



Cite this: DOI: 10.1039/d5md00630a

Harnessing photodynamic therapy for programmed cell death: the central role and contributions of metal complexes as next generation photosensitizers

Sreejani Ghosh, ^a Rinku Chakrabarty ^{*b} and Priyanka Paira ^{*a}

A fundamental biological mechanism, programmed cell death (PCD), is essential for tissue homeostasis, immunological control, and development. Its dysregulation is a characteristic of many diseases in multicellular organisms, including cancer, where unchecked proliferation is made possible by evading cell death. Therefore, one of the main tenets of contemporary anticancer therapies is the restoration or induction of PCD in cancer cells. One potential, least invasive method among these is photodynamic treatment (PDT). PDT uses light-activatable photosensitisers, which cause cancer cells to explode with reactive oxygen species (ROS) when exposed to light. These ROS harm important biomolecules, throw off the cellular redox equilibrium, and cause cells to die. PDT-induced cell death was previously believed to be mostly caused by autophagy, necrosis, or apoptosis. Recent research, however, has shown that it can trigger a wider range of unconventional cell death pathways. ROS can cause ferroptosis by oxidising membrane lipids, fragmenting DNA, and lowering intracellular glutathione (GSH) levels. Similarly, necroptosis or pyroptosis can result from severe oxidative stress activating death receptor signalling. Sometimes, in response, cells use survival strategies like autophagy, which can also lead to cell death. This review explores these new, unconventional methods of cell death and how PDT can be used to take advantage of them. Next-generation photosensitisers based on iridium (Ir), ruthenium (Ru), and rhenium (Re) complexes are given special attention because they provide deep tissue penetration, improved photostability, and adjustable ROS production. Their incorporation into PDT has revolutionary potential for improving cancer treatment precision and conquering therapeutic resistance.

Received 20th July 2025,
Accepted 25th September 2025

DOI: 10.1039/d5md00630a

rsc.li/medchem

1. Introduction

Due to its high prevalence, fatality rates, and the financial toll it takes on healthcare systems around the world, cancer continues to be a serious global health concern.¹ The World Health Organisation (WHO) recently estimated that cancer was the second largest cause of death worldwide in 2020, accounting for around 10 million fatalities.² Tumour heterogeneity and adaptive capacity frequently lead to medication resistance, disease recurrence, and metastasis, even with significant advancements in early diagnosis, diagnostics, and therapeutic modalities.³ As a result, oncological research is still motivated by the desire for more specialised, effective, and less harmful therapeutic alternatives. Photodynamic therapy (PDT), one of the newer

treatments, has drawn interest because of its distinct mode of action, which uses the production of reactive oxygen species (ROS) to photoactivate non-toxic substances and produce localised cytotoxic effects. Crucially, the effectiveness of PDT is being connected increasingly to its ability to control and trigger different types of programmed cell death (PCD), a process whose control is essential to the development of cancer and the response to treatment.⁴

A collection of biological processes known as “programmed cell death” has been conserved throughout evolution and is intended to preserve homeostasis, get rid of damaged or possibly dangerous cells, and influence the immune system.⁵ Although apoptosis has long been thought to be the most common type of PCD, over the last 20 years, a number of different but connected cell death mechanisms have been discovered, such as necroptosis, pyroptosis, ferroptosis, and autophagic cell death. Each of these pathways has distinct morphological characteristics, immunological effects, and molecular signalling cascades.⁶ Tumour cells frequently develop the capacity to avoid or

^a Department of Chemistry, School of Advanced Sciences, Vellore Institute of Technology, Vellore-632014, Tamil Nadu, India. E-mail: priyanka.paira@vit.ac.in
^b Department of Chemistry, Alipurduar University, Alipurduar-736122, West Bengal, India. E-mail: rckncs@gmail.com

inhibit various PCD pathways in the context of cancer, which aids in uncontrolled growth, treatment resistance, and immune surveillance evasion. As a result, cancer holds great promise for treatment approaches that might reactivate or avoid these death-resistance pathways. PDT stands out as a strong contender in this respect due to its ability to both geographically and temporally induce oxidative stress and begin numerous death pathways.⁷

A variety of tactics are used by cancer cells to evade apoptotic signals. Overexpression of anti-apoptotic proteins from the B-cell lymphoma 2 (Bcl-2) family, such as Bcl-2 and Bcl-xL, is a typical mechanism. These proteins impede the mitochondrial pathway of apoptosis by blocking the release of cytochrome c and the subsequent activation of caspase.⁸ On the other hand, tumours frequently downregulate or functionally inactivate pro-apoptotic members of the same family, such as Bak and Bax, which tips the scales in favour of cell survival. Furthermore, almost 50% of human malignancies have mutations in the TP53 gene, which codes for the tumour suppressor protein p53. Since wild-type p53 causes cell cycle arrest or apoptosis in response to a variety of cellular stressors, its deactivation eliminates a crucial obstacle to the growth of tumours. Moreover, inhibitors of apoptosis proteins (IAPs), which bind and block caspases, the primary apoptotic executors, can be upregulated in cancer cells.^{9,10} Together, these changes allow cancer cells to avoid dying, which leads to unchecked proliferation and resistance to traditional treatments.^{11,12}

The complex and dynamic milieu known as the tumour microenvironment (TME) is made up of several cellular and non-cellular elements that interact with tumour cells to affect the course, metastasis, and response to treatment of cancer.¹³ Cancer-associated fibroblasts (CAFs), immunological cells (including T cells, myeloid-derived suppressor cells, and tumour-associated macrophages), endothelial cells, and pericytes are important biological components of the TME. The extracellular matrix (ECM), growth factors, cytokines, chemokines, and extracellular vesicles are examples of non-cellular components. Through bidirectional communication, these components alter signalling pathways that control angiogenesis, immune evasion, cell proliferation, and survival in tumour cells.¹⁴

The TME's function in fostering resistance to cell death is an important feature. For example, CAFs express a range of soluble molecules that can decrease apoptotic signalling and activate survival pathways in cancer cells, including interleukins, transforming growth factor-beta (TGF- β), and ECM components. Similarly, within the TME, tumour-associated macrophages frequently take on an M2-like phenotype, producing growth factors and anti-inflammatory cytokines that promote tumour growth and suppress cytotoxic immune responses.¹⁵ Furthermore, hypoxia-induced factors (HIFs) can be stabilised by the hypoxic conditions frequently present in solid tumours as a result of abnormal vasculature.¹⁶ These HIFs then upregulate genes related to

angiogenesis, metabolism, and survival, further strengthening the tumour's resistance to apoptosis.¹⁷

Three components make up the system that powers photodynamic therapy: molecular oxygen, a particular light wavelength, and a photosensitiser (PS).¹⁸ When light activates the photosensitiser, it first changes from its ground state to an excited singlet state, then it crosses between systems to reach a triplet state.¹⁹ After that, the triplet-state PS can either interact with substrates to create free radicals through type I reactions or transfer energy to molecular oxygen through type II reactions, producing singlet oxygen ($^1\text{O}_2$) and other ROS. The oxidative damage caused by these highly reactive ROS to vital macromolecules such as proteins, lipids, and nucleic acids results in cellular malfunction and death.²⁰ While ROS's short half-life and small diffusion distance ($\sim 0.02\text{--}0.1\ \mu\text{m}$) guarantee that cytotoxicity is limited to the lit tumour site, minimising harm to surrounding normal tissue, PDT's spatial selectivity is attributed to the localised nature of light delivery (Fig. 1).²¹

For the treatment of cancer, tetrapyrrolic compounds conjugated with metal complexes have emerged as a promising class of PSs in PDT due to their enhanced photophysical and photobiological properties. The coordination of transition metals such as Ru, Cu, Pt, Fe, Rh, Ir, and Pd with compounds including porphyrins, chlorins, bacteriochlorins, and phthalocyanines results in enhanced singlet oxygen production, red-shifted absorbance, and greater photostability. The heavy atom effect, especially from high-Z metals (such as Ru, Ir, and Pt), makes it easier for systems to cross one another. This increases the generation of ROS, which, in turn, enhances phototoxicity. Tetra(2-naphthyl)tetracyanoporphyrine and its Fe(II) complex, for example, show promising PDT agents due to their strong ROS output and specific tumour accumulation. Strong near-infrared (NIR) absorption by palladium-conjugated porphyrinoids allows for deeper tissue penetration and better hypoxic tumour treatment.^{22–24} Because of their strong NIR absorption, metallo-bacteriochlorins minimise off-target toxicity by enabling deep tissue activation and demonstrating quick systemic elimination. Through synergistic mechanisms, ruthenium-based tetrapyrrole complexes have demonstrated dual phototoxic and chemotoxic effects, hence enhancing therapeutic efficacy. These metal-tetrapyrrole conjugates' nanoformulations also improve their overall photodynamic performance, targeted administration, and bioavailability. These chemicals have a lot of therapeutic promise despite issues, including poor solubility and possible toxicity. Multidisciplinary attempts to create next-generation PDT agents with strong anticancer activity and less systemic adverse effects are still drawn to their adaptability and tunability.^{25,26}

The potential of PDT to start different PCD pathways based on several factors, including the kind and subcellular location of the photosensitiser, the light dose and fluence rate, the cellular redox state, and the tumour microenvironment, is one of its distinguishing features.²⁷

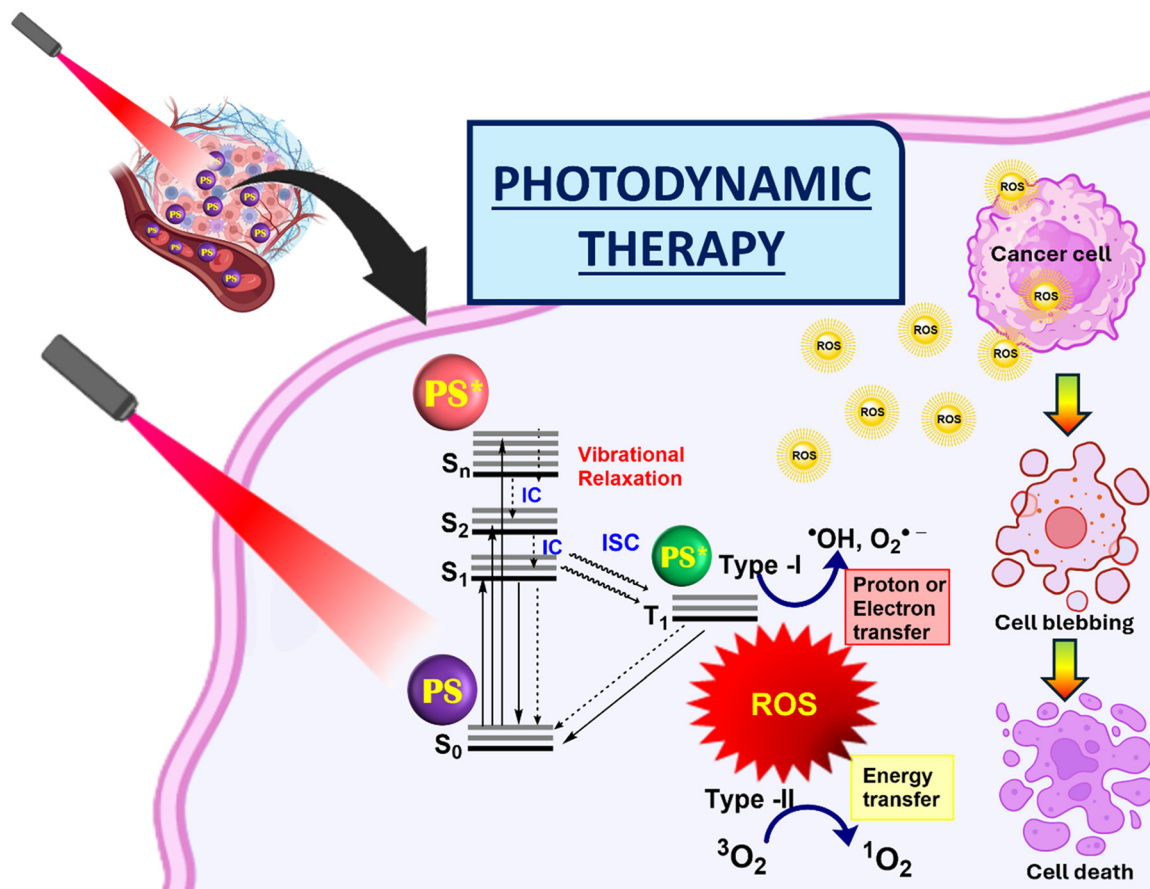


Fig. 1 Schematic diagram showing the mechanism of action of photodynamic therapy in cancer cells.

Certain porphyrins and chlorins are examples of photosensitizers that target mitochondria and can directly damage the integrity of the mitochondrial membrane, causing cytochrome *c* release, activation of the caspase cascade, and ultimately apoptotic cell death.²⁸ Alternatively, lysosome-localising photosensitizers can cause permeabilisation of the lysosomal membrane, which releases hydrolases such as cathepsins that either directly cause apoptosis or activate other types of PCD.²⁹ Moreover, depending on the strength of stress signals, photosensitizers that build up in the endoplasmic reticulum might cause ER stress and the unfolded protein response, which can result in apoptosis or immunogenic types of cell death.³⁰

The most researched type of PCD, apoptosis, is a tightly controlled, immunologically quiet process that involves both extrinsic and internal signalling pathways.³¹ The Bcl-2 protein family modulates mitochondrial outer membrane permeabilisation (MOMP), which in turn controls the intrinsic (mitochondrial) route.³² PDT-induced mitochondrial oxidative damage can increase pro-apoptotic proteins like Bak and Bax, which causes cytochrome *c* to be released and caspase-9 and executioner caspases-3/7 to be activated. Conversely, the extrinsic pathway entails the activation of death receptors, including TRAIL-R and Fas, which results in the recruitment of FADD and the activation of caspase-8.

Interestingly, there is a lot of interaction between the two pathways. For example, caspase-8 can cleave Bid to tBid, which encourages permeabilisation of the mitochondria.³³

Nevertheless, a lot of malignancies create defences against apoptosis by mutating death receptor signalling, losing pro-apoptotic proteins (such as p53 and Bax), or upregulating anti-apoptotic proteins (like Bcl-2 and Bcl-xL).³⁴ Alternative types of PCD become crucial in these situations. The receptor-interacting protein kinases RIPK1 and RIPK3, as well as the mixed lineage kinase domain-like (MLKL) pseudokinase, are responsible for necroptosis, a type of controlled necrosis.³⁵ Necroptosis is a pro-inflammatory process because, in contrast to apoptosis, it results in the rupture of the plasma membrane and the release of intracellular DAMPs.³⁶ When caspase activity is decreased or RIPK1/RIPK3 expression is elevated, PDT has been demonstrated to induce necroptosis, offering a useful pathway to cell death in malignancies that are resistant to apoptosis.³⁷

However, PDT can also trigger ferroptosis, an iron-dependent form of non-apoptotic cell death characterised by the accumulation of lipid peroxides. System Xc⁻ (cystine/glutamate antiporter), intracellular iron pools, and glutathione peroxidase 4 (GPX4) are the main controllers of ferroptosis.³⁸ Inhibiting GPX4 activity, promoting lipid

peroxidation, and overwhelming antioxidant defences are all ways whereby PDT-induced ROS, especially singlet oxygen, can cause ferroptotic cell death. The metabolic phenotype, iron load, and redox state of some cancer cells affect their susceptibility to ferroptosis, and PDT can alter these factors.³⁹

When overactivated, autophagy, a lysosome-mediated degradation system, can function as a type of PCD or as a survival strategy in metabolic stress. Depending on the amount and location of oxidative damage, PDT can alter autophagic flux.⁴⁰ While greater doses or specific lysosomal damage can result in faulty autophagy and cell death, moderate PDT doses may cause protective autophagy that postpones cell death. Furthermore, autophagy might affect the overall fate of cells by interacting with the pathways leading to necroptosis and apoptosis.⁴¹

The TME, which is crucial in determining therapy responses, is another important factor to take into account. By causing damage to the tumour vasculature, increasing vascular permeability, and upsetting the extracellular matrix, PDT-induced ROS can alter the TME. However, because PDT depends on molecular oxygen, tumour hypoxia—a typical characteristic of solid tumours—can reduce its effectiveness.⁴² The hypoxic tumour microenvironment, which restricts the effectiveness of traditional PDT due to oxygen dependence, has given rise to hypoxia-activated prodrugs (HAPs), a potential approach in PDT-based cancer phototherapeutics. Typically seen in solid tumours, HAPs are made to be inert in normoxic environments and preferentially activate in hypoxic ones. When hypoxia-responsive moieties such as nitroimidazoles, azobenzene, and quinones are included in photosensitiser frameworks, site-specific therapeutic effects and regulated activation are made possible. To increase ROS formation locally, nitroimidazole-conjugated porphyrin compounds, for instance, undergo bio-reduction under hypoxia to release the active photosensitiser. As demonstrated by azobenzene-linked BODIPY conjugates, azo-based linkers have been used to conceal photosensitizers or photosensitive medications that cleave reductively in low-oxygen settings.^{43–46} Additionally, quinone-based triggers in metal complexes, like photosensitisers based on Ir(III) or Ru(II), have been employed for hypoxia-activated phototoxicity with negligible off-target effects. For improved tumour accumulation, certain HAPs also add bio-reductive components to exosomes or nanocarriers. These clever designs provide a strong platform for treating aggressive and treatment-resistant tumours by enhancing PDT selectivity and safety while also enhancing combination therapies through synergistic chemo-photo effects.^{47–49}

From a translational standpoint, a number of variables, such as the optimisation of photosensitiser pharmacokinetics, light delivery methods, dosimetry, and treatment timing, are critical to the clinical effectiveness of PDT.⁵⁰ Although Photofrin and Foscan, two first- and second-generation photosensitisers, have shown promise in treating

some types of cancer, they have drawbacks such as low tissue penetration, prolonged photosensitivity, and restricted tumour selectivity.^{51,52} To improve therapeutic precision, third-generation photosensitizers combine theranostic functions, stimuli-responsive release mechanisms, and tumour-targeting ligands.⁵³ PDT is becoming more applicable to deep-seated tumours at the same time, thanks to developments in fibre-optic technology, light-emitting diode (LED) arrays, and upconversion nanoparticles.^{54,55}

Key obstacles to the clinical translation of metal-based PSs for PDT include low photostability, prolonged systemic retention that results in photosensitivity, poor solubility, and decreased ROS generation in hypoxic tumour settings. PDT's efficacy is further limited by its poor tumour selectivity and limited light penetration. But transition metal complexes, particularly Ru(II), Ir(III), and Os(II) molecules, have distinct benefits such as high ROS production, tunable photophysical characteristics, and activation under X-ray or near-infrared light.^{56–58} Targeted delivery and enhanced tumour accumulation are made possible by their capacity to undergo precise structural alterations. In order to improve systemic anticancer effects, emerging techniques concentrate on creating intelligent, tumour-activated PSs and combining PDT with immunotherapy. The increasing potential of metal-based PDT agents is demonstrated by clinical candidates such as purlytin, lutrin/antrin, TOOKAD soluble, and most notably TLD-1433 (a Ru(II) complex in trials). With these advancements, PDT will no longer be a localised treatment but rather a potent tool that may treat metastatic malignancies more precisely and with fewer adverse effects.^{59,60}

In conclusion, photodynamic therapy is a flexible and multidimensional approach to cancer treatment that can activate the immune system and specifically trigger a variety of pathways leading to programmed cell death. The interaction of subcellular targets, PDT-induced ROS, and PCD molecular regulators determines the treatment result and offers several avenues for intervention. In addition to helping to improve current PDT techniques, a better knowledge of these systems will open the door for the logical development of combination therapies that take advantage of weaknesses in the machinery that kills cancer cells. With a focus on the mechanistic diversity, therapeutic implications, and future options for incorporating PDT into contemporary cancer treatment paradigms, this study attempts to provide a thorough analysis of the state of PDT-induced PCD.

2. ROS-regulated programmed cell death pathway

2.1. Apoptosis

2.1.1. Apoptotic pathways and regulation. Apoptosis, a closely controlled and designed type of cell death, is essential for preserving cellular homeostasis and getting rid of damaged or dangerous cells, particularly ones that have the potential to cause cancer. Because it acts as a natural defence

against carcinogenesis, apoptosis is very important in the study of cancer biology. But cancer cells often have the capacity to avoid death, which leads to the growth of tumours, resistance to treatment, and unfavourable clinical results. The intrinsic (mitochondrial) and extrinsic (death receptor-mediated) signalling routes are the two main ways that apoptosis occurs. Both pathways lead to the activation of executioner caspases, which coordinate the methodical breakdown of cellular constituents.⁶¹

The Bcl-2 protein family controls MOMP, which is the main regulator of the intrinsic pathway. MOMP and the release of cytochrome c from the mitochondrial intermembrane gap into the cytosol are promoted by pro-apoptotic members like Bak and Bax.⁶² After cytochrome c, caspase-9, and apoptotic protease-activating factor-1 (Apaf-1) form the apoptosome, downstream effector caspases, including caspase-3 and -7, are activated. Anti-apoptotic Bcl-2 family proteins, such as Bcl-2 and Bcl-xL, on the other hand, prevent this process and increase cell survival.⁶³

On the other hand, extracellular death ligands like Fas ligand (FasL), tumour necrosis factor- α (TNF- α), and TNF-related apoptosis-inducing ligand (TRAIL) link to their corresponding transmembrane death receptors (Fas, TNFR1, DR4/DR5) to start the extrinsic route.⁶⁴ The death-inducing signalling complex (DISC), which is created as a result of this ligand-receptor interaction, attracts and activates

initiator caspase-8.⁶⁵ By cleaving the BH3-only protein Bid into its truncated version (tBid), which translocates to mitochondria and activates MOMP, activated caspase-8 can either directly cleave and activate effector caspases or enhance the apoptotic signal, connecting the intrinsic and extrinsic pathways (Fig. 2).⁶⁶

2.1.2. Apoptotic pathways induction through photodynamic therapy. PDT induces apoptosis by generating singlet oxygen ($^1\text{O}_2$) and other ROS upon light activation of photosensitizers. These ROS cause oxidative damage to vital cellular macromolecules—including proteins, lipids, and nucleic acids—leading to programmed cell death. The PS's chemical makeup and subcellular location, the amount of light used, and the oxygenation level of the TME are some of the variables that affect the apoptotic response to PDT.⁶⁷

PSs that target mitochondria, such as Photofrin, Verteporfin, and Foscan, have shown great effectiveness in triggering intrinsic apoptosis by triggering cytochrome c release, mitochondrial depolarisation, and MOMP in response to light activation. As a result, the intrinsic caspase cascade is activated, and the apoptosome is assembled. Furthermore, oxidative stress brought on by PDT can suppress anti-apoptotic proteins like Bcl-2 and survivin, increase the expression of pro-apoptotic proteins like Bax, Bak, and p53, and alter signalling pathways like mitogen-activated protein kinases (MAPKs), all of which contribute to

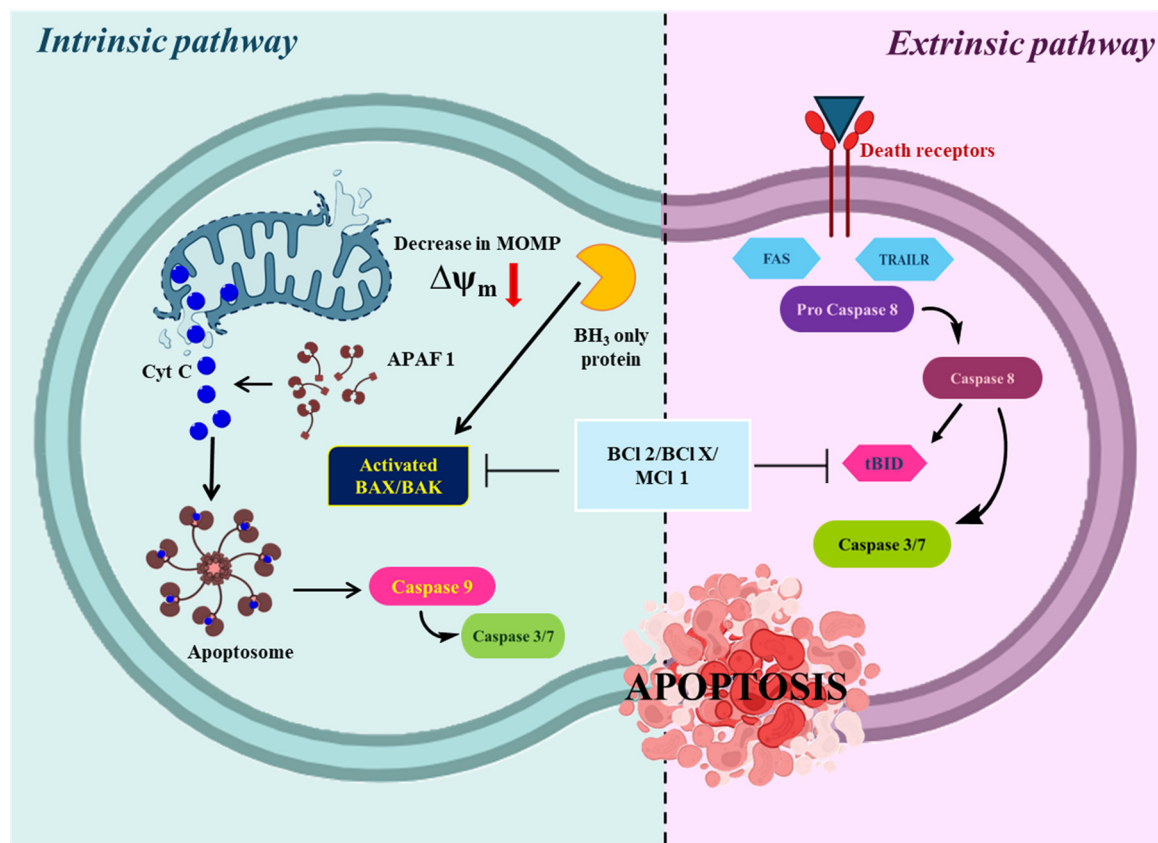


Fig. 2 Schematic representation of apoptotic cell death pathways.

the apoptotic result. Notably, PDT can also trigger the extrinsic route by increasing the expression of death receptors and their ligands, such as Fas and TRAIL-R, or by making cancer cells more susceptible to receptor-mediated apoptosis through receptor clustering and membrane remodelling brought on by ROS.⁶⁸

Crucially, PDT's capacity to trigger apoptosis in a regulated and immunologically advantageous way offers therapeutic benefits for the treatment of cancer. In contrast to necrosis, which frequently causes inflammation and collateral tissue damage, apoptosis is immunologically silent or even immunogenic in some circumstances, particularly when damage-associated molecular patterns (DAMPs) such as calreticulin, HMGB1, and ATP are released. By encouraging dendritic cell maturation and cytotoxic T lymphocyte activation, these compounds can improve anti-tumour immunity. Furthermore, PDT's selectivity for cancerous cells over healthy tissues reduces systemic toxicity due to selective

PS accumulation and localised light activation. Cancer is characterised by resistance to apoptosis, which is frequently caused by p53 mutations, overexpression of anti-apoptotic proteins, or downregulation of death receptors.⁶⁹

However, by concurrently activating several pro-apoptotic pathways and altering the tumour microenvironment, PDT presents a viable method to get past this resistance. For example, by reactivating p53-independent apoptotic pathways or downregulating Bcl-2 expression, PDT has been demonstrated to restore apoptosis sensitivity in resistant cancer morphologies.⁷⁰ All things considered, PDT's pro-apoptotic mechanisms offer a complex and effective way to destroy tumour cells while protecting the surrounding healthy tissues, which makes it a useful supplement or substitute for traditional cancer treatments. The development of novel PSs with enhanced tumour selectivity, deeper tissue penetration, and subcellular targeting capabilities, as well as combinatorial strategies that combine PDT with apoptosis-

Table 1 Cyclometalated iridium III complexes inducing apoptosis *via* photodynamic therapy

Sl. no.	Cyclometalated iridium(III) complex	Cancer cell lines	IC ₅₀ (light)	Apoptosis mechanism	Localisation	Reference
1	1	HepG2	4.4 ± 0.7 μM	Mitochondrial disruption and Trx inhibition	Mitochondria	72
2	2	HeLa	0.83 ± 0.06 μM	Mitochondria-membrane disruption and PI3K/AKT signaling pathway	Mitochondria	73
3	3	A549	2.23 ± 0.08 μM	Decrease in MMP, caspase, and Bcl-2 regulation	Mitochondria	74
4	4	SGC-7901	0.6 ± 0.1 μM	Mitochondrial dysfunction, Ca ²⁺ level regulation, decrease in ATP levels	Mitochondria	75
5	5	A549	0.2 ± 0.05 μM	Mitochondrial injury and lipid peroxidation	Mitochondria and endoplasmic reticulum	76
6	6	MDA-MB-231	0.26 μM	Mitochondrial disruption and ER stress	Mitochondria	77
7	7	HeLa	1.8 μM	Mitochondria-membrane disruption and ROS generation	Mitochondria	78
8	8	A549	24.0 nM	Mitochondrial dysfunction and ROS generation	Mitochondria	79
9	9	PC-3	2.4 ± 1.4 μM	Decreasing MMP and NADH oxidation, and DNA photocleavage	Mitochondria	80
10	10	A549	0.426 ± 0.041 μM	Caspase activation, GSH depletion and lipid peroxidation	Mitochondria	81
11	11	HCT116	30.93 nM	Decrease in MMP, pro-apoptotic gene activation, and caspase activation	Mitochondria	82
12	12	HCT116	0.1095 ± 1.2 μM	DNA fragmentation and cellular blebbing	Lysosomes and mitochondria	83
13	13	MDA-MB-231	5.31 μM	Cytochrome C release and caspase activation	Mitochondria	84
14	14	MCF-7	10 ± 1.90 μM	Proapoptotic protein activation and mitochondrial membrane damage	Mitochondria	85
15	15	A549R	0.83 ± 0.10 μM	ROS accumulation and mitochondrial membrane potential depolarisation	Mitochondria	86
16	16	A549	0.23 ± 0.08 μM	ROS accumulation, MMP depletion, and caspase activation,	Mitochondria	87
17	17	HeLa	0.00070 ± 0.0002 μM	NADH oxidation, DNA damage and mitochondrial damage	Mitochondria	88
18	18	A549	11.0 ± 0.4 μM	Elevated pro-apoptotic Bax protein and Cyt C release and downregulation of Bcl-2	Mitochondria	89
19	19	HepG2	0.5 μM	ROS damage to mitochondria	Mitochondria	90
20	20	Hep G2	1–10 μM	Cytochrome C release and NADH photo-oxidation	Mitochondria	91
21	21	A375	1.1 ± 0.4 μM	MMP depletion, ROS generation	Mitochondria	92

sensitising agents, immune checkpoint inhibitors, or traditional chemoradiation, are ongoing research efforts to further improve PDT's apoptotic efficacy.⁷¹

2.1.3. Photosensitizer inducing apoptosis *via* PDT.

Cyclometalated iridium(III) complexes are strong photodynamic agents that, after being activated by light, cause apoptosis by a carefully planned series of intracellular processes. Therefore, it is a hot topic among researchers who want to create phototherapeutics that can destroy tumour cells. Mono-metallic and Bi-metallic iridium complexes using ligands with extended conjugation were designed and synthesized by Miao Zhong *et al.* (1), Shu-fen He *et al.* (2), Qin Zhou *et al.* (3), Jing Hao *et al.* (4), Wenlong Li *et al.* (5), Zheng-Yin Pan *et al.* (6), Rui Tu *et al.* (7), Zanru Tan *et al.* (8), Elisenda Zafon *et al.* (9) and, Li-Zhen Zeng *et al.* (10). The potency of these complexes as apoptosis inducing phototherapeutics were investigated. These metal complexes are mostly cationic in nature, thus making them specific towards mitochondria (Table 1).^{72–81}

When these complexes are exposed to radiation, they change into an excited triplet state and release energy to molecular oxygen, producing reactive oxygen species (ROS), especially singlet oxygen (¹O₂). The ROS build up in cancer cells, particularly in subcellular organelles such as the endoplasmic reticulum, lysosomes, or mitochondria, depending on where the complex is located within the cell. When mitochondria-targeting iridium(III) complexes damage mitochondrial membranes oxidatively, pro-apoptotic substances, including cytochrome c, are released into the cytosol, and mitochondrial membrane potential ($\Delta\Psi_m$) is lost. The cell enters apoptosis, which is marked by chromatin condensation, membrane blebbing, and DNA breakage, when this release triggers initiator caspase-9, which in turn triggers executioner caspases such as caspase-3 and -7. Further sensitising the cells to apoptosis, these complexes can also downregulate anti-apoptotic proteins (like Bcl-2) and upregulate pro-apoptotic proteins (like Bax). These complexes can selectively kill cancer cells by apoptosis while reducing off-target toxicity because they can accurately control ROS formation both geographically and temporally with light.

A prospective therapeutic target, myeloid cell leukaemia-1 (Mcl-1) is an antiapoptotic oncoprotein that is overexpressed in a variety of malignancies. Even though there are several small-molecule Mcl-1 inhibitors, it is still difficult to distribute them precisely. Using the location of Mcl-1 on the outer mitochondrial membrane, a series of mitochondria-targeting luminous cyclometalated iridium(III) prodrugs were created by Tejal Dixit *et al.* (11), containing Mcl-1 inhibitors *via* ester linkage. According to mechanistic research, 11 quickly builds up in mitochondria and is triggered by overexpressed esterase, which releases two cytotoxic agents: the ROS-generating iridium(III) complex and the Mcl-1 inhibitor (I-2). Through cell cycle arrest and the mitochondria-mediated route, this dual action causes the depolarisation of the mitochondrial membrane and initiates apoptosis. Significant morphological alterations and a

decrease in tumour growth in 3D multicellular tumour spheroids of HCT116 cells further demonstrated the compound's effectiveness.⁸²

A possible approach to next-generation PDT with increased efficacy and fewer adverse effects is organelle-targeted PSs. Twelve of the cyclometalated iridium(III) complexes that were synthesised and characterised by Monika Negi *et al.* (12), which demonstrated outstanding photophysical characteristics, such as a long photoluminescence lifetime and a high singlet oxygen quantum yield. When exposed to blue light (456 nm), 12 effectively produces hydroxyl and singlet oxygen radicals, which cause cancer cells to undergo apoptosis. It causes considerable cytotoxicity (PI > 400) and morphological disruption in 3D tumour spheroids, particularly accumulating in mitochondria and lysosomes. The effectiveness of PDT is increased by this dual organelle targeting through type I/II mechanisms.⁸³

The majority of Ir(III)-based photosensitisers are mononuclear, although little is known about binuclear systems. Nishna Neelambaran *et al.* introduced a dinuclear Ir(III) complex (13) containing 2-(2,4-difluorophenyl)pyridine and 4'-methyl-2,2'-bipyridine ligands. 13 showed much better photoluminescence quantum yield ($\Phi_p = 0.70$) and singlet oxygen generation ($\Phi_s = 0.49$). Additionally, 13 demonstrated significant photocytotoxicity and robust cellular uptake against MDA-MB-231 breast cancer cells. Without the need for further targeting moieties, its dual positive charge promoted intrinsic mitochondrial localisation. Si-DMA staining, annexin V-FITC/PI flow cytometry, cytochrome c release, and NaN₃ inhibition tests were used to confirm ROS-induced apoptosis. This demonstrates how effective image-guided photodynamic therapy can be with 13.⁸⁴

To meet their high energy needs for development and metastasis, cancer cells mostly rely on mitochondria. Cyclometalated iridium(III) probes were created by Chandana Reghukumar *et al.* (14) to target this susceptibility. In MCF-7 breast cancer cells, 14 showed better photosensitising efficacy and less dark toxicity. Its positive charge and intense red fluorescence (colocalization coefficient = 0.90) facilitate mitochondrial targeting. When 14 is activated by light, it produces singlet oxygen ($\Phi_\Delta = 0.79$), alters the potential of the mitochondrial membrane, hinders respiration, and causes death. SERS analysis and Annexin V staining were used to validate these effects. 14 is therefore a powerful theranostic agent that combines both fluorescence and Raman-based imaging capabilities with laser-activated mitochondrial damage.⁸⁵

After synthesising and comprehensively characterising four iridium(III) complexes, 15 was shown to be a promising photosensitiser by Kai Xiong *et al.*, that targets mitochondria because of its high singlet oxygen production and precise mitochondrial localisation. While 15 showed little toxicity to normal HLF cells, it showed strong phototoxicity to A549 lung cancer cells and their cisplatin-resistant version, A549R. Because cancer cells internalise more of the complex, this

selective cytotoxicity is explained by differential cellular absorption. **15** efficiently overcame drug resistance in A549R cells by inducing mitochondria-mediated apoptosis upon 405 nm light irradiation. These results demonstrate **15**'s potential as a targeted photodynamic treatment agent for resistant cancer types, providing a method to kill cancer cells only while leaving healthy tissues intact.⁸⁶

Complexes of cyclometalated iridium(III) have a lot of potential as metallodrugs to treat cancer. The anticancer potential of three phosphorescent complexes that target mitochondria was assessed by Yi Li *et al.* (**16**) in this investigation. IC₅₀ values for all three examined cancer cell lines ranged from 0.23 to 5.6 μ M, indicating much higher antiproliferative action than cisplatin. Their preponderance in mitochondria was confirmed by colocalization tests. According to mechanistic studies, these complexes cause mitochondrial malfunction, which is manifested by apoptosis, increased intracellular ROS levels, and depolarisation of the mitochondrial membrane potential (MMP). According to these results, all the complexes are potent candidates for the creation of next-generation anticancer treatments because they appear to cause cytotoxicity by interfering with mitochondrial integrity and redox equilibrium.⁸⁷

Carlos Gonzalo-Navarro *et al.* (**17**) coordinated π -expanded ligands to Ir(III) half-sandwich complexes to enhance excited-state lifetimes and promote ¹O₂ generation. Derivatives of the form [CpIr(C[^]N)Cl] and [CpIr(C[^]N)L]BF₄ were synthesised, with greater π -expansion leading to higher phototoxicity (PI > 2000) and notable activity under red light (PI = 63). TD-DFT calculations supported the effect of π -expansion. These complexes induce reactive oxygen species (ROS) generation, mitochondrial membrane depolarisation, DNA cleavage, NADH oxidation, and lysosomal damage, triggering apoptosis and secondary necrosis. This work introduces the first class of half-sandwich iridium cyclometalated complexes for effective PDT.⁸⁸

The anticancer potential of four neutral cyclometalated iridium(III) dithioformic acid complexes was evaluated by Yuting Wu *et al.* (**18**). Assays for toxicity showed remarkable effectiveness, especially when used against human non-small cell lung cancer (A549) cells. **18** displayed potent anticancer action (IC₅₀ = 11.0 \pm 0.4 μ M), was almost twice as effective as cisplatin, and successfully stopped A549 cell migration. These complexes specifically targeted mitochondria, resulting in apoptosis, cell cycle arrest, increased intracellular reactive oxygen species (ROS) production, and a decrease in mitochondrial membrane potential (MMP). According to Western blot examination, apoptotic signalling cascades were triggered by the considerable release of cytochrome c (Cyt-c), the elevation of pro-apoptotic Bax, and the downregulation of Bcl-2. When taken together, these results demonstrate their many uses in cancer treatment, including as apoptotic induction, anti-metastatic action, and mitochondrial imaging.⁸⁹

Because of their unique photophysical characteristics, cyclometalated iridium(III) complexes are great options for applications like fluorescent lifetime imaging microscopy (FLIM) probes and photosensitisers. For FLIM-guided photodynamic treatment (PDT), a novel iridium(III) complex, with aggregation-induced emission (AIE) properties, was created by Dandan Chen *et al.* (**19**) in this work. Variations in fluorescence lifetime showed that **19** was highly sensitive to changes in mitochondrial viscosity. In the near-infrared spectrum, it also demonstrated advantageous multiphoton absorption (two-photon: 700–800 nm; three-photon: 1150–1450 nm). Notably, FLIM allowed for real-time monitoring of changes in mitochondrial viscosity during PDT. This study demonstrates how **19** can be used as a therapeutic agent and a diagnostic tool, allowing for self-reporting PDT responses and accurate detection of cellular microenvironmental alterations.⁹⁰

As a hydride donor, nicotinamide adenine dinucleotide-reduced (NADH) is essential for preserving cellular equilibrium. To identify endogenous NADH levels, a quinoline-appended iridium complex is presented in this work by Shanmughan Shamjith *et al.* (**20**) as a dual-mode molecular probe for both fluorescence and surface-enhanced Raman spectroscopy (SERS). **20** has detection limits of 25.6 nM (fluorescence) and 15 pM (SERS) after undergoing a NADH-triggered switch that turns on luminescence (turn-ON) and turns off SERS signals (turn-OFF). The energy barrier for the hydride transfer from NADH to **20**, which forms N-**20**, is 19.7 kcal/mol, according to density functional theory (DFT) calculations. Furthermore, by preventing photoinduced electron transfer (PeT), N-**20** acts as a photosensitiser, producing singlet oxygen and NAD radicals. This makes it an effective tool for multiphase photodynamic treatment and NADH sensing.⁹¹

Zanru Tan *et al.* (**21**) created a series of dinuclear cyclometalated Ir(III) complexes as photodynamic anticancer drugs that work with two photons. These complexes selectively accumulate in mitochondria and show significant two-photon absorption (2PA) cross-sections (σ_2 = 66–166 GM). Notably, **21** displayed a phototoxicity index (PI) of 24 and an IC₅₀ of 2.0 μ M. **21** efficiently generates reactive oxygen species (ROS) when excited by two photons, causing damage to the mitochondria and the death of cancer cells. To improve 2PA for PDT applications, this study demonstrates how dinuclear complexes with conjugated planar bridges can significantly increase optical characteristics (Fig. 3).⁹²

2.2. Ferroptosis

2.2.1. Ferroptotic pathways and regulation. In 2012, the research group of B. Stockwell discovered a new cell death modality selectively triggered by the oncogenic RAS selective lethal small molecule, elastin. This cell death modality was named ferroptosis. The term “ferroptosis” is derived from the Greek word “ptosis” (falling) and the Latin word “ferrum” (iron).⁹³ Ferroptosis represents a controlled necrotic cell

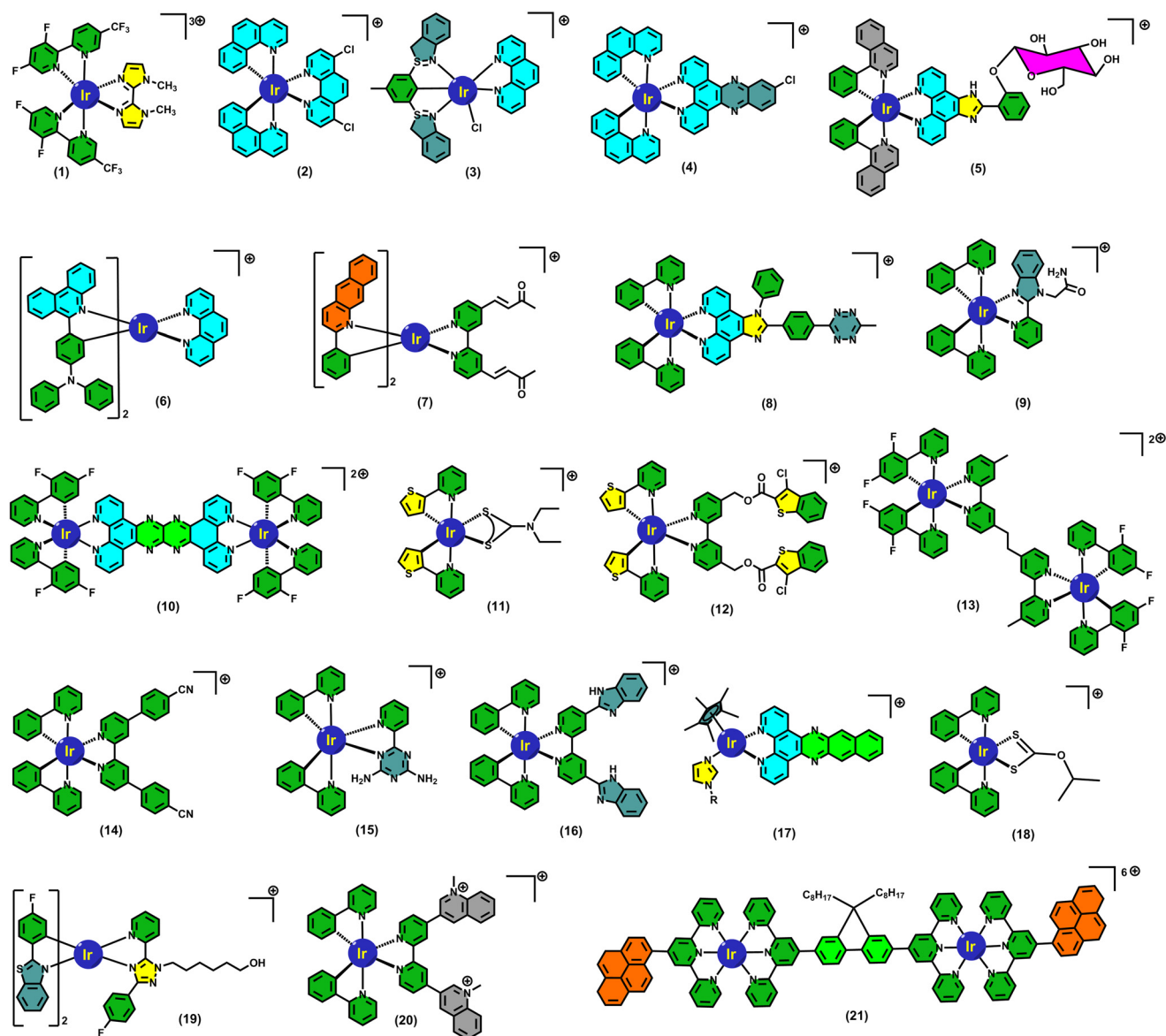


Fig. 3 Selective cyclometalated Ir(III) complexes which trigger apoptosis as phototherapeutics.

death pathway that primarily triggers oxidative alterations in phospholipid membranes linked to iron concentration in the microenvironment. Ferroptosis can be distinctly identified from other conventional cell death pathways due to its notable morphological, biochemical, and genetic traits.⁹⁴ Several ferroptosis inhibitors are known to exist, including ferrostatin 1, liproxstatin-1, an inhibitor of ROS and lipid peroxidation, and deferoxamine, an iron chelator. Ferroptosis is morphologically defined by outer mitochondrial membrane rupture, decreased or absent mitochondrial cristae, and shrinkage of the mitochondria with increasing membrane density. There is no chromatin condensation or margination, and the nucleus size is constant. Ferroptosis is associated with cellular shrinkage and the emergence of homogeneous circular protrusions of the plasma membrane, along with a gradual loss in its

elasticity, according to recent atomic force microscopy investigations conducted in murine fibrosarcoma L929 cells. The cytoskeleton is unaffected, and membrane blebs are discernible even if surface roughness forms in the early phases of ferroptosis.⁹⁵ A recent review found that ferroptosis is controlled by several genes, mostly associated with iron homeostasis and lipid peroxidation metabolism (*e.g.*, GPX4, TFR1, SLC7A11, NRF2, NCOA4, P53, HSPB1, ACSL4, FSP1). The hunt for the new, specialised ferroptosis activator genes continues to linger on, though.⁹⁶ Ferroptosis was first identified biochemically as being associated with inhibition of glutathione peroxidase 4 (GPX4) or blocking of the cystine/glutamate antiporter (system Xc). The activity of system Xc, a heterodimer composed of the SLC7A11 and SLC3A2 subunits, ordinarily distributes cystines and holds the

cellular antioxidant environment in check, inhibiting the buildup of ROS. A selenium protein named GPX4 is essential for lipid peroxide detoxification and for reducing the detrimental effects of phospholipid peroxidation inducers.⁹⁷ As the system is compromised or GPX4 levels are reduced, the antioxidant cysteine–glutathione (GSH) metabolism is exhausted. Accordingly, lipid peroxides are incapable of being metabolised, and Fe^{2+} oxidises lipids through the Fenton reaction, which causes the production of extremely detrimental lipid peroxides and the death of cells. Therefore, a key element in regulating ferroptotic processes is the intricate interaction between lipid, iron, and cysteine metabolism.⁹⁸ Lipid peroxides have been proposed to be a crucial indicator of ferroptosis; the more lipid peroxides are present within the cell, the greater the extent of ferroptosis is observed. Other known inducers of ferroptosis include the small molecule compound Ras selective lethal 3 (RSL3), which inactivates GPX4, FIN56, which triggers ferroptosis and promotes GPX4 degradation whilst plummeting the level of the antioxidant CoQ10, and FINO2, which directly oxidises iron and indirectly inhibits GPX4 enzymatic function, contributing to widespread lipid peroxidation.⁹⁹

2.2.2. Ferroptotic pathways induction through photodynamic therapy. The ability of PDT to cause ferroptosis in tumour cells has been demonstrated by mounting data in recent years, providing a viable avenue for improving anticancer efficacy. 5-Aminolevulinic acid (5-ALA) is one prominent example. It has shown strong anticancer effects in esophageal squamous cell carcinoma (ESCC) models, notably in BALB/cAJcl-nu/nu mice that have had KYSE30 cells subcutaneously implanted. Mechanistic studies showed that 5-ALA-mediated PDT contributes to the buildup of lipid peroxides and oxidative stress in tumour cells by downregulating important ferroptosis-suppressing proteins, such as glutathione peroxidase 4 (GPX4) and heme oxygenase 1 (HMOX1). The development of third-generation PSs and attempts to use PDT to induce ferroptosis have grown intimately related. These next-generation PS platforms include PSs coupled with targeting moieties like sugars, monoclonal antibodies, or peptides, PSs encapsulated within liposomes, and nanocomplexes and nanocarriers designed to include PSs alongside chemotherapeutic drugs. These nanostructures' synthesis and design are very beneficial since they overcome several drawbacks of traditional PDT. These nano-constructs primarily improve tumour selectivity and reduce off-target cytotoxicity by increasing the targeted distribution of therapeutic drugs and PSs to tumour cells.^{27,100}

Importantly, these systems can include PSs that absorb in the 600–1000 nm NIR region, which enables more effective light activation of the PS and deeper tissue penetration. This ability minimises phototoxic effects on nearby healthy tissues by allowing a decrease in PS dosage without compromising therapeutic efficacy. Furthermore, the co-administration of pharmaceutical drugs *via* nano-platforms not only speeds up

the induction of cell death but also stimulates strong antitumor immune responses, which are crucial for eradicating remaining tumour cells and stopping the spread of the disease. Within this context, oxygen-enhanced PDT is a particularly novel method that aims to address a significant obstacle to effective PDT: the hypoxic nature of solid tumours. These oxygen-augmented platforms contain elements that can increase local oxygen levels in the tumour microenvironment, which increases the production of ROS when exposed to radiation. Ferroptotic cell death is greatly increased by the oxidative stress that follows. Crucially, increased interferon-gamma ($\text{IFN-}\gamma$) release indicates that this oxygen-rich environment encourages T cell infiltration and activation. Ferroptosis is exacerbated by the cytokine-induced downregulation of SLC3A2 and SLC7A11, which are parts of the cystine/glutamate antiporter system Xc^- . This further disturbs intracellular redox equilibrium.¹⁰¹

Moreover, photosensitisers alone or in combination with drugs that induce ferroptosis can be included into nano-constructs. These designs successfully induce ferroptosis in both configurations, highlighting their potential as therapeutics. But even with these developments, there are still major obstacles to overcome. Finding a careful balance between the danger of systemic iron-induced toxicity and efficient iron administration is a major challenge. Iron overloading tissues can cause oxidative damage that is not intended, while low iron availability can hinder the development of ferroptosis and reduce the effectiveness of treatment. Therefore, the ability of nano-constructs to maintain effective photodynamic reactions and promote robust ferroptosis must be given equal weight with their biocompatibility and tumour selectivity in the rational design of these structures. For ferroptosis-activating PDT techniques to be clinically translated and integrated into precision oncology paradigms, these design issues must be resolved.¹⁰²

2.2.3. Photosensitizer inducing ferroptosis *via* PDT. An iridium(III) complex that uses proton-coupled electron transfer (PCET) to cause strong photoactivated cell killing was created by Jing Chen *et al.* (22). Ferrostatin-1 (Fer-1), a canonical inhibitor of ferroptosis, efficiently inhibits the ferroptosis-like cell death mechanism that 22 activates upon light irradiation. However, conventional iron chelators and ROS scavengers do not affect this mechanism, which points to a nonclassical ferroptotic pathway. Using a polyunsaturated fatty acid model, mechanistic investigations showed that 22 directly stimulates lipid peroxidation (LPO) through a PCET-mediated mechanism. Studies on subcellular localisation revealed that 22 primarily builds up in the ER and mitochondria, where it causes ER stress, LPO buildup, mitochondrial enlargement, and the downregulation of GPX4, a crucial regulator of ferroptosis. Surprisingly, 22 retains its photocytotoxic effectiveness in hypoxic environments, and *in vivo* tests confirmed that it can effectively stop tumour growth when activated by a two-photon laser. To treat hypoxic and drug-resistant tumours, this study presents a unique paradigm in which

photoactivated PCET promotes LPO and ferroptosis-like cell death, independent of both iron and oxygen.¹⁰³

To improve therapeutic efficacy, Yu Pei *et al.* constructed a pH-responsive iridium-ferrocene combination (**23**) that cleverly takes advantage of the features of the TME. **23** dissociates in the acidic lysosomal environment after being internalised by cancer cells, avoiding the quenching of photoinduced electron transfer (PET) and increasing its brightness and photosensitising properties. **23** produces significant amounts of reactive oxygen species (ROS) under light irradiation *via* both type I and type II photodynamic processes. Notably, the complex's Fe^{2+} moiety catalyses Fenton reactions to create hydroxyl radicals ($\cdot\text{OH}$) when there is no light present. The Fe^{3+} produced during this process is then recycled back into Fe^{2+} by GSH-mediated redox cycling. Lipid peroxidation (LPO) and ferroptosis are the results of this enzymatic loop's substantial GSH depletion and ongoing $\cdot\text{OH}$ generation. PDT effectiveness is further increased by oxygen creation during Fenton reactions, which also reduces tumour hypoxia. Both photodynamic and ferroptotic effects are amplified when GSH depletion and TME oxygenation occur together. Studies conducted both *in vitro* and *in vivo* showed that **23** has strong anticancer efficacy and outstanding biocompatibility. All things considered, **23** is a multipurpose theranostic drug that can target lysosomes, activate in response to pH changes, and synergistically increase therapeutic effects, providing a potential method for accurate and successful cancer treatment.¹⁰⁴

Using iridium hydrides, Xinyang Zhao *et al.* (**24**) created a unique iridium(III) complex that is especially designed to trigger ferroptosis by targeting the mitochondria. Given that GPX4 plays a crucial role in controlling ferroptosis, the researchers purposefully included triphenylphosphine as a mitochondria-targeting moiety to improve the complex's transport to the mitochondrial compartment, where GPX4 is mostly found. To increase the complex's cytotoxic effects through ferroptotic pathways, **24**, a ligand that induces ferroptosis, was also added to functionalise it. By dual inhibiting ferroptosis suppressor protein 1 (FSP1) and GPX4, two important negative regulators of ferroptosis, this Ir(III) compound successfully triggered ferroptosis in human fibrosarcoma HT1080 cells. Crucially, the complex also had fluorescent characteristics, which made it possible to follow its intracellular location in real time when excited by visible light (488 nm). This made it a useful tool for theranostic and mechanistic research. Furthermore, the **24** ligand's intrinsic toxicity was greatly decreased by its coordination to the Ir(III) centre, improving the complex's overall biocompatibility and qualifying it for *in vivo* application. This work opens up new possibilities for the development of tailored cancer treatments with integrated diagnostic capabilities by presenting a viable approach for the design of mitochondria-targeted metallodrugs that cause ferroptosis.¹⁰⁵

Xiangdong He *et al.* established a folate receptor-targeted Iridium complex (**25**) for PDT, which consists of three

essential parts: a terminal folic acid ligand for tumour-specific targeting, polyethylene glycol (PEG) for self-assembly and solubility, and a cyclic Ir(III) core. Cellular absorption studies have established that folic acid promotes selective accumulation in tumour cells overexpressing folate receptors, while the PEG moiety allows **25** to create stable, water-soluble nanoparticles. Under 420 nm irradiation, **25** shows a significant $^1\text{O}_2$ quantum yield, causing oxidative stress that manifests as LPO buildup, glutathione (GSH) depletion, and GPX4 downregulation. Ferroptosis is brought on by these alterations taken together. In a mouse tumour xenograft model, the compound showed strong anticancer effects by a hybrid mechanism that combines ferroptosis and apoptosis. **25** is a viable option for clinical PDT applications due to its excellent therapeutic performance, tumour selectivity, and favourable biocompatibility.¹⁰⁶

Lu Zhu *et al.* (**26**) created two chirality-dependent iridium(III) phenyl quinazolinone complexes that inhibit FSP1 to cause ferroptosis in pancreatic cancer cells. Despite their structural similarities, the two enantiomers showed varied PDT responses and significantly differing ferroptosis-inducing capacities. Molecular simulations and proteomic investigations demonstrated that the L-isomer selectively binds to and inhibits metallothionein-1 (MT1), making cancer cells more susceptible to ferroptosis. A series of biological processes, including increased formation of ROS, lipid peroxidation, glutathione depletion, and FSP1 inactivation, were set off by this interaction. The D-isomer, on the other hand, only slightly increased ferroptotic activity. The study showed that the L-isomer may be produced efficiently *via* simple chiral resolution, allowing for precise regulation of ferroptosis in pancreatic cancer cells. The promise of stereoselective ferroptosis inducers for focused and effective pancreatic cancer treatment is highlighted by these findings, which offer a fresh viewpoint on the use of chirality in the creation of metallodrugs.¹⁰⁷

A hydrogen sulphide (H_2S)-responsive iridium(III) complex has been created by Yi Li *et al.* (**27**) as a cancer-selective ferroptosis inducer. Because of its high sensitivity and specificity for intracellular H_2S , **27** can selectively activate H_2S -rich cancer cells and make it easier to distinguish between malignant and healthy tissues *in vitro* and *in vivo* based on H_2S content. The complex primarily builds up in mitochondria, where it intercalates into mitochondrial DNA (mtDNA), seriously damaging it and impairing mitochondrial function. This impact is greatly amplified when exposed to light. Ferroptosis is brought on by **27**-mediated PDT, which produces a lot of ROS and depletes GSH. This results in the buildup of LPO and the downregulation of GPX4. Additionally, the cyclic GMP-AMP synthase-stimulator of interferon genes (cGAS-STING) pathway is activated by substantial mtDNA damage. This leads to ferritinophagy and iron homeostasis disruption, which intensifies ferroptotic cell death in both *in vitro* and *in vivo* scenarios. **27**-mediated PDT mostly affects genes linked to ferroptosis, autophagy, and cancer immunity, according to transcriptomic research using

RNA sequencing. The first cancer-specific small-molecule photosensitizer that can both induce ferroptosis and activate the cGAS–STING pathway is presented in this work, providing a new paradigm for the creation of multipurpose, cancer-selective therapeutic agents that combine immune

modulation and ferroptosis induction for increased anti-cancer efficacy.¹⁰⁸

A cyclometalated Ir(III) complex with a ferrocene moiety (28) was created by Yu-Yi Ling *et al.* This complex acts as a self-amplifying photosensitizer that can catalyse type I and

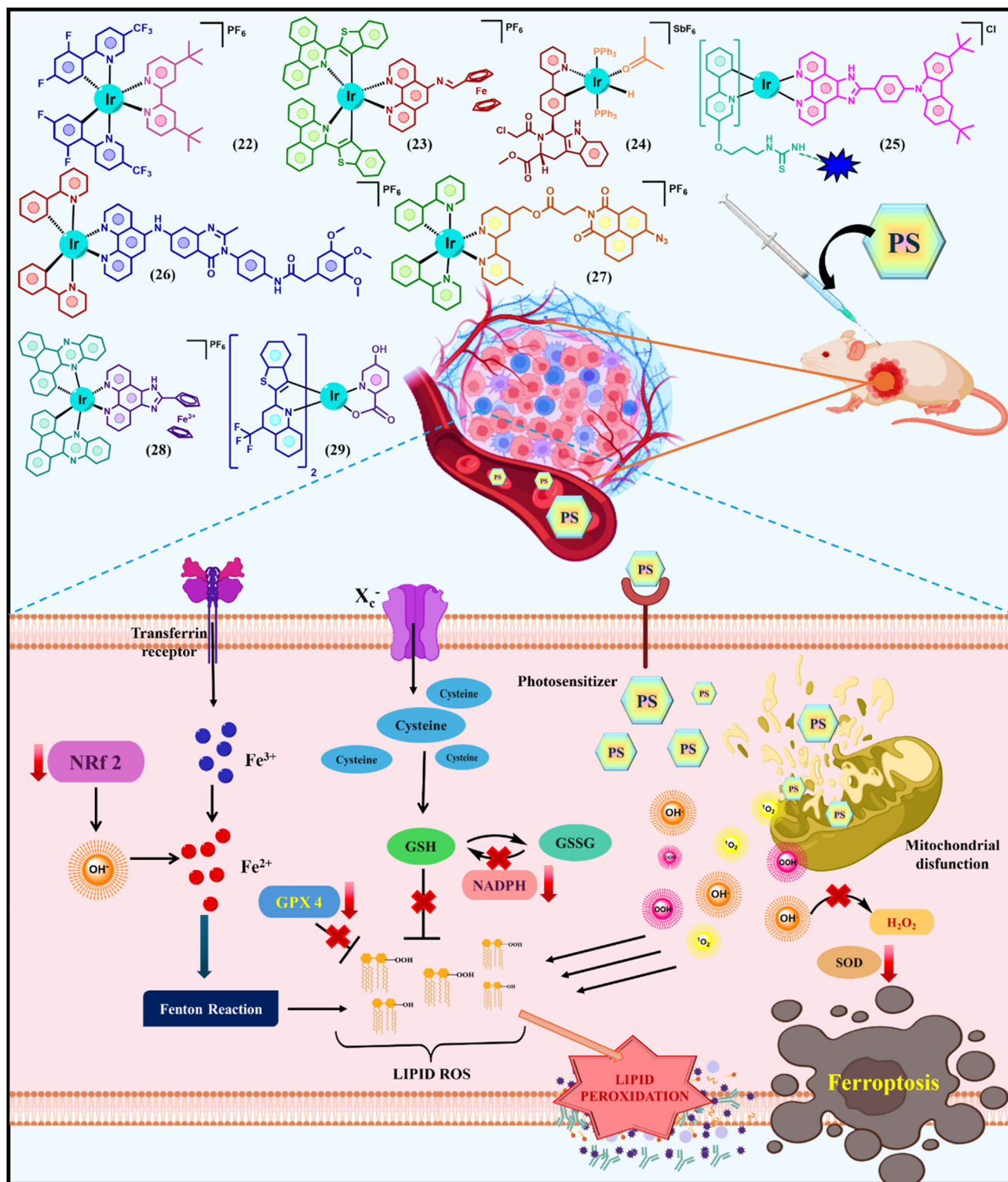


Fig. 4 Illustration explaining the mode of action of photosensitizers for the induction of ferroptosis in cancer cells.

type II PDT processes by producing $\cdot\text{OH}$ and $^1\text{O}_2$. Through a robust association with apotransferrin (Apo-Tf), which is mediated by the overexpression of transferrin receptors (TfR) on MDA-MB-231 breast cancer cells, **28** demonstrates significant selectivity towards these cells. **28** effectively stimulates ferroptosis, lipid peroxidation, and peroxynitrite (ONOO^-) production in both normoxic and hypoxic environments upon light activation. Interestingly, immunogenic cell death (ICD) is also triggered by **28**-induced PDT, which improves ferroptosis-mediated cancer immunotherapy. Further *in vivo* research has shown that **28** can trigger systemic anticancer immune responses by suppressing distant tumours in addition to the main tumour growth. The applicability of complex **28** is restricted by its visible light excitation, which limits tissue penetration despite its encouraging therapeutic profile. The authors suggest methods include using two-photon excitation, adding ligands with extended π -conjugation, or combining upconversion nanomaterials or organic dyes with long-wavelength absorption to get over this restriction. All things considered, this work provides the first instance of a self-amplifying, small-molecule-based photosensitizer that can induce ferroptosis to enhance cancer immunotherapy, providing important information for the development of next-generation photoimmunotherapeutic drugs.¹⁰⁹

Using a logical molecular design approach, Qing Zhang *et al.* designed a PDT agent based on a small-molecule iridium complex (**29**) to increase the production of ROS. They evaluated the capacity of **29** to transmit energy to molecular

oxygen and generate triplet excited states by theoretical calculations, emphasising its favourable energy levels, high molar extinction coefficient, and effective oxidative potential. The photocytotoxicity of **29** was superior to that of traditional iridium-based photosensitisers ($\text{IC}_{50} = 91 \text{ nM}$). Changes in intracellular ROS, GSH, malondialdehyde (MDA), LPO, and MMP further demonstrated that laser-activated **29** causes ferroptosis. Importantly, in order to show *in vitro* and *in vivo* that **29** promotes ferroptosis by decreasing GPX4, the researchers used CRISPR/Cas9-generated GPX4-knockout cells and GPX4-overexpressing cells. Interestingly, **29** also demonstrated strong anti-tumour activity and positive biosafety characteristics. The understanding of the mechanistic functions of photosensitizers based on iridium complexes in PDT is greatly advanced by this work (Fig. 4) (Table 2).¹¹⁰

2.3. Paraptosis

2.3.1. Paraptotic pathways and regulation. Sperandio and colleagues coined the term “paraptosis” in 2000 to describe its unique features. They are “*para*–”, which means “beside” or “alongside”, and “–ptosis”, which means “falling” or “death” and is the same suffix as “apoptosis”. Because “paraptosis” literally means “a form of cell death simultaneous to apoptosis”, it is a distinct type of programmed cell death even if it employs a caspase-independent mechanism.¹¹¹ Paraptosis is a non-apoptotic, caspase-independent kind of controlled cell death that differs

Table 2 Photosensitizers instigating various cell death pathways as cancer phototherapeutics

Sl. no.	Photosensitizer	Cell line	Photo-cytotoxicity	Cell death pathway	Reference
1	22	HeLa	$1.18 \pm 0.51 \mu\text{M}$	Ferroptosis	103
2	23	4 T1	<90%		104
3	24	HT1080	$7.48 \mu\text{M}$		105
4	25	HeLa	$12.66 \pm 0.25 \mu\text{M}$		106
5	26	PANC-1	$2.70 \pm 0.11 \mu\text{M}$		107
6	27	HeLa	$1.45 \pm 0.22 \mu\text{M}$		108
7	28	MDA-MB-231	$0.05 \pm 0.03 \mu\text{M}$		109
8	29	4 T1	91 nM		110
9	30	A549	$0.93 \pm 0.1 \mu\text{M}$	Paraptosis	118
10	31	HepG2	$1.6 \mu\text{M}$		119
11	32	MCF-7	$0.86 \mu\text{M}$		120
12	33	Jurkat cells	$7\text{--}16 \mu\text{M}$		121
13	34	Jurkat cells	$0.4\text{--}7.2 \mu\text{M}$	Pyroptosis	122
14	35	Jurkat cells	$8.8\text{--}18 \mu\text{M}$		123
15	36	MDA-MB-231	$4.6 \pm 0.13 \mu\text{M}$		134
16	37	MDA-MB-231	$0.1 \pm 0.06 \mu\text{M}$		135
17	38	U14	$1.9 \pm 0.3 \mu\text{M}$		136
18	39	4 T1	$7.1 \mu\text{M}$		137
19	40	MDA-MB-231	$0.0200 \pm 0.0006 \mu\text{M}$	Necroptosis	138
20	41	A549	$0.48 \mu\text{M}$		150
21	42	BEL-7402	$0.47 \pm 0.11 \mu\text{M}$		151
22	43	MV4- 11	$1.69 \pm 0.23 \mu\text{M}$		152
23	44	A549	$1.94 \pm 0.14 \mu\text{M}$	Autophagy	153
24	45	A549R	$2.2 \pm 0.2 \mu\text{M}$		154
25	46	A549	$5.6 \pm 0.4 \mu\text{M}$		163
26	47	HeLa	$0.636 \mu\text{M}$		164
27	48	A549	$0.7 \mu\text{M}$		165
28	49	EMT6	$0.6 \mu\text{M}$		166

from necrosis and apoptosis due to its distinct morphological and molecular characteristics. Unlike apoptosis, paraptosis does not exhibit the characteristics of DNA breakage, chromatin condensation, or apoptotic body formation. Instead, its most distinctive features are the lack of membrane blebbing, the progressive growth of the mitochondria and ER, and the notable cytoplasmic vacuolization. The non-acidic vacuoles produced during paraptosis have nothing to do with autophagic or lysosomal activity. They are mostly caused by the distension of the ER and, to a lesser degree, by the enlargement of the mitochondria.¹¹²

Paraptosis may be brought on by several events, including the activation of insulin-like growth factor receptor I (IGF-IR), the administration of particular phytochemicals (such as celastrol or curcumin), proteasome inhibitors, and medications that cause ER stress. Paraptosis is significantly influenced by mitogen-activated protein kinase (MAPK) signalling pathways, such as the JNK and ERK1/2 pathways. These signalling pathways allow both increased protein synthesis and ER stress, both of which are critical for vacuole development. Although cycloheximide and other inhibitors can halt the process, paraptosis also necessitates continuous protein translation, indicating a dependence on newly synthesised proteins that may accumulate and strain the ER.¹¹³

Mitochondrial dysfunction, including increased production of ROS and loss of MOMP, also affects how paraptosis is executed. Importantly, paraptosis is mechanically independent of apoptosis, as evidenced by the fact that it is not suppressed by pan-caspase inhibitors or conventional anti-apoptotic proteins like Bcl-2. The biological importance of paraptosis includes possible roles in neurological disorders and tumour suppression. It is particularly interesting in cancer therapy because it offers a mechanism to destroy cells that are resistant to apoptosis by initiating a distinct and irreversible death process.¹¹⁴

2.3.2. Paraptotic pathways induction through photodynamic therapy. Although it has long been believed that PDT primarily causes cell death by apoptosis, there is growing evidence that PDT can also cause other, non-apoptotic processes, like paraptosis. Paraptosis is a distinct kind of programmed cell death characterised by extensive cytoplasmic vacuolization, endoplasmic reticulum (ER) dilatation, mitochondrial swelling, and the absence of caspase activation, DNA breakage, or chromatin condensation.¹¹⁵

ROS-mediated oxidative stress, which jeopardises the structural and functional integrity of the mitochondria and the ER, is the primary mechanism by which PDT may induce paraptosis. The accumulation of unfolded or misfolded proteins in the ER causes ROS-induced ER stress and unfolded protein response (UPR) activation. When this stress surpasses the adaptive capacity of the cell, it results in ER dilatation and vacuole formation, which are characteristics of paraptosis. At the same time, mitochondrial dysfunction,

which is marked by swelling and loss of membrane potential, exacerbates cellular stress and promotes paraptosis. Since paraptosis does not include caspase activation and is not inhibited by anti-apoptotic proteins such as Bcl-2 or pan-caspase inhibitors, it is mechanistically distinct from apoptotic cell death.¹¹⁶

Furthermore, PDT-induced paraptosis requires ongoing protein synthesis, as seen by the inhibitory effects of translational blockers such as cycloheximide. A role in controlling stress responses and promoting vacuolization has also been suggested by the involvement of MAPK signalling pathways, specifically ERK1/2 and JNK. Importantly, PDT has a therapeutic advantage in treating cancers that are resistant to apoptosis because of its ability to induce paraptosis. PDT interacts with multiple cell death mechanisms, including paraptosis, to increase the overall efficacy of cancer treatments and offers a practical method for avoiding apoptotic resistance in malignant cells.¹¹⁷

2.3.3. Photosensitizer inducing paraptosis via PDT. Four new cyclometalated phosphorescent Ir(III) complexes were synthesized by Liang He *et al.* (30). These complexes display outstanding photophysical properties, including high luminescence quantum yields, long phosphorescence lifetimes, and two-photon excited phosphorescence. They display potent anticancer activity against human cancer cell lines tested. Cell imaging and ICP MS results show that they are preferentially accumulated in the mitochondria, probably due to their positive charge and lipophilicity. Anticancer mechanisms studies show that 30 possesses an entirely different mode of action from cisplatin. 30 induces mitochondria-derived cytoplasmic vacuolation associated with caspase-independent paraptotic cell death. 30 affects the UPS and MAPK signaling pathways, both of which have been reported to be associated with paraptosis. The complex disrupts the physiological functions of mitochondria severely and quickly, which are indicated by the loss of mitochondrial membrane potential, reduction of cellular ATP production, mitochondrial respiration inhibition, and ROS elevation. The severe and rapid damage to mitochondria and the UPS results in the collapse of mitochondria and the subsequent cytoplasmic vacuolation before the cells are ready to start the mechanisms of apoptosis and/or autophagy. ROS inhibition assays further confirm that increased mitochondrial superoxide has a critical role in 30-induced cell death. *In vivo* studies have demonstrated the anticancer efficacy of 30. Overall, this work has identified caspase-independent non-apoptotic paraptosis as the major mode of cell death caused by 30, which is unique and may have potential in cancer treatment. Furthermore, this work also gives useful insights into the design and anticancer mechanisms of new metal-based anticancer agents.¹¹⁸

Immunotherapy has emerged as a highly effective strategy for cancer treatment by harnessing the innate immune system to selectively recognize and eliminate malignant cells while sparing normal tissues. Jiaxin Liao *et al.* designed and synthesized three novel cyclometalated iridium(III) complexes

and assessed for their antitumor properties (31). Upon co-incubation with HepG2 cells, 31 was found to accumulate in lysosomes, where it triggered paraptotic cell death and induced endoplasmic reticulum (ER) stress. Notably, 31 also elicited immunogenic cell death (ICD), which facilitated dendritic cell maturation, thereby enhancing the recruitment of effector T cells to tumor sites. Additionally, 31 downregulated the presence of immunosuppressive regulatory T cells within the tumor microenvironment and stimulated systemic antitumor immune responses. To date, 31 represents the first documented iridium(III)-based complex capable of inducing paraptosis while concurrently promoting tumor cell ICD. Importantly, 31 achieved this without altering cell cycle progression or elevating ROS levels in HepG2 cells.¹¹⁹

Six mononuclear Ir complexes using polypyridyl pyrazine-based ligands and $\{[cp^*IrCl(\mu Cl)]_2$ and $[(ppy)_2Ir(\mu Cl)]_2\}$ precursors have been synthesised and characterised by Tripathy *et al.* (32). The complexes have shown potent anticancer activity against various human cancer cell lines (MCF7, LNCap, Ishikawa, DU145, PC3, and SKOV3) while one of the complexes is found to be inactive. Flow cytometry studies have established cellular accumulation of the complexes the highest in 32, which is in accordance with their observed cytotoxicity. No changes in the expression of PARP, Caspase 9, and Beclin1, Atg12, discard apoptosis and autophagy, respectively. Overexpression of CHOP, activation of MAPKs (P38, JNK, and ERK), and massive cytoplasmic vacuolisation collectively suggest a paraptotic mode of cell death induced by proteasomal dysfunction as well as endoplasmic reticulum and mitochondrial stress. An intimate relationship between p53, ROS production, and the extent of cell death has also been established using p53 wild, null, and mutant type cancer cells.¹²⁰

K. Yokoi *et al.* reported the design and synthesis of a green-emitting iridium complex-peptide hybrid (33), which has an electron-donating hydroxy acetic acid (glycolic acid) moiety between the Ir core and the peptide part. It was found that 33 is selectively cytotoxic against cancer cells, and the dead cells showed a green emission. Mechanistic studies of cell death indicate that 33 induces a paraptosis-like cell death through the increase in mitochondrial Ca^{2+} concentrations *via* direct Ca^{2+} transfer from ER to mitochondria, the loss of mitochondrial membrane potential ($\Delta\Psi_m$), and the vacuolization of cytoplasm and intracellular organelles. Although typical paraptosis and/or autophagy markers were upregulated by 33 through the MAPK signalling pathway, as confirmed by Western blot analysis, autophagy is not the main pathway in 33-induced cell death. The degradation of actin, which consists of a cytoskeleton, is also induced by high concentrations of Ca^{2+} , as evidenced by co-staining experiments using a specific probe.¹²¹

The same group further described that (34), an inhibitor of a mitochondrial sodium (Na^+)/ Ca^{2+} exchanger, induces paraptosis in Jurkat cells *via* intracellular pathways similar to those induced by 33. The findings allow us to suggest that

the induction of paraptosis by 33 and 34 is associated with membrane fusion between mitochondria and the ER, subsequent Ca^{2+} influx from the ER to mitochondria, and a decrease in the mitochondrial membrane potential ($\Delta\Psi_m$). On the contrary, celastrol, a naturally occurring triterpenoid that had been reported as a paraptosis inducer in cancer cells, negligibly induces mitochondria-ER membrane fusion. Consequently, we conclude that the paraptosis induced by 33 and 34 (termed as “paraptosis II” by the group) proceeds *via* a signalling pathway different from that of the previously known paraptosis induced by celastrol, a process that negligibly involves membrane fusion between mitochondria and the ER (termed as “paraptosis I” by the group).¹²²

Once again, the same group conducted a detailed mechanistic study of cell death induced by (35), a typical example of iridium complex-peptide hybrids, and describe how 35 induces paraptotic programmed cell death like that of celastrol, a naturally occurring triterpenoid that is known to function as a paraptosis inducer in cancer cells. It is suggested that 35 (50 μM) induces ER stress and decreases the mitochondrial membrane potential ($\Delta\Psi_m$), thus triggering intracellular signalling pathways and resulting in cytoplasmic vacuolization in Jurkat cells (which is a typical phenomenon of paraptosis), while the change in $\Delta\Psi_m$ values is negligibly induced by celastrol and curcumin. Other experimental data imply that both 35 and celastrol induce paraptotic cell death in Jurkat cells, but this induction occurs *via* different signalling pathways (Fig. 5) (Table 2).¹²³

3. Inflammation-regulated programmed cell death pathways

3.1. Pyroptosis

3.1.1. Pyroptotic pathways and regulation. A unique, pro-inflammatory type of controlled cell death, pyroptosis, was first discovered in *Shigella flexneri*-infected macrophages and then in response to *Salmonella typhimurium*.¹²⁴ Over time, pyroptosis has been linked to a variety of clinical situations, such as ischaemic stroke, myocardial infarction, microbial infections, and different phases of cancer development. Numerous terms, including pyronecrosis, gasdermin-dependent cell death, and caspase-1-dependent cell death, have been used to describe this type of cell death.¹²⁵ However, the Nomenclature Committee on Cell Death has officially recognised the term “pyroptosis”, which was created by Cookson and Brennan in 2001 and is derived from the Greek words “pyro”, which means fire or fever, and “ptosis”, which means falling.¹²⁶

Although it shares some characteristics with both necrosis and apoptosis, pyroptosis is distinguished from both by a combination of morphological and biochemical characteristics. At first, pyroptotic cells show signs of death, including chromatin condensation and DNA fragmentation. But these are followed by events that resemble necrosis, such as swelling of the cells, rupture of the membrane, and the consequent release of intracellular pro-inflammatory

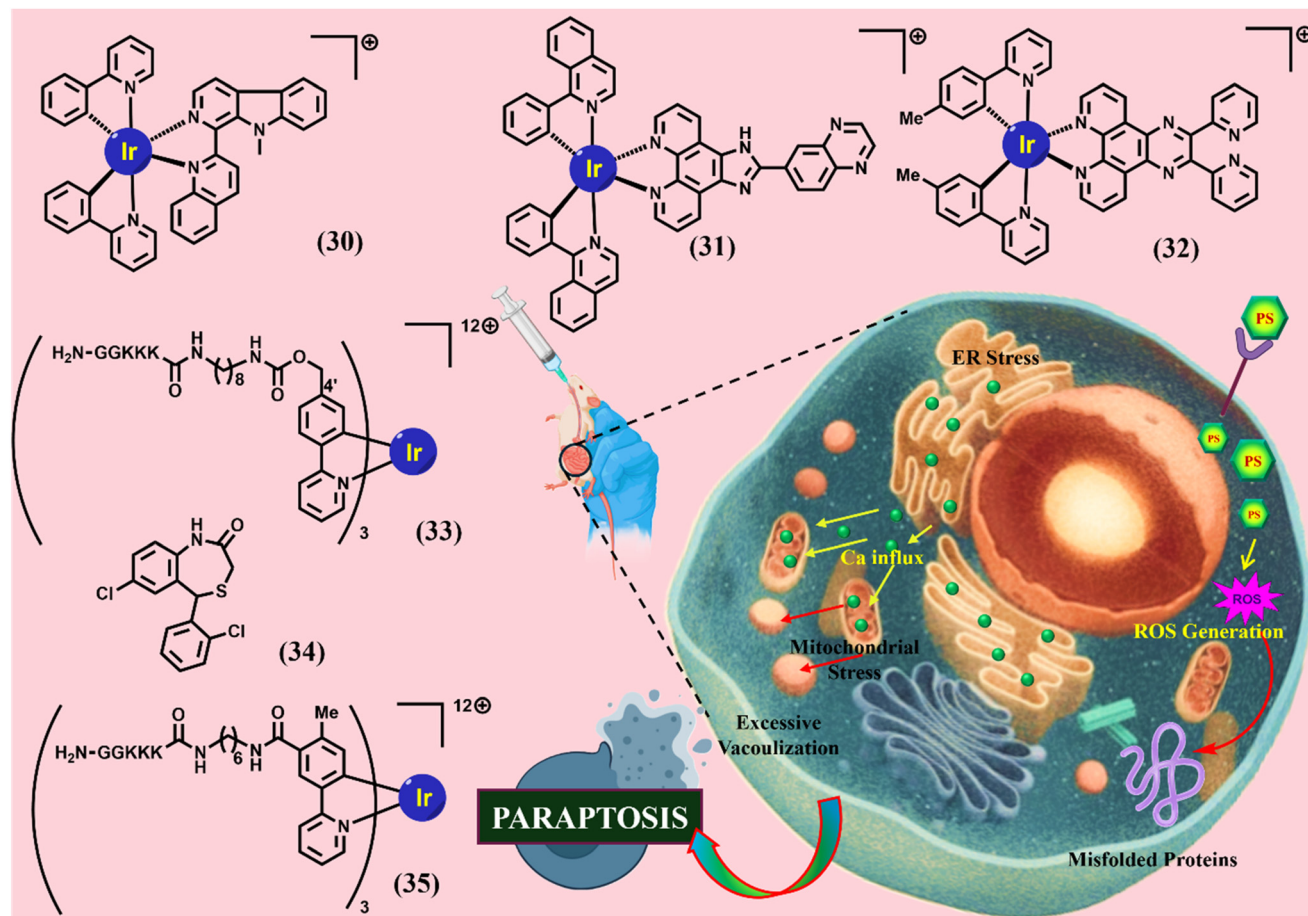


Fig. 5 A graphical representation of how photosensitizers work to cause cancer cells to undergo paraptosis.

substances such as cytokines and DAMPs. Mechanistically, the activation of inflammatory caspases—most notably caspase-1, but also human caspases 4 and 5 and mouse caspase 11—is strongly linked to pyroptosis.¹²⁷ Usually, the formation of multiprotein complexes called inflammasomes, which comprise adaptor proteins like ASC (apoptosis-associated speck-like protein containing a CARD domain) and sensor proteins like NOD-like receptors (NLRP3, NLRC4), AIM2, and Pyrin, activates these caspases. Caspases-1 trigger strong inflammatory reactions by cleaving pro-IL-1 β and pro-IL-18 into their mature, secretory forms when they are activated. The gasdermin family of proteins, especially gasdermin D (GSDMD), is a crucial pyroptotic executor. When the N-terminal segment of GSDMD is broken down by inflammatory caspases, it moves to the plasma membrane, where it oligomerizes and creates big, non-selective holes. By upsetting ionic gradients and allowing water to enter, these pores cause cellular lysis and swelling, which releases DAMPs and inflammatory cytokines into the extracellular environment.¹²⁸

Pyroptosis can occur through a non-canonical pathway in addition to the canonical pathway driven by caspase-1. In this route, cytosolic lipopolysaccharides (LPS) from Gram-negative bacterial infections directly activate caspase-4 and -5 (in

humans) or caspase-11 (in mice). GSDMD is also cleaved by these caspases, which promotes pore formation and cell death. Crucially, either directly or by activating secondary caspase-1, this mechanism also aids in the development of IL-1 β and IL-18. Apoptotic caspase-3 and its association with gasdermin E (GSDME) constitute a third pathway. Cells expressing this gasdermin isoform undergo pyroptosis when caspase-3 cleaves GSDME under specific stressors. A point of confluence between apoptotic and pyroptotic pathways is highlighted by the caspase-3/GSDME axis, which is becoming more widely acknowledged as being important in chemotherapy-induced cancer cell death.¹²⁹

In conclusion, pyroptosis is a complex and strictly controlled type of cell death that plays a vital role in the interaction between inflammation and innate immunity. Its distinctive characteristics—rupturing the plasma membrane, releasing inflammatory cytokines, and engaging gasdermin proteins—highlight its possible significance in immunogenic cell death, especially in cancer treatment. In the context of infectious disease, cancer, and inflammatory disorders, a better knowledge of the molecular regulators of pyroptosis may open the door to new therapeutic approaches that utilise or alter this process.¹³⁰

3.1.2. Pyroptotic pathways induction through photodynamic therapy. Novel membrane-anchored photosensitisers (PSs) with aggregation-induced emission capabilities, such as TBD-3C, have been developed recently in PDT. These PSs efficiently induce apoptosis and pyroptosis, with pyroptosis being the primary effect, in a variety of cancer cell lines, including 4 T1, HeLa, and C6. ROS-mediated caspase-1 activation, GSDMD cleavage, and the production of pro-inflammatory cytokines IL-1 β and IL-18 are the hallmarks of this cell death.¹³¹ Similarly, pyroptosis in HepG2 cells has been demonstrated to be triggered by curcumin-loaded PLGA microbubbles in sono-PDT. A non-canonical pyroptosis mechanism, including downregulation of pyruvate kinase M2 (PKM2), activation of caspase-8 and -3, and GSDME cleavage, was discovered through mechanistic studies of PDT utilising 5-ALA, protoporphyrin IX dimethyl ester, and chlorin e6 in esophageal squamous carcinoma cells. Pyroptosis was inhibited by overexpression of PKM2, indicating that it may be a therapeutic target to improve the effectiveness of PDT.¹³²

Pyroptosis is still not well understood in PDT, despite its importance. There is good reason to look at pyroptosis as a powerful and immunogenic cell death pathway in tumours treated with PDT, since ROS plays a key role in both PDT and pyroptotic signalling. Although PDT-induced inflammation is advantageous for immune activation, it must be carefully controlled because too much cytokine synthesis, including IL-1 β , might have detrimental effects. To keep this balance, the light dose and PS concentration must be optimised. All things considered, pyroptosis presents a viable path to improve PDT's immunological and therapeutic effectiveness, especially in malignancies that are resistant. The molecular regulators of this process and their potential in combination therapy should be better defined in future studies.¹³³

3.1.3. Photosensitizer inducing pyroptosis via PDT. Recent developments in the realm of photoactive metal complexes have demonstrated their exceptional ability to combine immune activation and direct photodynamic tumour death through intricately coordinated mechanistic pathways, especially by triggering innate immune signalling and pyroptosis. By creating a cholic acid-modified iridium(III) photosensitiser (36) that preferentially localised in the endoplasmic reticulum (ER), Yun-Shi Zhi *et al.* initially brought attention to this potential. Complex 36 experienced effective intersystem crossing at the Ir(III) centre upon light irradiation, producing type I and type II ROS. The overabundance of ROS disrupted ER homeostasis, causing ER stress and GSDME cleavage-mediated pyroptotic cell death. Simultaneously, the complex caused the release of extracellular HMGB1, ATP secretion, and exposure to calreticulin (CRT), which are examples of traditional damage-associated molecular patterns (DAMPs). These signals were essential for antigen presentation and dendritic cell maturation, which allowed for T cell activation and the *in vivo* destruction of primary and metastatic tumours.¹³⁴

This strategy was furthered by Bin-Fa Liang *et al.* with cholic acid-modified ruthenium(II) complexes (37), which had the same ER-targeting ability but, for theranostics, an unusual combination of singlet oxygen (¹O₂) production and near-infrared aggregation-induced emission (AIE) phosphorescence. By activating the cyclic GMP-AMP synthase-stimulator of interferon genes (cGAS-STING) pathway, ROS-mediated ER disruption by 37 mechanistically triggered the phosphorylation of TBK1 and IRF3, which in turn triggered the release of cytokines and type I interferon. This cascade produced strong *in vivo* antitumor immunity with an extraordinarily high phototoxicity index (PI = 83.3) by reinforcing pyroptosis and amplifying innate immune signalling. When combined, these investigations show that ER stress and ROS overproduction are important upstream triggers; however, the Ru(II) systems took use of STING-mediated immune amplification, whereas the Ir(III) complexes focused on DAMP-driven ICD.¹³⁵

Going beyond Ir and Ru, Yu-Yi Ling *et al.* created Pt-based photosensitisers (38), which were intended to be the initial photoactivators of the cGAS-STING pathway. These Pt complexes, in contrast to ER-focused approaches, caused photoirradiation-induced damage to nuclear and mitochondrial DNA as well as the nuclear envelope. Cytosolic DNA fragments released by such genotoxic stress directly activated the cGAS enzyme, resulting in cyclic GMP-AMP (cGAMP) and initiating downstream STING signalling. Innate immune sensing and immunogenic lytic death were integrated at the same time that ROS buildup and DNA damage caused pyroptotic cell death. Crucially, this dual method not only destroyed cancer cells but also enhanced robust adaptive immune responses, demonstrating that nuclear and mitochondrial targeting is a different but no less successful way to activate photo-immunotherapeutic immunity.¹³⁶

In conjunction with this DNA-targeting strategy, Min Wu *et al.* developed AIE-based photosensitisers (39-PSs) coupled with cationic chains for membrane anchoring, which they presented as a plasma membrane-centred approach. These PSs produced ROS at the plasma membrane upon activation by light, causing pyroptotic rupture, lipid peroxidation, and integrity loss. Finding a correlation between the degree of pyroptosis and the strength of membrane anchoring was a significant mechanistic discovery, indicating that subcellular localisation plays a crucial role in determining the mode of cell death. The range of photo-induced pyroptosis-based interventions was increased by this non-invasive, membrane-targeted PDT technique, which provided precise spatiotemporal control and minimal side effects, in contrast to conventional chemotherapeutic inducers of pyroptosis, which frequently face resistance and systemic toxicity.¹³⁷

By using a CAIX-anchored rhenium(I) photosensitiser, Xuxian Su *et al.* presented a hypoxia-adapted design, further enhancing the mechanistic diversity (40). Complex 40 showed effective tumour-specific accumulation by binding carbonic anhydrase IX, which is overexpressed in hypoxic tumour

careful regulation of metal complex localisation, ROS type, and immune signalling pathways might determine not only cytotoxicity but also the strength and calibre of anticancer immune responses, according to these complementary mechanistic discoveries. Together, they provide a comprehensive framework for logically creating photoactive metal complexes that combine strong immunogenic regulation with tumour killing.

3.2.1. Necroptotic pathways and regulation. A caspase-independent, non-apoptotic mechanism of programmed cell death that physically mimics classical necrosis, necroptosis is a controlled form of necrotic cell death that was initially identified by Junying Yuan in 2005. Necroptosis has been thoroughly described since its discovery and is now officially acknowledged in the Nomenclature on Cell Death, indicating its importance as a legitimate mechanism leading to PCD. Necroptosis is mediated by a specific collection of signalling proteins and follows a genetically regulated process, in contrast to accidental necrosis.¹³⁹

Necroptosis can be initiated by a variety of upstream signals. These include activation of cell surface death receptors such as tumor necrosis factor receptor 1 (TNFR1),

The figure displays four chemical structures (36-39) and a schematic of pyroptosis signaling pathways.

Chemical Structures:

- (36)** An Iridium (Ir) complex with a terpyridine-like ligand and a steroid derivative.
- (37)** A Ruthenium (Ru) complex with a terpyridine-like ligand and a steroid derivative.
- (38)** A Platinum (Pt) complex with a terpyridine-like ligand and a steroid derivative.
- (39)** A complex molecule featuring a triazine ring, a nitrile group, and a steroid derivative.

Pyroptosis Schematic:

The diagram illustrates the signaling pathways leading to pyroptosis, a form of programmed cell death. Key components include:

- Cell Membrane:** The outer boundary of the cell, showing phospholipids (PS) and receptors (TNFR).
- TNF Signaling:** Tumor Necrosis Factor (TNF) binds to its receptor (TNFR), activating the pathway.
- Caspase Activation:** Caspase 1, Caspase 8, Caspase 3, and Caspase 9 are shown as key enzymes in the pathway.
- Mitochondrial Disfunction:** Cytochrome C release from the mitochondria is shown, leading to ROS production.
- GSDMD and GSDME:** These proteins are involved in the execution of pyroptosis, leading to cell lysis.
- Alarmins:** These molecules are released from the cell, signaling to neighboring cells.
- ATP and HMGB1:** These molecules are released from the cell, further signaling to neighboring cells.
- IL-18 and IL-1β:** These cytokines are released from the cell, further signaling to neighboring cells.

Fig. 6 Schematic representation of pyroptosis induction by photosensitizers.

death receptors DR4 and DR5, and FAS; pattern recognition receptors (PRRs) including Toll-like receptors 3 and 4 (TLR3 and TLR4); and cytosolic nucleic acid sensors such as Z-DNA binding protein 1 (ZBP1). Upon stimulation, these pathways converge to initiate the formation of the necrosome complex, a signaling platform involving receptor-interacting serine/threonine-protein kinase 1 (RIPK1) and RIPK3. Subsequent phosphorylation of mixed lineage kinase domain-like pseudokinase (MLKL) by RIPK3 leads to MLKL oligomerization and translocation to the plasma membrane, where it disrupts membrane integrity by forming large pores (>200 nm), culminating in cell lysis and release of intracellular contents.¹⁴⁰

Necroptotic cells differ from apoptotic cells in their morphological characteristics. These include mild chromatin condensation, early loss of plasma membrane integrity, and swelling of cells and organelles (oncosis). Notably, apoptotic characteristics, including caspase activation, internucleosomal DNA cleavage, and nuclear fragmentation, are absent in necroptosis. Necroptotic cells have been further characterised by nano-topographical studies, which demonstrate that they swell and separate from their substrate rather than shrinking like apoptotic cells do. The cytoskeletal structure initially stays intact during early necroptosis, but cellular flexibility eventually decreases. This could be a mechanobiological indicator of the advancement of necroptosis.¹⁴¹

The RIPK1-RIPK3-MLKL signalling axis must be activated for necroptosis to be performed. Clarifying the processes of this system has been made possible by pharmacological inhibitors that target important elements of it. Necrostatin-1 s (Nec-1 s) can inhibit RIPK1, GSK-872 can inhibit RIPK3, and necrosulfonamide (which works well in human cells) can inhibit MLKL. Crucially, pan-caspase inhibitors like zVAD-fmk, which stop apoptosis, do not affect necroptotic cell death because necroptosis is resistant to caspase inhibition. Indeed, by blocking the caspase-8-mediated checkpoint that typically inhibits the formation of the RIPK1-RIPK3 complex, zVAD-fmk-induced caspase-8 suppression can make cells more susceptible to necroptosis.¹⁴²

To perform necroptosis, the RIPK1-RIPK3-MLKL signalling axis needs to be triggered. Pharmacological inhibitors that target key components of this system have made it possible to clarify its functions. Necrostatin-1 s (Nec-1 s) can inhibit RIPK1, GSK-872 can inhibit RIPK3, and MLKL can be inhibited by necrosulfonamide, which is effective in human cells. Importantly, because necroptosis is resistant to caspase inhibition, pan-caspase inhibitors such as zVAD-fmk, which prevent apoptosis, do not affect necroptotic cell death. ZVAD-fmk-induced caspase-8 suppression can increase a cell's susceptibility to necroptosis by disrupting the caspase-8-mediated checkpoint that normally prevents the formation of the RIPK1-RIPK3 complex.¹⁴³

Nonetheless, necroptosis might have dualistic immunological effects that vary depending on the situation.

By encouraging tumour shrinkage and immunological activation, necroptosis may be a therapeutic ally; nevertheless, it may also have unanticipated pro-tumorigenic consequences. The pro-inflammatory tumour microenvironment (TME) may be facilitated by the enormous and uncontrollable production of cytokines and DAMPs during necroptosis. Thus, immune evasion, angiogenesis, and metastasis may be facilitated by the recruitment of immunosuppressive cells like tumor-associated macrophages (TAMs) and myeloid-derived suppressor cells (MDSCs). Furthermore, through the paracrine effects of released cytokines, necroptotic signalling has been linked to promoting the growth of cancer cells that are still alive.¹⁴⁴

Thus, necroptosis presents a promising approach to overcome resistance to traditional apoptosis-inducing therapies, such as chemotherapy, radiation, cancer vaccines, and oncolytic virotherapy; however, its application in clinical oncology necessitates a sophisticated comprehension of the immune milieu and tumour context. The secret to using this route for efficient and immunogenic cancer treatment may lie in the capacity to reduce pro-tumorigenic inflammation while selectively inducing necroptosis in tumour cells.¹⁴⁵

3.2.2. Necroptotic pathways induction through photodynamic therapy. In a groundbreaking study, Coupienne *et al.* examined the effects of 5-aminolevulinic acid (5-ALA)-based PDT on human glioblastoma LN18 cells, establishing the ability of PDT to cause necroptosis. According to their research, PDT's therapeutic effects, which were mediated by the generation of singlet oxygen, caused a necroptotic pathway that was reliant on receptor-interacting protein kinase 3 (RIPK3) to light up. Notably, RIPK1 and RIPK3 were shown to cluster in an unusual necrosome complex that did not contain the traditional necrosome components FADD and caspase-8, indicating a mechanism of cell death that is not dependent on caspase. Traditionally linked to apoptotic or necrotic results, this observation suggests that, in certain circumstances, it may also initiate controlled necrotic pathways like necroptosis.^{27,146}

The type of tumour being targeted, the type and concentration of the PS, and the light exposure parameters all seem to have a complex impact on the likelihood that PDT may cause necroptosis. These factors have the ability to alter not only the kind of ROS produced but also where they are found inside cells and the signalling pathways that lead to cell death.¹⁴⁷

For example, apoptosis was the main cause of cell death in studies assessing hypoxia-mediated PDT in both *in vitro* and *in vivo* models of osteosarcoma, such as human HOS cell lines and murine DLM-8. However, autophagy was triggered as an adaptive survival response when lower concentrations of the photosensitiser were applied, particularly in human osteosarcoma cells. This autophagy seems to reduce cytotoxic stress, indicating a defence mechanism that could affect resistance to treatment. Interestingly, hiporfin-PDT also enhanced RIPK1 expression in DLM-8 murine osteosarcoma

cells, and necrostatin-1, a selective RIPK1 inhibitor, was able to lessen the cytotoxic effects. This demonstrated the co-activation or shift towards necroptosis under particular microenvironmental conditions and PS concentrations. Similarly, it has been demonstrated that the amount of photosensitizer affects how glioblastoma cells react to PDT. Low doses of talaporfin sodium (mono-L-aspartyl chlorine e6, or NPe6) activated necroptosis in T98G glioblastoma cells, but greater quantities of the same molecule caused a type of necrosis that was not identifiable by necroptotic markers. The notion that the predominate mechanism of cell death can be changed by precisely adjusting PDT settings is supported by this dose-dependent dichotomy.¹⁴⁸

Studies using nanomaterial-assisted PDT provide more proof. For instance, in the absence of photoactivation, modest concentrations of nitrogen-doped titanium dioxide (N-TiO₂) nanoparticles caused human melanoma A375 cells to undergo a non-toxic autophagic response. Autophagy was successfully suppressed in response to light-induced ROS formation, though, and a transition towards RIPK1-mediated necroptosis was noted, along with the release of HMGB1, a recognised indicator of immunogenic cell death. This illustrates how increased oxidative stress can direct the cell towards controlled necrosis by overriding cytoprotective mechanisms like autophagy. Taken together, these studies collectively highlight that necroptosis is a context-dependent response to PDT, influenced by multiple interrelated factors including photosensitizer type and dose, cell type, and light energy. The balance between autophagy, apoptosis, necroptosis, and unregulated necrosis is delicately modulated by the intracellular oxidative environment established during PDT. Understanding these nuances not only provides insight into the mechanistic complexity of PDT-induced cell death but also opens avenues for optimizing therapeutic strategies to exploit necroptosis as a means of overcoming resistance to conventional apoptotic cell death in cancer therapy.¹⁴⁹

3.2.3. Photosensitizer inducing necroptosis via PDT. Two iridium(III) complexes created by Ruilin Guan *et al.* aim to cause necroptosis in cisplatin-resistant lung cancer cells (A549R) (**41**). These complexes aggregated specifically in mitochondria, causing MMP disturbance and oxidative stress. Annexin V/propidium iodide co-staining and western blot analysis, which showed the activation of RIPK3 and MLKL, were used to corroborate the induction of necroptosis. Their method of action was further confirmed by additional necroptotic indicators, including lactate dehydrogenase (LDH) release and extracellular calcium influx. Notably, **41** also interfered with the development of the cell cycle, causing arrest at the G0/G1 phase by the downregulation of several cell cycle regulators, including cyclins A2 and D2, CDK1, CDK2, CDK4, and CDK6. The two mechanisms, which include inducing necroptosis and inhibiting the cell cycle, demonstrate the potential of **41** as potent therapeutic candidates for the treatment of drug-resistant cancers.¹⁵⁰

Wenjuan Li *et al.* changed the structure of cyclometalated Ir(III) dimers and modified the hydrogen atom(s) at the N-3 position to create a variety of Ir(III) complexes based on 2-hydroxy-1-naphthaldehyde thiosemicarbazone ligands (**42**). They discovered a lead chemical, **42**, that demonstrated both strong fluorescence and great cytotoxicity against cancer cells after methodically examining their structure-activity and structure-fluorescence correlations. *In vivo*, **42** effectively suppressed tumour growth and spread, showed selective mitochondrial targeting, and was able to overcome cisplatin resistance. According to mechanistic investigations, **42** acted on many elements of the tumour microenvironment (TME) to produce its anticancer effects. This included inducing necroptosis in liver cancer cells and triggering immune responses linked to necroptosis.¹⁵¹

Eva Řezníčková *et al.* (**43**) created a dinuclear complex that outperformed its mononuclear counterpart in terms of cytotoxicity against a variety of human cancer cell lines, with GI₅₀ values ranging from 1.7 to 3.0 µM. Notably, it was discovered that **43** stimulated the MV4-11 acute myeloid leukaemia cells' Keap1/Nrf2 oxidative stress response system. **43** had NADH-oxidising activity in solution, as demonstrated by ¹H NMR spectroscopy, confirming its redox-based mode of action. In contrast, NAD⁺ was unaffected when formate was used as the hydride donor. Remarkably, this NADH oxidation was considerably inhibited by the presence of endogenous reductants, including ascorbate and reduced glutathione. In line with these *in vitro* results, **43** treatments of MV4-11 cells resulted in intracellular oxidation of NADH and a simultaneous decrease in NAD⁺ levels, which led to a significant depletion of both NADH and NAD⁺. These findings provide important new information on the redox-driven metabolic pathways that catalytic anticancer drugs use to cause cytotoxicity.¹⁵²

Two new unsymmetrical Ir(III) complexes were created by Lina Xie *et al.* (**44**); these compounds could potentially be used as chemotherapeutic agents. **44**, which has a hydrophilic nature, showed limited nuclear penetration and accumulated preferentially in the mitochondria. The lipophilic **44**, on the other hand, might go into the nucleus. Both complexes show remarkable anticancer potential, despite the unexplained processes by which such a small structural variation results in significant variances in cellular absorption and subcellular localisation. Interestingly, **44** showed strong cytotoxic effects on cancer cells, especially cisplatin-resistant ones, indicating they can overcome chemoresistance. Both complexes caused excessive reactive oxygen species (ROS) production by impairing cellular metabolism and rupturing mitochondrial membrane potential upon accumulation. Unlike its partner complex, **44**'s nuclear location enabled it to initiate several cell death pathways. In particular, the other complex caused cisplatin-resistant A549R cells to undergo mitochondria-mediated apoptosis, while **44** encouraged PARP-1-dependent necroptosis, possibly as a result of its capacity to damage

DNA. This study highlights the therapeutic potential of necroptosis inducers for the treatment of drug-resistant malignancies and provides insightful information about the structure–activity relationships of metal-based chemotherapeutics.¹⁵³

Using 1,1-(pyrazin-2-yl) pyrene [4,5-*e*] [1,2,4] triazine as the primary ligand and a variety of auxiliary ligands, Kai Xiong *et al.* created a range of ruthenium(II) complexes in this environment (45). 45, which had a mixture of the primary ligand with bipyridyl and phenylpyridyl groups, was the one that demonstrated improved nuclear-targeting properties. 45 is an uncommon dual catalytic inhibitor that can inhibit topoisomerases I and II's endogenous activity at the same time. A signalling cascade that eventually results in necroptotic cell death is started by this dual inhibition. The study provided a precise description of the mechanism relating topoisomerase inhibition to necroptosis. Interestingly, 45 showed strong antitumor activity *in vivo*, even in drug-resistant cancer models. 45 is the first known ruthenium-based chemotherapeutic drug that can cause necroptosis, highlighting its promise as a cutting-edge

therapeutic option for the treatment of cancers that are resistant to current treatments (Fig. 7) (Table 2).¹⁵⁴

4. Immunity-induced programmed cell death pathways

4.1. Autophagy

4.1.1. Autophagy pathways and regulation. The term autophagy, which comes from the Greek words “auto”, which means “self”, and “phagein”, which means “to eat”, describes a basic catabolic mechanism by which cells break down and recycle their own components in order to preserve homeostasis and endure stress. Belgian biochemist Christian de Duve first proposed the biological idea of autophagy in 1963. In the 1990s, Japanese researcher Yoshinori Ohsumi conducted ground-breaking research that clarified the mechanism underlying autophagy. Ohsumi won the 2016 Nobel Prize in Physiology or Medicine for his groundbreaking research, which included identifying autophagy-related (Atg) genes in yeast and proving conserved autophagic pathways in higher eukaryotes.¹⁵⁵ There are two levels of autophagy:

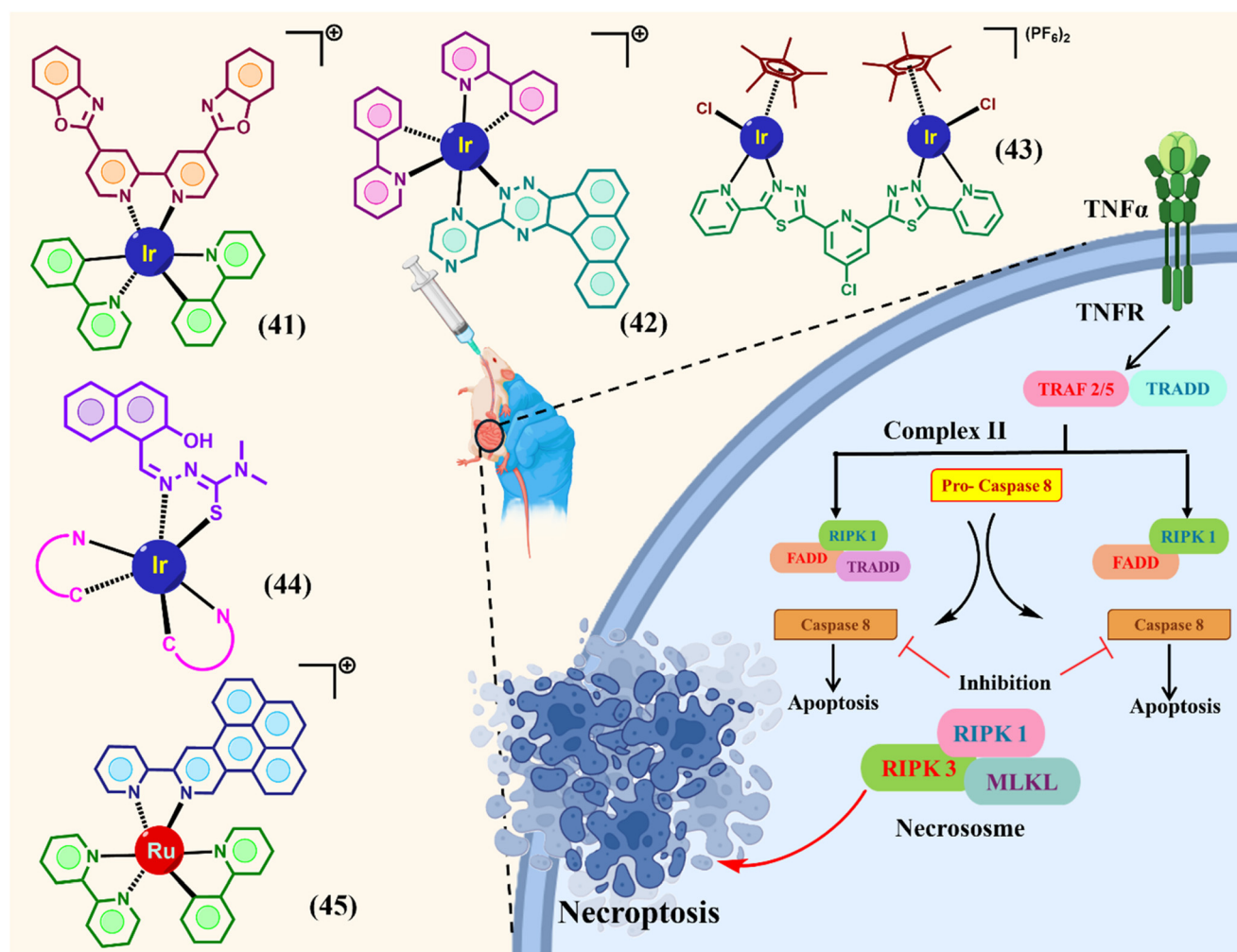


Fig. 7 Mechanism of action of necroptosis triggering photosensitizers.

stress-induced autophagy, which is triggered as a survival strategy in response to nutrient deprivation, hypoxia, or cytotoxic insult, and basal autophagy, which is constitutively active under normal physiological conditions to promote turnover of damaged organelles and misfolded proteins. Although this process is usually protective, its functions vary based on the intensity and cellular environment. Moderate autophagy, on the one hand, promotes cell survival by recycling intracellular components to provide energy and biosynthetic precursors, thereby reducing cellular stress. Conversely, self-digestion and, in certain cases, autophagy-dependent cell death can result from excessive or dysregulated autophagy.¹⁵⁶

Autophagy's dualistic nature makes treatment extremely difficult, especially in oncology. In order to withstand harsh microenvironmental conditions such as hypoxia, food deprivation, and therapeutic interventions, cancer cells frequently use autophagy as a cytoprotective response. By offering a different pathway for metabolic adaptability and energy conservation, autophagy can paradoxically undermine the effectiveness of cancer treatments like starvation therapy, which attempts to deprive tumour cells of vital nutrients.¹⁵⁷ Therefore, autophagy acts as a survival barrier that lessens the cytotoxic effects of therapies meant to cause tumour tissues to experience metabolic stress. Recent attempts at cancer treatment have evolved towards tactics that either concurrently suppress autophagy or take advantage of its dynamics to cause irreversible cellular damage in recognition of this protective process.¹⁵⁸

One such creative method was put up by Tang and associates, who created a strategy based on PDT that was especially intended to take advantage of and interfere with autophagy-mediated survival pathways in cancer cells. PDT has showed great promise as a localised, minimally invasive therapy method since it depends on the production of ROS when PSs are activated by light. However, the activation of autophagy by cancer cells in response to oxidative stress caused by PDT can compromise its therapeutic effectiveness.¹⁵⁹ By combining fasting therapy with autophagy-responsive photosensitisers (TPAQ and TPAP), which show selective fluorescence activation and ROS generation within autophagic lysosomes, Tang's group hoped to turn this therapeutic resistance into an opportunity. This two-pronged approach is based on the observation that autophagy facilitates the transport of intracellular components to lysosomes for destruction, especially when hunger is present. Under normal circumstances, TPAQ and TPAP are designed to be non-fluorescent and photodynamically inactive; however, they become active in the acidic environment of autolysosomes, which is a characteristic of autophagic flux. These PSs react to light irradiation by generating large amounts of ROS once they have been localised to the lysosomes. The produced ROS cause lysosomal membrane permeabilisation (LMP) by specifically causing oxidative damage to the lysosomal membranes. Because lysosomal integrity is compromised,

hydrolytic enzymes such as cathepsins can be released into the cytoplasm, causing mitochondrial malfunction, caspase activation, and eventually apoptotic cell death. Therefore, the creation of ROS brought on by PDT not only overwhelms the autophagic machinery but also uses it as a weapon against the cancer cells, transforming their survival strategy into a self-destruction pathway. Importantly, this tactic turns autophagy from a defence mechanism into a weakness. The PSs employed in Tang's research take advantage of autophagy for specific subcellular targeting and ROS generation, rather than just avoiding it. Because TPAQ and TPAP's colourimetric shift upon activation within autolysosomes enables real-time imaging of autophagic progression and treatment response, their fluorescence emission features also serve a dual diagnostic role. To improve the selectivity and efficacy of PDT in the treatment of cancer, this clever PS design provides both spatiotemporal control over ROS generation and dynamic monitoring of autophagy-associated cell fate.^{160–162}

4.1.2. Photosensitizer inducing autophagy *via* PDT.

Because of their unique method of action and the hypoxic nature of solid tumours, nitrogen mustards (NMs), one of the first chemotherapeutic drugs created for the treatment of cancer, have limited therapeutic efficacy. Meng-Meng Wang *et al.* created (**46**), a multifunctional organoiridium(III) prodrug, to combat tumour hypoxia and improve the therapeutic efficacy of NMs to overcome these constraints. **46** combines three useful elements: an Ir-arene fragment that produces ROS, a hypoxia-responsive azolinker, and a nitrogen mustard-based DNA-alkylating moiety. Notably, our work is the first to successfully treat hypoxic lung cancer using DNA damage response (DDR)-induced autophagy. Mechanistically, **46** decreases the expression of hypoxia-inducible factor 1- α (HIF-1 α) and increases the levels of catalase (CAT), which helps to convert excess hydrogen peroxide into oxygen in order to lessen hypoxic stress. GSH depletion and increased ROS generation are two of the several therapeutic responses that **46** triggers under hypoxic conditions. The DDR process is activated by this dual redox modulation, which also causes substantial DNA cross-linking damage and increases oxidative stress. In particular, the medication increases downstream signalling through the PIK3CA/PI3K-AKT1-mTOR-RPS6KB1 cascade and initiates DDR-mediated autophagy through the ATM/Chk2 axis. The strong antiproliferative effects of **46** on hypoxic tumours were validated by both *in vitro* and *in vivo* investigations.¹⁶³

Through lysosome-autophagosome fusion, autophagy breaks down damaged components, acting as an essential cellular quality control mechanism. On the other hand, excessive autophagy can increase cell survival and lead to medication resistance in cancer. Although precisely controlling ROS within autophagic pathways is still challenging, targeting autophagy through oxidative stress is a promising therapeutic method. To prevent autophagy, Mingyu Park *et al.* created biocompatible, neutral Ir(III)-based photosensitisers (**47**), which are intended to suppress ROS generation specific to lysosomes. Comparisons with non-

targeting analogues validated these complexes' lysosomal selectivity and biocompatibility. Proteomics, mass spectrometry, and live-cell imaging were among the mechanistic investigations that showed how complex-generated ROS oxidised important autophagy-related proteins, especially those involved in lysosomal function and vesicle fusion, hence reducing autophagy. *In vivo*, the red-light-activated **47** likewise demonstrated potent anti-tumour effectiveness.¹⁶⁴

The performance and design of photosensitizer, especially its capacity to promote effective intersystem crossing to produce reactive oxygen species, are crucial to the therapeutic effectiveness of photodynamic treatment. A major obstacle in the sector is still obtaining a logical design for PSs with improved ISC rates. In this regard, two positional isomers based on a boron-dipyrromethene (BODIPY) core functionalised with a cyclometalated iridium(III) moiety were successfully synthesised by Na Xu *et al.* (**48**). The purpose of this tactical change was to get beyond the inherent drawbacks of using BODIPY and Ir(III) complexes separately as PSs for PDT. The direct conjugation between the BODIPY scaffold and the Ir(III) fragment was demonstrated to dramatically improve the ISC process, hence increasing the efficiency of ROS generation, through thorough theoretical modelling and experimental validation. Strong ROS generation during irradiation caused lysosomal membrane permeabilization (LMP), which in turn caused calcium dysregulation and the consequent cytosolic release of lysosomal enzymes. Lysosome-dependent cell death, which is

typified by mitochondrial apoptosis, autophagy suppression, and cellular acidosis, was brought on by this cascade. Furthermore, it was shown *in vivo* utilising bilateral tumour models that the disruption of calcium homeostasis stimulates a photodynamically triggered immunotherapeutic response. All things considered, this work offers a promising NIR-activated photosensitizer that combines photodynamic and immunotherapeutic modalities to boost the effectiveness of cancer treatment while also addressing the energy gap reduction difficulty through efficient ISC augmentation.¹⁶⁵

Using a cyclometalated iridium(III) complex, Yu Chen *et al.* were able to create (**49**), a lysosome-targeted photosensitizer and photoredox catalyst. The lysosomal environment and the acidic tumour microenvironment (TME) are ideally suited to pH-sensitive phosphorescence properties **49** and increased photodynamic therapy (PDT) efficacy in acidic environments. Interestingly, **49** also had the potential to photocatalytically oxidise nicotinamide adenine dinucleotide (NADH) in hypoxic environments, which is a useful property for oxygen-deficient solid tumours. **49**'s therapeutic action was linked to a lysosome-mediated mechanism of cell death. With IC₅₀ values of 2.0 μM in 4 T1 cells and 0.6 μM in EMT6 cells under light activation, the chemical demonstrated strong photocytotoxicity. Additionally, a 4 T1 tumour-bearing mouse model was used to confirm the *in vivo* anti-tumour activity of **49**, showing a substantial reduction in tumours upon exposure to light. The potential of PDT in cancer treatment is advanced by this study's convincing strategy for creating lysosome-targeted photosensitisers and photoredox catalysts

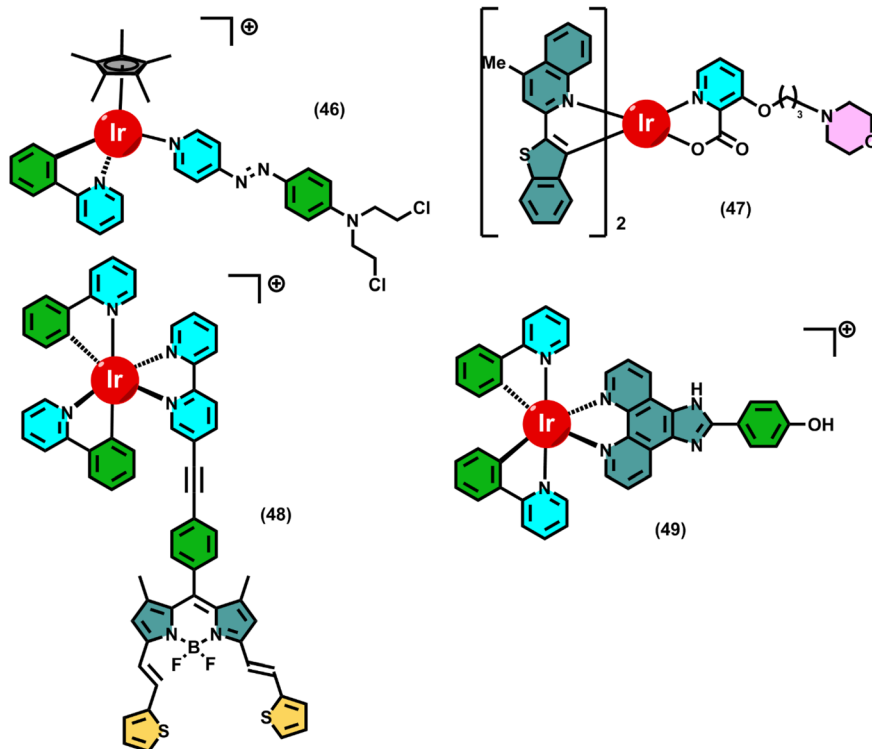


Fig. 8 Iridium complexes triggering autophagy in cancer cells.

that can overcome the difficulties presented by hypoxic tumour settings (Fig. 8) (Table 2).¹⁶⁶

5. Unexplored cell death pathways

5.1. Cuproptosis

The therapeutic potential of copper ionophores—small compounds that may bind copper ions extracellularly and facilitate their transport into cells—has been brought to light by recent developments in the field of copper-induced cell death.¹⁶⁷ As prospective agents in the development of copper-based anticancer treatments, these compounds have attracted more and more interest. Significant advancements in the study and creation of copper ionophores were made between 2011 and 2023, which was a pivotal time in the development of this medicinal approach.¹⁶⁸ As illustrated in the figure, the research shows that copper ionophores could cause fibrosarcoma cells to die, as well as the discovery that the tumour suppressor protein p53 controlled the process of copper-induced cell death.¹⁶⁹ The growing corpus of research on copper ionophores raises the possibility that this type of metal-induced cytotoxicity could be a useful therapy strategy for cancer. These ionophores can cause elevated intracellular

copper levels, which can damage membrane structures, increase the production of ROS, and interfere with vital cellular functions, all of which can jeopardise cell integrity.¹⁷⁰ All of these actions work together to cause oxidative stress, damage to cells, and eventually cell death. Therefore, further research into copper ionophores presents a viable path for the creation of innovative anticancer treatments (Fig. 9).¹⁷¹

5.2. Disulfidptosis

Even while research on disulfidptosis is still in its preliminary stages, new findings have significantly advanced our knowledge of this unusual type of controlled cell death. A number of research avenues need to be investigated in order to better understand its underlying mechanisms, identify any possible pathophysiological roles, and enable its therapeutic translation.¹⁷² First, it's still unknown what specific molecular processes cause disulfidptosis. Whether the actin cytoskeleton's collapse is the only mechanism causing this type of cell death or if other processes also play a role is still unknown. Second, there are currently just a few methods available for causing disulfidptosis. Future research should examine if disulfide stress may be directly induced, the

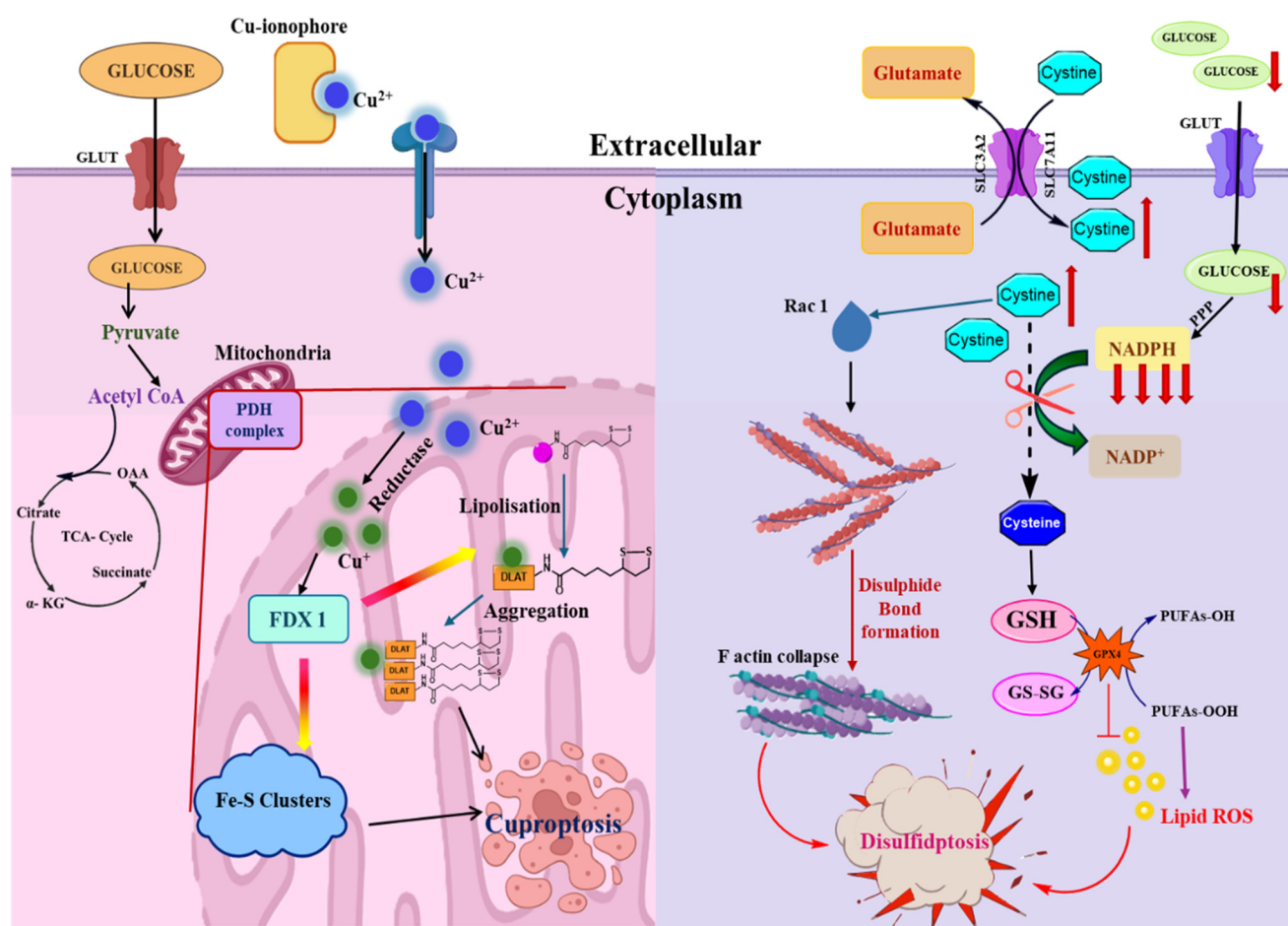


Fig. 9 Illustration describing cuproptosis and disulfidptosis pathways.

pentose phosphate pathway inhibited, or intracellular NADPH depleted as effective triggers. Third, the therapeutic window and application of metabolic therapies that target cancer cells may be limited because they may also affect non-cancerous cells, such as immune cells. This possible off-target effect poses a significant obstacle for practical translation and is particularly pertinent in the setting of GLUT inhibition-induced disulfidptosis. Fourth, preclinical research has shown that GLUT inhibitors as monotherapy have a limited tumor-suppressive activity, which seems to be largely dependent on SLC7A11 overexpression. Therefore, in order to determine which patients are most likely to benefit from GLUT-targeted medicines, biomarkers that detect high SLC7A11 expression must be developed and optimised.¹⁷³ Furthermore, more research should be done on the possibility of combining GLUT inhibitors with other therapeutic drugs. SLC7A11 overexpression has historically been linked to tumour growth and ferroptosis suppression, but this conventional wisdom is called into question by the discovery that it also promotes disulfidptosis.¹⁷⁴ SLC7A11

seems to have two functions: it inhibits ferroptosis and promotes disulfidptosis at the same time. This paradox calls into question how targeted cancer therapeutics might prevent such unintended outcomes and whether therapeutic approaches that attempt to increase ferroptosis by SLC7A11 suppression may inadvertently suppress disulfidptosis. Addressing these questions will be vital for guiding future research and for the design of more effective, selective cancer treatment strategies (Fig. 9).^{175,176}

5.3. Parthanatos

Parthanatos is a unique type of programmed cell death that differs from necrosis, apoptosis, and other controlled cell death routes in both morphology and mechanism. The main cause of it is the overactivation of the nuclear enzyme poly(ADP-ribose) polymerase-1 (PARP-1), which aids in DNA repair and preserves genomic integrity. Poly (ADP-ribose) (PAR) polymers are produced in excess when PARP-1 is overactivated in response to significant DNA damage.

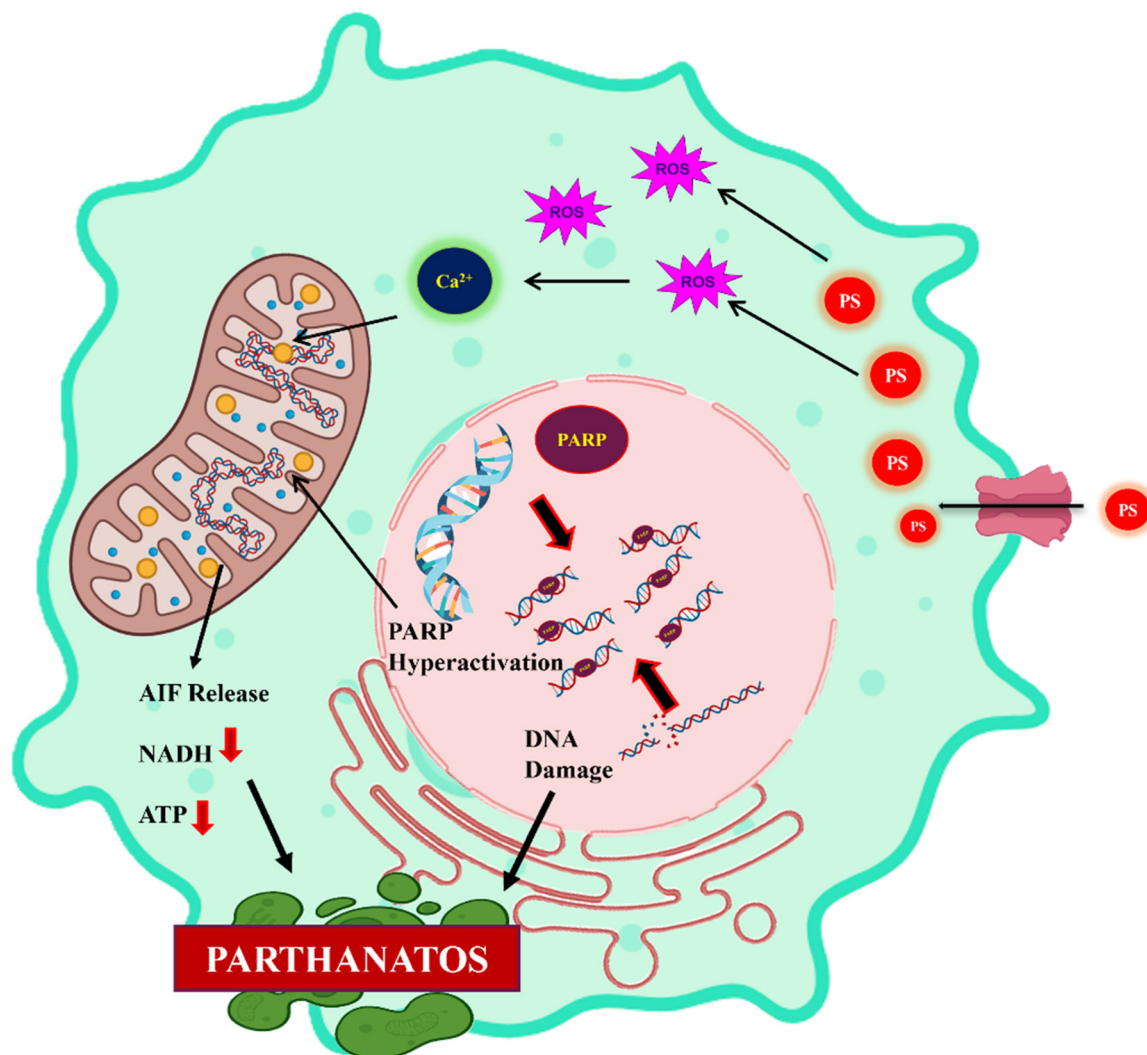


Fig. 10 Parthanatos cell death pathway induced by photosensitizers.

Bioenergetic failure is the final result of the buildup of these PAR polymers, which causes the depletion of vital cellular molecules like ATP and NAD⁺.¹⁷⁷ Significantly, PAR polymers move into the mitochondria and encourage the release of a flavoprotein called apoptosis-inducing factor (AIF), which is found in the intermembrane space of the mitochondria. In contrast to apoptosis, parthanatos does not exhibit apoptotic body formation or membrane blebbing, and it proceeds without caspase activation. After being released, AIF moves into the nucleus, where it causes chromatin condensation and extensive DNA fragmentation, which ultimately leads to cell death.¹⁷⁸ Parthanatos can be caused *via* PDT. When activated, photosensitizers produce ROS that cause irreversible damage to nuclear DNA; they dramatically activate PARP-1, which starts the manufacture of poly(ADP-ribose) (PAR) polymers and sets off the parthanatos pathway.¹⁷⁹ One important factor influencing cellular fate is the level of PARP-1 activation; moderate activation promotes DNA repair, whereas excessive activation has cytotoxic consequences. Furthermore, ROS generated during PDT may damage mitochondrial integrity, allowing AIF to be released and relocated to the nucleus. Therapeutic potential of PDT is enhanced by the involvement of parthanatos, especially when it comes to addressing malignancies that show resistance to apoptosis. Parthanatos avoids conventional apoptotic resistance mechanisms since it is caspase-independent, unlike apoptosis. Improved knowledge of the relationship between PARP-1 hyperactivation and PDT-induced oxidative stress could help develop methods to increase PDT's ability to eradicate cancerous cells. Furthermore, this pathway has shown clinical relevance and the possibility of controlled intervention by emerging as a possible target for therapeutic regulation through the use of PARP-1 inhibitors or drugs that block AIF nuclear translocation (Fig. 10).¹⁸⁰

6. Induction of multiple cell death pathways

Three cyclometalated iridium(III) complexes were synthesised and studied by Lin Zhou *et al.*, with DBDIP-2-(2,3-dihydrobenzo[*b*][1,4]dioxin-6-yl)-1*H*-imidazo[4,5-*f*][1,10]phenanthroline serving as the primary ligand (50). These substances demonstrated strong cytotoxic effects when activated by visible light, especially against A549 lung cancer cells. Cellular migration, subcellular localisation, mitochondrial membrane potential and permeability, intracellular ROS levels, and calcium ion flux were among the biological tests that collectively showed the compounds cause apoptosis through the mitochondrial pathway. Furthermore, ROS-induced oxidative stress increased the production of the pore-forming protein GSDMD and promoted the release of damage-associated molecules. The integrity of the cell membrane had been impaired, as evidenced by the greater release of lactate dehydrogenase (LDH) that accompanied this. Moreover, GPX4 expression was depleted with an increase in malondialdehyde (MDA), a hallmark of lipid peroxidation. These results imply that the iridium(III) complexes raise cancer cell

death by stimulating ferroptotic and pyroptotic pathways in addition to inducing apoptosis. All of the evidence implies the possibility of cyclometalated iridium(III) complexes as viable solutions for photodynamic cancer treatment.¹⁸¹

The ligand 5-bromo-2-amino-2'-(phenyl-1*H*-imidazo[4,5-*f*][1,10]phenanthroline) (BAPIP) and its associated cyclometalated iridium(III) complexes were synthesised and characterised using a new method by Chunxia Huang *et al.* (51). Employing the MTT assay, the cytotoxic characteristics of these complexes were methodically evaluated against a panel of cell lines, which included B16, HCT116, HepG2, A549, HeLa, and LO2. It's interesting to note that although compounds showed minimal cytotoxicity when they were free, liposomal formulations were created in an attempt to increase their antiproliferative action. With IC₅₀ values between 4.9 and 7.6 μ M, these liposome-encapsulated complexes showed noticeably improved cytotoxic effects, primarily against A549 lung cancer cells. In line with mechanistic research, these liposomal formulations predominantly aggregate within mitochondria, where they induce ROS generation and mitochondrial malfunction, resulting in apoptosis. Reduced GSH levels, downregulation of GPX4, increased expression of HMGB1, and increased lipid peroxidation were further studies that further verified the development of ferroptosis, as well as Pyroptotic cell death pathways concurrently. RNA sequencing-based transcriptomic research sheds light on the intricate signalling networks at play. The therapeutic promise of complexes was confirmed by *in vivo* investigations, which demonstrated that they could effectively inhibit tumour growth.¹⁸²

Two iridium-based complexes have been well demonstrated by Shuang Tian *et al.* (52). Complex 52 showed substantial cytotoxicity against distinct cancer cell lines, while its counter complex exhibited little cytotoxic effects, as demonstrated by *in vitro* cytotoxicity tests. Interestingly, both complexes showed increased anticancer activity when exposed to light; 52 showed notable phototoxic efficacy, in comparison to its counter complex. Both complexes were encapsulated in liposomes to enhance their therapeutic potential even further. These liposomal forms significantly reduced the growth of SGC-7901 gastric cancer cells when exposed to radiation. Assays for wound healing and colony formation corroborated this improved efficacy and validated the strong anti-proliferative properties of the irradiated formulations. Treatment with 52 lip generated cell cycle arrest in the S phase, according to cell cycle analysis. According to the mechanistic investigation, the free complexes and their liposomal counterparts both caused apoptosis by disrupting the potential of the mitochondrial membrane, promoting the release of cytochrome c, activating caspase-3, and modifying the expression of Bcl-2 family proteins. Ferroptotic pathways were implicated since photodynamic stimulation concurrently resulted in an increase in lipid peroxidation and malondialdehyde (MDA) and a decrease in intracellular GSH levels. Together, these results show that both complexes and their liposome-

encapsulated forms use the combined processes of ferroptosis and apoptosis under light irradiation to cause cancer cell death. The creation of dual-mode photodynamic therapeutic drugs with potential for clinical use in the treatment of cancer is better understood thanks to this study.¹⁸³

Huiwen Zhang *et al.* presented the synthesis, design, and characterisation of a novel ligand, TFBIP [2-(4'-trifluoromethyl-[1,1'-biphenyl]-4-yl)-1*H*-imidazo[4,5-*f*][1,10]phenanthroline] and three of its corresponding cyclometalated iridium(III) complexes (53). When examined utilising the MTT assay against several cancer cell lines, the *in vitro* cytotoxicity of these complexes was shown to be negligible, with IC₅₀ values more than 100 μ M. Thus, they were encapsulated into liposomal carriers to enhance the anticancer potential of the iridium complexes. These liposomal formulations revealed modest to high activity and substantially elevated cytotoxicity. Interestingly, 53 Lipo obtained a significantly lower IC₅₀ value than its free complex form, demonstrating significant inhibitory effects on cell proliferation. To clarify how these liposomal complexes work, mechanistic investigations were carried out. It was discovered that complexes significantly increased apoptosis, as evidenced by a high early apoptotic population of 37%. Additional research verified the depolarisation of the mitochondrial membrane potential, the passage of mitochondrial permeability transition pores, and the boosted generation of ROS. Moreover, cytochrome *c* release and increased intracellular calcium levels were detected. The participation of mitochondrial-mediated apoptosis was supported by Western blot analysis, which showed alteration of Bcl-2 family protein expression. Furthermore, the study suggested that caspase-3 selectively cleaves PARP to trigger apoptosis or GSDME to initiate pyroptosis, complying with cytochrome *c* activation, confirming the coexistence of both cell death pathways.¹⁸⁴

A cyclometalated iridium(III) complex that targets mitochondria (54), was developed and synthesised by Panpan Wang *et al.* and shows aggregation-induced enhancements in photodynamic activity. When exposed to light, this complex produces copious amounts of ROS and self-assembles into nanoaggregates in aqueous settings. According to *in vitro* cytotoxicity tests, 54 exhibits specific toxicity towards irradiated cancer cells and significant photo-cytotoxicity when activated by light. The selective localisation of 54 in the mitochondria has been established by confocal laser scanning microscopy and inductively coupled plasma mass spectrometry (ICP-MS) studies. Mechanistic studies showed that 54-induced ROS triggers mitophagy by damaging mitochondrial integrity when exposed to light. A compound that simultaneously suppresses the synthesis of GSH and promotes ferroptosis suggests a complicated mode of action that involves both ferroptotic and autophagic pathways. On top of that, 54 significantly downsizes tumour size in *in vivo* models and inhibits the expansion of three-dimensional multicellular tumour spheroids (3D MCTS). These findings

emphasise the potential of AIE-active iridium complexes for integrated cancer diagnostics and treatment and support the therapeutic approach of combining AIE features with PDT.¹⁸⁵

The design and synthesis of five new cyclometalated iridium(III) complexes incorporating isoquinoline-based C^N ligands were reported by Yuan Lu *et al.* (55). Out of all of these, the complex known as Ir-1 showed the strongest *in vitro* cytotoxicity. In MDA-MB-231 triple-negative breast cancer (TNBC) cells, mechanistic investigations revealed the complex triggers autophagy-dependent ferroptosis, which in turn triggers ferroptosis-mediated ICD and simultaneously inhibits indoleamine 2,3-dioxygenase (IDO) through ROS-induced endoplasmic reticulum (ER) stress. A strong antitumor immune response, marked by CD8⁺ T cell activation and Foxp3⁺ regulatory T cell depletion, was induced in immunocompetent BALB/c mice vaccinated with Ir-1-treated dying TNBC cells, as determined by immunological evaluation, enabling persistent antitumor immunity. Furthermore, overall therapeutic efficacy *in vivo* had been significantly enhanced by combination therapy employing 55 and an anti-PD-1 immune checkpoint inhibitor. With its therapeutic impact synergistically mediated through ICD induction and IDO inhibition, these findings place the shown complex as a prospective candidate for chemoimmunotherapy in TNBC, therefore increasing both innate cytotoxic effects and adaptive immunological responses.¹⁸⁶

Yajie Niu *et al.* designed a new DMHBT as a ligand and synthesised three complexes with cyclometalated iridium(III) (56). Single-state oxygen and superoxide anion assays showed that all complexes can increase ¹O₂ and O₂^{•−} as photosensitizers for the treatment of cancer in photodynamic therapy. *In vitro* cytotoxicity experiments revealed that all complexes exhibited moderate or low cytotoxicity against various tumour cell lines, whereas the *in vitro* toxicity of the complexes was greatly improved upon light irradiation, with the strong ability to kill B16 cells. The cellular uptake demonstrated that the complexes enter the cells and accumulate in the cell nuclei. Colocalization experiments revealed that the complexes were able to localise at the mitochondria. Since apoptosis *via* the intrinsic pathway is mediated by oxidatively damaged mitochondria, we found that the complexes led to a massive inward flow of Ca²⁺ and a great enhancement of ROS, which in turn sustained the opening of the MPTP and the decrease of MMP, resulting in mitochondrial dysfunction and inducing B16 cells to undergo apoptosis. The mechanism studies found that photo-activated complex also triggered Bcl-2 family proteins and caused a caspase cascade reaction to induce apoptosis. The complexes can arrest the cell cycle at the G0/G1 phase, blocking DNA synthesis and contributing to cell death. We also found that photo-activated complex inhibits the AKT/PI3K/mTOR signalling pathway, downregulates p62, and promotes the expression of Beclin-1, which induces cells to undergo autophagy. In addition, the photo-activated complex caused a dramatic

increase in ROS levels in B16 cells. Further experiments revealed that overloaded ROS reacted with polyunsaturated fatty acids to initiate lipid peroxidation, inhibited the Xc-system-glutathione (GSH)-glutathione peroxidase 4 (GPX4) antioxidant defence system, and up-regulated the expression of the damage-associated molecule HMGB1 to cause ferroptosis. It also promotes the release of CRT and HSP70, which activate tumour-specific immune responses to trigger immunogenic cell death. In summary, **56** as photosensitizers target the DNA and induce cell death *via* the following five pathways: (I) ROS mediated mitochondrial dysfunction apoptosis; (II) blocking the cell cycle at G0/G1 phase and inhibiting cell proliferation; (III) inducing cellular autophagy; (IV) causing ferroptosis and (V) immunogenic cell death.¹⁸⁷

According to recent findings, mitochondrial metabolism affects how well BC treatments work. One intriguing anticancer therapy strategy that might get around the drawbacks of traditional BC treatments is the mitochondria-targeted photosensitizer (PS). Two iridium(III) PSs that target the mitochondria have been developed by Jianguo Zheng *et al.* (**57**) for the treatment of BC. Through white light activation, **57** mechanically reduced the mitochondrial membrane potential, which in turn caused a drop in the B-cell lymphoma 2 protein (Bcl-2)/Bcl-associated X protein (Bax) ratio and an increase in cleaved caspase3. Ferroptosis and apoptosis were simultaneously activated by the reduction of glutathione, the deactivation of glutathione peroxidase 4, the increase of acyl-CoA synthetase long chain family member 4, and the buildup of lipid peroxide. The findings showed that **57** had great biosafety and outstanding anticancer effectiveness *in vivo*. An inventive therapy platform for BC is offered by this research using light-activated and mitochondrial-targeted PS.¹⁸⁸

Tao Feng *et al.* suggested a coordination-driven method for combining iridium(III) photosensitisers with Fe(III) ions to create (**58**), which are nanopolymers intended for combined photodynamic and chemodynamic cancer treatment. These nanopolymers were designed to break down in the acidic lysosomal milieu of cancer cells, releasing Fe ions and molecular Ir(III) complexes, despite their remarkable stability in physiological settings. The released Ir(III) complexes produced ROS under two-photon irradiation, such as superoxide anion radicals and singlet oxygen, which caused cancer cell death by both autophagy and apoptosis. Concurrently, lipid peroxidation, GSH depletion, and GPX4 downregulation were all facilitated by the liberated iron ions, which in turn facilitated ferroptosis. The **58** nanopolymers were subsequently encapsulated into exosomes generated from melanoma to form **58@EXO** nanoparticles, which improved therapeutic efficacy and tumour selectivity. In a mouse model of melanoma xenograft, this formulation showed preferential tumour accumulation and prolonged systemic circulation. **58@EXO** successfully prevented lung metastasis and accomplished near-complete tumour ablation in a single treatment session after intravenous injection and

two-photon irradiation at 730 nm. The therapeutic potential of **58@EXO** as a multifunctional nanoplatform that can trigger ferroptosis, apoptosis, and autophagy is highlighted by this study. A possible avenue for the creation of sophisticated, multimodal cancer treatments is the combination of photodynamic and chemodynamic modalities.¹⁸⁹

Maniklal Shee *et al.* strategically synthesised four iridium(III)-based catalysts (**59**) with bioinspired proton-coupled electron transfer (PCET)-active ancillary ligands and investigated their photophysical characteristics and possible biological uses as organelle-specific phototherapeutic agents that target lysosomes and mitochondria. Leveraging an electron-accepting BIP (benzimidazolium-imidazole-pyridine) platform, the PCET framework was utilised to refine the efficacy of type I PDT and open the door for the acceleration of oxygen reduction reactions. Large two-photon absorption cross sections (TPACS), strong photostability, and notable *in vitro* (photo)cytotoxicity against hypoxic 4 T1 and MCF-7 cancer cell lines were among the advantageous photophysical characteristics displayed by all synthesised Ir(III) complexes. The one with the best phototherapeutic performance was the mitochondrial-targeting **59** complex, which was functionalised with an *N,N*-bis(2-chloroethyl)azane moiety. Its effectiveness in preventing the establishment of solid hypoxic tumours in mice was validated by *in vivo* investigations. Mechanistically, **59** effectively decreased molecular oxygen and photo-oxidised endogenous NADH to produce ROS, which in turn caused ferroptosis to occur in tandem with apoptosis. These results demonstrate the potential of PCET-guided Ir(III) complexes as potent agents for hypoxic photodynamic cancer therapy.¹⁹⁰

With the goal to strengthen anticancer immune responses, You-Liang Zeng *et al.* sought to investigate the synergistic activation of ferroptosis and pyroptosis—an area with considerable therapeutic promise but little research to date. In order to achieve this, they created two photosensitisers based on iridium(III)-triphenylamine (**60**), which have the ability to upset intracellular redox balance and start photoinduced cascade damage to DNA and Kelch-like ECH-associated protein 1 (KEAP1). These photosensitisers caused DNA damage that initiated the cytoplasmic nucleic acid-sensing pathway dependent on absent in melanoma 2 (AIM2), which in turn prompted pyroptosis mediated by GSDMD. At the same time, disruption of iron metabolism *via* the KEAP1/Nuclear factor erythroid 2-related factor 2 (NRF2)/heme oxygenase-1 (HO⁻¹) signalling axis promoted ferroptosis by downregulating GPX4 and facilitated GSDME-dependent non-canonical pyroptosis. A strong antitumor immune response was triggered, and immunogenic cell death resulted from the synergistic action of pyroptosis and ferroptosis induction. This dual-modality strategy successfully inhibited tumour growth, as shown by *in vivo* tests, underscoring the therapeutic promise of the complexes in the creation of immune-activating photodynamic cancer treatments.¹⁹¹

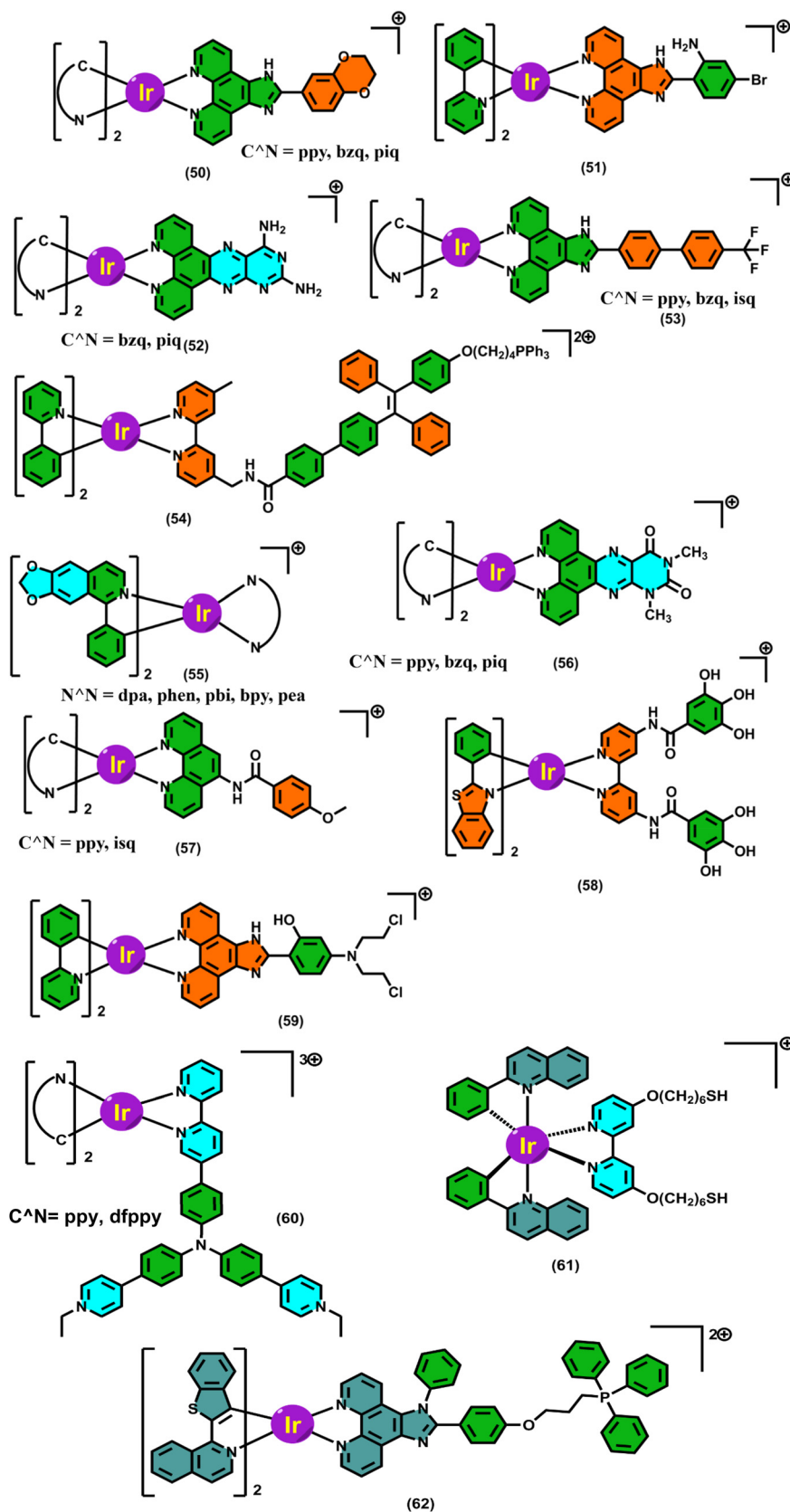


Fig. 11 Iridium complexes portray the synergism of various PCDs.

In the study reported by Libing Ke *et al.*, oxidative polymerisation was employed to produce a biodegradable iridium(III) coordinated polymer (**61**) that will be applied to photodynamic cancer treatment. A substantial diminution in intracellular GSH levels resulted from the polymeric nanoparticles' selective disintegration into monomeric Ir(III) complexes within cancer cells upon cellular internalisation; this process was visible through the use of phosphorescence lifetime imaging microscopy (PLIM). The decrease in GSH, a crucial intracellular antioxidant that scavenges ROS, was credited with the therapeutic improvement. Mechanistic studies revealed that the nanoparticles were garnered predominantly in the mitochondria, where they generated singlet oxygen and superoxide anion radicals through photoactivation, resulting in mitochondrial oxidative stress. This led to mitochondrial fragmentation and dysfunction. Furthermore, the nanoparticles stimulated lipid peroxidation, and this led cancer cells to undergo both ferroptosis and apoptosis. The nanoparticles were encased in an amphiphilic biotin-functionalized polymer to enhance their selective absorption by tumour tissues and achieve tumour-specific distribution. A single dose of therapeutically relevant two-photon laser irradiation resulted in near-complete tumour ablation and considerable tumour accumulation in tumour-bearing mice used in *in vivo* experiments. These results highlight this Ir(III)-based coordination polymer's promising clinical translation potential. Its capacity to lower the normally high glutathione levels in cancer cells gives rise to a far more favourable outcome.¹⁹²

Two novel cyclometalated Ir(III) complexes generated from benzo[b]thiophenyl isoquinoline (BTIQ), were engineered by Hao Yuan *et al.* (**62**) to serve as powerful photosensitisers for PDT. Interestingly, **62** was designed to target mitochondria primarily. Under hypoxic conditions, both complexes demonstrated type I photodynamic activity and might cause tumour cells to undergo photoactivated ferroptosis. Lipid peroxide buildup, mitochondrial shrinkage, downregulation of GPX4, and suppression by the ferroptosis inhibitor ferrostatin-1 (Fer-1) were the hallmarks of the observed ferroptotic cell death. When exposed to photoirradiation in hypoxic conditions, **62** triggered apoptosis, decreased ATP

synthesis, and collapsed MMP. In comparison to other complexes, **62** simultaneous productions of ferroptosis and apoptosis generated superior anticancer efficacy by effectively halting the proliferation of MCF-7, PANC-1, and MDA-MB-231 cells as well as multicellular tumour spheroids. This work demonstrates the therapeutic potential of combining ferroptosis and apoptosis to uplift the potency of PDT, especially against hypoxic solid tumours *via* type I photoreactions (Fig. 11) (Table 3).¹⁹³

7. Immuno-photodynamic therapy (immuno-PDT)

A promising synergistic approach, immuno-photodynamic therapy (immuno-PDT), combines photodynamic therapy with cancer immunotherapy, intending to enhance anticancer immune responses by inducing immunogenic cell death. Crucially, ICD, which is marked by the release of DAMPs such as calreticulin exposure, ATP secretion, and HMGB1 release, can be brought on by this oxidative stress. These DAMPs then encourage dendritic cell maturation and antigen presentation to cytotoxic T cells. Numerous photosensitizers have been found to have strong ICD-inducing properties. In preclinical models, chlorin-based PSs like Photofrin and m-THPC (temoporfin) have been demonstrated to produce potent ICD responses. Furthermore, by antibody-conjugated targeting, phthalocyanine derivatives such as IR700DX, which are employed in near-infrared photoimmunotherapy (NIR-PIT), have shown exceptional tumour selectivity and immune activation. Redaporfin and other bacteriochlorins have drawn interest because of their high singlet oxygen quantum yield and extensive tissue penetration, which further improve ICD induction. Inorganic complexes, especially those based on transition metals, have become viable substitutes; photosensitisers based on iridium(III) and ruthenium (II) can induce pyroptotic cell death and ER stress while also stimulating the immune system. For example, it has been demonstrated that Ir(III) complexes that target the endoplasmic reticulum can trigger memory T-cell responses and strong anti-tumour immunity. PDT and immune

Table 3 Cyclometalated Ir complexes ablate cancer cells *via* a combination of various PCDs

Sl. no.	Photosensitizer	Cell line	Photo-cytotoxicity (μM)	Cell death pathway	Reference
1	50	A549	0.31 ± 0.1	Ferroptosis and pyroptosis	181
2	51	A549	4.9 ± 1.0	Ferroptosis and pyroptosis	182
3	52	SGC-7901	2.4 ± 0.2	Apoptosis and ferroptosis	183
4	53	HeLa	5.6 ± 0.03	Apoptosis and pyroptosis	184
5	54	MCF-7	8	Ferroptosis and autophagy	185
6	55	MDA-MB-231	1.82 ± 0.01	Ferroptosis and autophagy	186
7	56	A549	1.0 ± 0.1	Apoptosis and ferroptosis	187
8	57	SW780	0.37 ± 0.01	Apoptosis and ferroptosis	188
9	58	A375	20	Apoptosis-autophagy-ferroptosis	189
10	59	MCF-7	0.78	Apoptosis and ferroptosis	190
11	60	MDA-MB-231	0.012 ± 0.004	Pyroptosis and ferroptosis	191
12	61	A549	2.4	Apoptosis and ferroptosis	192
13	62	MCF-7	0.20 ± 0.05	Apoptosis and ferroptosis	193

checkpoint blockade, such as anti-PD-1 or anti-CTLA-4 antibodies, have been shown in recent combination trials to boost therapeutic efficacy synergistically, reducing tumour burden and preventing metastasis. As a result, immuno-PDT is a revolutionary method that can turn immunologically “cold” tumours into “hot” immune-responsive settings, providing a strong foundation for cancer treatments of the future.^{194–199}

7.1. Photosensitizer inducing immunogenic cell death in synergy with PDT

A hydrogen peroxide (H_2O_2)-responsive and self-quenchable photosensitizer (**63**), was created by Jing Li *et al.* using a donor–acceptor (D–A) structural framework that successfully balanced the enhanced postoperative safety with the immunogenic photodynamic therapy (IPDT) efficacy. The molecule was showcasing notable AIE properties as a result of the addition of a triphenylamine core. Strong photodynamic activity at low doses was made possible by the expanded π -conjugation system, which also improved reactive oxygen species (ROS) formation and red-shifted optical characteristics (excitation at 500 nm, emission at 707 nm). By reacting primarily to H_2O_2 , **63** transformed into its luminous, low-toxicity derivative, which made accurate tumour imaging possible. At the same time, the reaction byproduct quinone methide (QM) enhanced ROS-mediated cytotoxicity by contributing to the depletion of GSH in the TME. Because of its off-state photosensitisation in non-cancerous tissues, this dual-action mechanism enabled **63** to accomplish effective tumour cell ablation with little collateral damage. Interestingly, **63** also promoted dendritic cell maturation and macrophage M1 polarisation, which enhanced the systemic anti-tumour immune response and enabled robust immunological activation. Together, these characteristics highlight **63**'s promise as a cutting-edge IPDT agent that provides immune modulation, tumour-selective therapy, and superior biocompatibility. The potential of self-quenchable photosensitizers for upcoming clinical translation in immuno-photodynamic cancer therapy is highlighted by the multifunctional design of **63**.²⁰⁰

Xiao-Yan Liu *et al.* rationally developed two new ruthenium(II) complexes by coordinating biquinoline and phenanthroline ligands with a Ru(II) centre (**64**). They were thoroughly examined for their potential in immunotherapeutic and chemo-photodynamic treatment applications. Using a combination of type I and type II PDT methods, both complexes efficiently induced cell death against the lung cancer cell line A549 and the breast cancer cell line 4 T1. In particular, compound **64** had low micromolar IC_{50} values (1.50–1.76 μM) upon laser activation, showed inherent chemotherapeutic activity, and demonstrated enhanced therapeutic performance under hypoxic settings, indicating its dual-function capabilities. In addition to causing direct cytotoxicity, **64** might trigger ICD, which activates and matures antigen-presenting cells and

ultimately aids CD8 T-cell-mediated antitumour immunity. The therapeutic potential of **64** was further validated by *in vivo* investigations, which showed significant tumour growth inhibition in both breast and lung cancer models, with tumour suppression rates of 97.3% and 94.6%, respectively. These results demonstrate the Ru(II) complexes' multifunctional therapeutic efficacy, especially **64**, as strong type-I/II photosensitisers with extra immunomodulatory capabilities, highlighting their potential for advancement in combined chemo-photo-immunotherapy approaches.²⁰¹

Qiaoshan Lie *et al.* presents a novel photoactivatable ferrocene–iridium(III) complex (**65**), as a powerful therapeutic drug that targets melanoma stem cells by causing ICD upon light activation and destroying their stemness. **65** exhibits preferential mitochondrial accumulation and cleaves in response to photoirradiation, releasing Fe^{2+} ions and a cytotoxic iridium(III) photosensitizer. Interestingly, even in hypoxic environments, **65** maintains its ability to produce superoxide anions ($\text{O}_2^{\cdot-}$) and hydroxyl radical (OH^{\cdot}), allowing for efficient photodynamic activity. In addition to causing ferroptosis and autophagy and significantly impairing the stemness of melanoma stem cells, this also activates ICD in melanoma cells and melanoma stem cells. **65** was encapsulated in DSPE-PEG2000 to create **65@PEG** nanoparticles, which improved its pharmacokinetic and biocompatibility profiles and allowed for tumour-targeted delivery by systemic injection. **65@PEG** showed preferential tumour accumulation after intravenous injection, and after light irradiation, tumour tissues showed a marked downregulation of stemness-associated markers. **65@PEG** successfully stopped the growth of primary and distant tumours when used therapeutically. Immunological evaluations further showed that **65@PEG** polarises macrophages towards the M1 phenotype, which changes the immunosuppressive environment and boosts both innate and adaptive immune responses. It also stimulates dendritic cell maturation and alters the tumour microenvironment. This complex system provides a strong immuno-photodynamic strategy in addition to combating medication resistance in melanoma. When taken as a whole, the results highlight **65@PEG**'s potential as a next-generation agent for photodynamic and photoactivated chemotherapy (PDT/PACT), offering a viable therapeutic approach for the management of drug-resistant solid tumours.²⁰²

Gloria Vigueras *et al.* illustrates the synthesis and assessment of four phosphorescent Ir(III) complexes (**66**) that were created using ligands based on benzimidazoles, which are known to have photosensitising properties. **66** was the most successful contender among all, with superior biological and photophysical characteristics. In melanoma and HeLa cell lines, all complexes demonstrated strong catalytic activity in oxidising NADH under blue light and little dark toxicity, even at doses as high as 300 μM . **66** exhibited strong intracellular ROS production, preferential mitochondrial accumulation, superior phototoxicity, and partial endoplasmic reticulum localisation upon irradiation.

Its cytotoxic effects may be exacerbated by damage to vital organelles, as suggested by this localisation profile. Crucially, **66** increased immune cell phagocytosis by inducing ICD markers such as ATP and HMGB1 release and calreticulin exposure. Additionally, following light activation, it demonstrated preferential cytotoxicity against CD20⁺ cancer stem cell (CSC)-like melanoma cells, with activity similar to that of abamectin, a known CSC-targeting drug. **66** is a good

option for photoimmunotherapy because it is the first Ir(III) molecule known to target CSCs while eliciting ICD. It is a powerful method for getting around tumour resistance, metastasis, and the drawbacks of traditional chemotherapy because of its light-triggered selectivity and immunostimulatory potential.²⁰³

Jia-Ying Zhou *et al.* created two new iridium(III)-based photosensitisers that interact with phospholipids and ER-

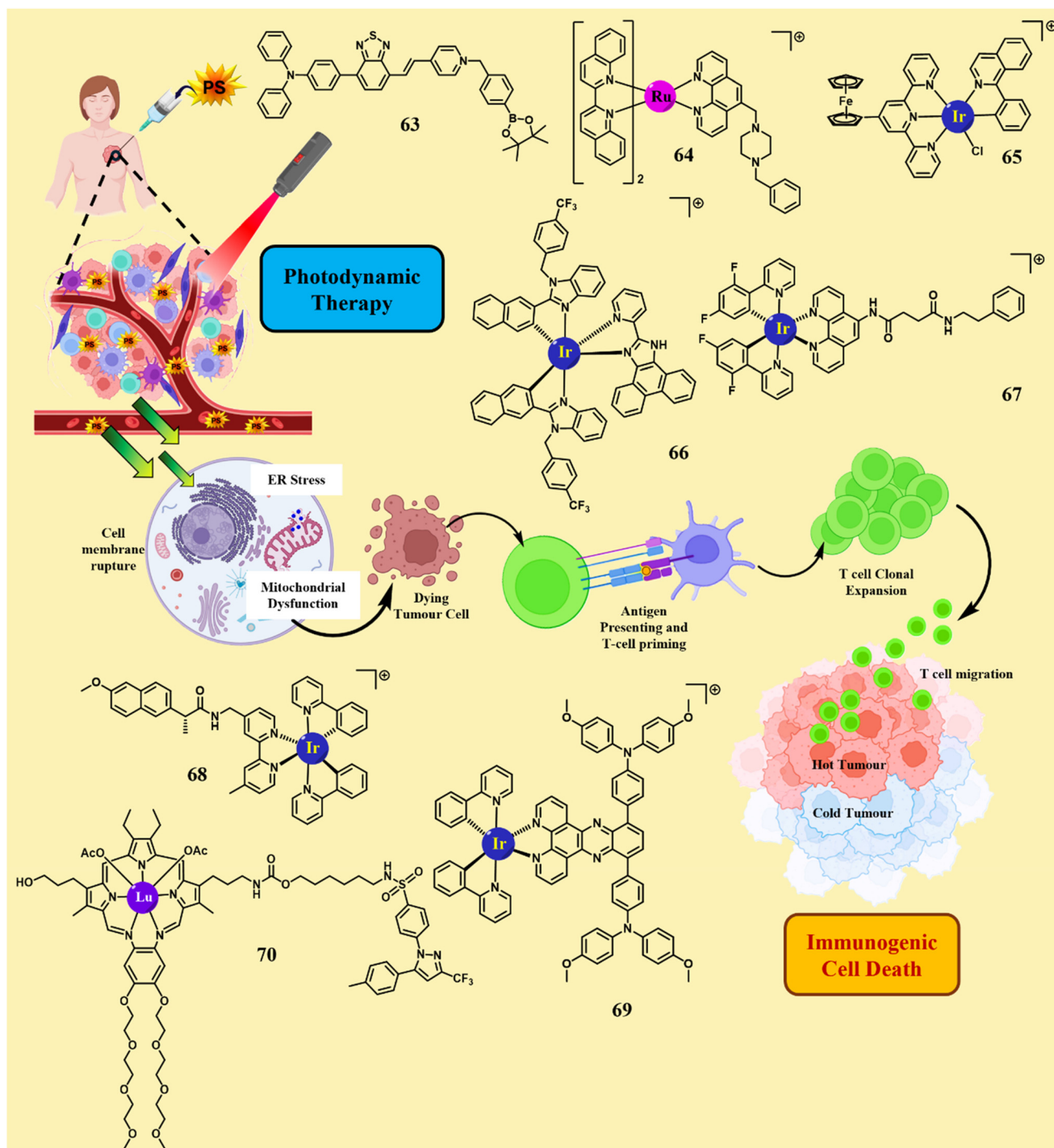


Fig. 12 Photosensitizers inducing diverse cell death mechanisms in synergy with cancer immunotherapy.

associated proteins to target the endoplasmic reticulum (ER) (67). Among these, it was demonstrated that **67** efficiently produces ROS through type I and type II photodynamic pathways, causing ER stress in cells of oral squamous cell carcinoma (OSCC) when activated by light. The basis for a combination therapeutic approach was established when **67**-mediated PDT induced ICD, which is marked by the release of DAMPs. This, in turn, increased the expression of PD-L1. When used in conjunction with a PD-L1 immune checkpoint inhibitor, the medication improved T cell infiltration and activation in the TME, promoted dendritic cell (DC) maturation, and showed synergistic effectiveness. This combination therapy effectively transformed immunologically “cold” tumours into “hot” tumours, as demonstrated in rat carcinogenesis models and cell-derived xenograft (CDX) models. All things considered, this work offers a potential new strategy for OSCC immunotherapy by demonstrating for the first time how to combine PD-L1 blockage with a metal-based ICD-inducing photosensitizer to enhance anti-tumour immune responses.²⁰⁴

Jingyue Zhao *et al.* used naproxen (NPX), a cyclooxygenase (COX) inhibitor, as a ligand to create a cyclometalated iridium(III) complex, **68**, with the goal of utilising its potential to trigger immunogenic responses in tumour cells. Compared to cisplatin, **68** showed reduced cytotoxicity towards normal human lung fibroblast (HLF) cells and strong anticancer activity, especially against cisplatin-resistant A549R cells. This suggests that **68** may be able to overcome cisplatin resistance while reducing side effects. According to subcellular localisation studies, **68** primarily builds up in the endoplasmic reticulum (ER) and mitochondria, where it increases ER stress and causes severe mitochondrial dysfunction. Alongside these effects, there was a significant decrease in intracellular ATP levels and an increase in ROS formation. The release of DAMPs caused by the increased ER stress resulted in ICD in A549R cells, providing a possible dual modality that combines immunotherapy and chemotherapy. Additionally, multicellular tumour spheroids made from A549R cells were substantially reduced in their proliferation and colony formation by **68**. Additionally, it hampered tumour cell motility by upsetting the cytoskeletal organisation of actin. All together, these studies offer a convincing approach to creating metal-based ICD inducers

that have a variety of anticancer effects *via* immunomodulatory and cytotoxic pathways. These results provide crucial mechanistic understandings of the immunogenic potential of complexes based on iridium and lend credence to the viability of combining bioactive small molecules with cyclometalated metal centres to improve therapeutic effectiveness.²⁰⁵

Two cyclometalated iridium(III) complexes were developed and synthesised by Feng Chen *et al.* They have a donor-acceptor-donor architecture with triphenylamine (TPA) electron-donating groups positioned advantageously to improve photophysical properties (**69**). Both complexes showed good biosafety profiles and outstanding photostability. Significantly, **69** outperformed other complexes in terms of photophysical properties, such as a smaller energy bandgap, a lower oxidation potential, and a larger spin-orbit coupling (SOC) constant, which led to red-shifted absorbance and increased production of type I ROS. In both normoxic and hypoxic circumstances, **69** effectively generated $O_2^{\cdot-}$ and OH^{\cdot} during red-light irradiation, resulting in noticeably higher photocytotoxicity than the other complexes. Studies conducted *in vitro* verified that ROS produced by **69** under red-light activation caused cancer cells to release DAMPs, which in turn started antitumor immune responses. Additionally, inoculation with dead tumour cells that had been pre-treated with **69** and exposed to red-light irradiation significantly inhibited tumour growth, according to *in vivo* immunisation trials conducted on C57BL/6 J mice with syngeneic tumours. These results highlight **69**'s potential as a strong inducer of ICD. All things considered, this work offers a novel molecular design approach for creating effective type I ROS-generating iridium-based complexes, emphasising its potential use in photoimmunotherapy to treat cancer.²⁰⁶

To determine whether structurally altering LuTex to promote the production of $O_2^{\cdot-}$ during photoirradiation could improve the effectiveness of IPDT, this study was conducted by Jusung An *et al.* **70**, a new small molecule photosensitizer conjugate (SMPC), was created by covalently joining a LuTex core with the COX-2 inhibitor celecoxib in order to test this theory. The intramolecular donor-acceptor interactions between the LuTex and celecoxib moieties successfully reduced the singlet-triplet energy gap (ΔE_{t1-s0}), hence

Table 4 Photosensitizers triggering various cell death pathways in combination with cancer immunotherapy

Sl. no.	Photosensitizer	Cell line	Photo-cytotoxicity (μM)	Immune response	Reference
1	63	4 T1	30	Promoting dendritic cell maturation and polarising M2 to M1 macrophages	200
2	64	4 T1	1.90 ± 0.04	Initiated an ICD Cascade, triggering a CD8+T cell antitumor immune response	201
3	65	A549	8.36 ± 0.97	Promotes macrophage-mediated phagocytosis	202
4	66	A375	6.9 ± 0.4	Induces DAMPs characteristic of ICD	203
5	67	SCC1	0.12 ± 0.05	Dendritic cell maturation, T lymphocyte infiltration and antitumor cytokine secretion	204
6	68	A549R	2.9 ± 0.3	DAMPs release, CRT exposure, HMGB1 migration, and ATP secretion	205
7	69	A549	2.8 ± 0.10	Induces DAMPs characteristic of ICD	206
8	70	Hepa1-6	10	Promoting T-cell mediated anti-tumor immunity	207

increasing efficient $O_2^{\cdot-}$ generation, as demonstrated by both experimental evidence and theoretical calculations. Through COX-2 binding, the celecoxib unit further enhanced tumour-targeting specificity, assisting in the localisation of the photosensitiser to malignant tissues and lowering the possibility of non-specific photoactivation. Apart from its photosensitising capabilities, **70** demonstrated chemotherapeutic efficacy, specifically *via* antiangiogenic pathways, which improved the overall results of photodynamic therapy. The CD133 cancer stem cell marker-specific aptamer-decorated exosomes (called Ex-apt@70) were used as carriers for targeted administration, enabling accurate distribution to breast and liver cancer cells in both *in vitro* and *in vivo* settings. This exosome-based delivery method greatly increased biocompatibility decreased systemic toxicity, and improved tumor-targeting specificity. Furthermore, Ex-apt@70 appeared to reduce tumour stemness in addition to improving treatment efficacy by specifically targeting cancer stem cells (Fig. 12) (Table 4).²⁰⁷

8. Conclusion and future outlook

In the creation of photosensitisers for photodynamic treatment, transition metal complexes of iridium, ruthenium, and rhenium constitute a new frontier because of their high spin-orbit coupling, customisable photophysical characteristics, and capacity to initiate a variety of programmed cell death pathways. In particular, these complexes allow subcellular targeting, generate ROS effectively under customised excitation, and trigger alternative cell death mechanisms like ferroptosis, pyroptosis, and necroptosis in conjunction with immunogenic cell death, as this review emphasises.

But there are still a lot of obstacles to overcome. Due to their weak water solubility, limited tumour selectivity, and oxygen dependence, many metal-based PSs are less effective in tumour microenvironments with low oxygen levels. Moreover, it is still an open but crucial challenge to accurately direct PS-induced cell death onto the specified pathway.

The logical design of PSs with distinct subcellular targeting motifs and ROS profiles, which allow for the selective activation of particular cell death processes, must be the field's top priority going ahead. It will be crucial to comprehend the structural and electrical factors, such as photostability, metal oxidation state, and ligand environment, that affect these results. Additionally, there is an increasing demand for PSs that can operate in the near-infrared spectrum, penetrate deeper tissues, and perform well in hypoxic environments. These restrictions might be addressed by techniques including bioorthogonal activation, oxygen-independent ROS creation, energy transfer systems, and heavy-atom engineering.

In order to improve therapeutic results, future research should also incorporate these metal complexes into multipurpose platforms, integrating PDT with

immunotherapy or drug delivery methods. Crucially, moving PSs from the bench to the bedside will necessitate striking a compromise between pharmacological viability, potency, and biocompatibility; this equilibrium should ideally be bolstered by strong preclinical models and translational research.

In final analysis, Ir, Ru, and Re complexes have the potential to be revolutionary next-generation PDT agents. Realising their clinical significance in the treatment of resistant and late-stage tumours will require ongoing innovation in their design, mechanistic knowledge, and application tactics.

Conflicts of interest

There are no conflicts to declare.

Cell line abbreviations

HCT116	Human colon cancer cell line
MCF-7	Human breast cancer cell line
MDA-MB-231	Mesenchymal human breast cancer cell line
A549	Lung carcinoma epithelial cells
A549R	Chemotherapeutic drug resistant lung carcinoma epithelial cells
HepG2	Human liver cancer cell line
HeLa	Human cervical cancer cells
SGC-790	Human gastric adenocarcinoma cell line
PC-3	Human prostate cancer cell line
A375	Human melanoma cell line
4 T1	Murine (mouse) mammary carcinoma cell line
HT1080	Human fibrosarcoma cell line
PANC-1	Human epithelioid carcinoma cell line
Jurkat cells	Human T lymphocyte cell line
U14	Mouse squamous cell carcinoma cell line
BEL-7402	Human hepatoma cell line
MV4-11	Human leukemia cell line
EMT6	Murine mammary carcinoma cell line
SW780	Human bladder cancer cell line
SCCI	Squamous cell carcinoma (SCC) of the head and neck
CT26	Murine colon carcinoma cell line
Hepa1-6	Murine hepatoma cell line from a C57L mouse

Data availability

No new data was generated.

Acknowledgements

The authors express gratitude to the Department of Science and Technology, Government of India, for their support of this research through the DST-SERB CRG project grant (CRG/2021/002267). Additionally, this work was financially supported by Vellore Institute of Technology (VIT), Vellore under the Faculty Seed Grant (REGMS) (Sanction Order No.: SG20250014). Recognition is also extended to DST, New Delhi, India, for the DST-FIST project.

References

- H. Jin, L. Wang and R. Bernards, *Nat. Rev. Drug Discovery*, 2023, **22**, 213–234.
- J. Ferlay, M. Colombet, I. Soerjomataram, D. M. Parkin, M. Piñeros, A. Znaor and F. Bray, *Int. J. Cancer*, 2021, **149**, 778–789.
- N. Behranvand, F. Nasri, R. Zolfaghari Emameh, P. Khani, A. Hosseini, J. Garssen and R. Falak, *Cancer Immunol., Immunother.*, 2022, **71**, 507–526.
- N. Alvarez and A. Sevilla, *Int. J. Mol. Sci.*, 2024, **25**, 1023.
- S. E. Qian, Y. Long, G. Tan, X. Li, B. Xiang, Y. Tao, Z. Xie and X. Zhang, *MedComm*, 2024, **5**, e70024.
- A. P. Mishra, B. Salehi, M. Sharifi-Rad, R. Pezzani, F. Kobarfard, J. Sharifi-Rad and M. Nigam, *Mol. Diagn. Ther.*, 2018, **22**, 281–295.
- X. An, W. Yu, J. Liu, D. Tang, L. Yang and X. Chen, *Cell Death Dis.*, 2024, **15**, 556.
- S. K. Kim and S. W. Cho, *Front. Pharmacol.*, 2022, **13**, 868695.
- Q. Wang, X. Shao, Y. Zhang, M. Zhu, F. X. Wang, J. Mu, J. Li, H. Yao and K. Chen, *Cancer Med.*, 2023, **12**, 11149–11165.
- O. Morana, W. Wood and C. D. Gregory, *Int. J. Mol. Sci.*, 2022, **23**, 1328.
- M. Castells, B. Thibault, J. P. Delord and B. Couderc, *Int. J. Mol. Sci.*, 2012, **13**, 9545–9571.
- W. Wang, T. Li and K. Wu, *Cell Death Discovery*, 2025, **11**, 93.
- S. K. Kim and S. W. Cho, *Front. Pharmacol.*, 2022, **13**, 868695.
- X. Lei, Y. Lei, J. K. Li, W. X. Du, R. G. Li, J. Yang, J. Li, F. Li and H. B. Tan, *Cancer Lett.*, 2020, **470**, 126–133.
- H. Tang, J. Qiao and Y. X. Fu, *Cancer Lett.*, 2016, **370**, 85–90.
- X. Jing, F. Yang, C. Shao, K. Wei, M. Xie, H. Shen and Y. Shu, *Mol. Cancer*, 2019, **18**, 1–15.
- V. Petrova, M. Annicchiarico-Petruzzelli, G. Melino and I. Amelio, *Oncogenesis*, 2018, **7**, 10.
- Á. Juarranz, P. Jaén, F. Sanz-Rodríguez, J. Cuevas and S. González, *Clin. Transl. Oncol.*, 2008, **10**, 148–154.
- W. Jiang, M. Liang, Q. Lei, G. Li and S. Wu, *Cancers*, 2023, **15**, 585.
- P. Mroz, A. Yaroslavsky, G. B. Kharkwal and M. R. Hamblin, *Cancers*, 2011, **3**, 2516–2539.
- A. C. Moor, *J. Photochem. Photobiol., B*, 2000, **57**, 1–13.
- N. Plekhova, O. Shevchenko, O. Korshunova, A. Stepanyugina, I. Tananaev and V. Apanasevich, *Bioengineering*, 2022, **9**, 82.
- A. T. Rice, M. I. Martin, M. C. Warndorf, G. P. Yap and J. Rosenthal, *Inorg. Chem.*, 2021, **60**, 11154–11163.
- L. N. Shestakova, T. S. Lyubova, S. A. Lermontova, A. O. Belotelov, N. N. Peskova, L. G. Klapshina, I. V. Balalaeva and N. Y. Shilyagina, *Pharmaceutics*, 2022, **14**, 2655.
- P. Pallavi, K. Harini, V. Anand Arumugam, P. Gowtham, K. Girigoswami, S. Muthukrishnan and A. Girigoswami, *J. Evidence-Based Complementary Altern. Med.*, 2022, **2022**, 3011918.
- H. Abrahamse and M. R. Hamblin, *Biochem. J.*, 2016, **473**, 347–364.
- T. Mishchenko, I. Balalaeva, A. Gorokhova, M. Vedunova and D. V. Krysko, *Cell Death Dis.*, 2022, **13**, 455.
- A. P. Castano, T. N. Demidova and M. R. Hamblin, *Photodiagn. Photodyn. Ther.*, 2005, **2**, 1–23.
- N. Kavčič, K. Pegan and B. Turk, *Biol. Chem.*, 2017, **398**, 289–301.
- M. Korbelik, *Lasers Surg. Med.*, 2018, **50**, 491–498.
- V. Labi and M. Erlacher, *Cell Death Dis.*, 2015, **6**, e1675.
- D. Kashyap, V. K. Garg and N. Goel, *Adv. Protein Chem. Struct. Biol.*, 2021, **125**, 73–120.
- A. A. A. Azzwali and A. E. Azab, *Clin. Med.*, 2019, **7**, 80–82.
- D. Kanduc, A. Mittelman, R. Serpico, E. Sinigaglia, A. A. Sinha, C. Natale, R. Santacroce, M. G. Di Corcia, A. Lucchese, L. Dini and P. Pani, *Int. J. Oncol.*, 2002, **21**, 165–170.
- Z. Su, Z. Yang, Y. Xu, Y. Chen and Q. Yu, *Mol. Cancer*, 2015, **14**, 1–14.
- X. Meng, T. Dang and J. Chai, *Cancer Control*, 2021, **28**, 10732748211066311.
- S. Fulda, *Cancer Biol. Ther.*, 2013, **14**, 999–1004.
- Y. Mou, J. Wang, J. Wu, D. He, C. Zhang, C. Duan and B. Li, *J. Hematol. Oncol.*, 2019, **12**, 1–16.
- H. Yu, P. Guo, X. Xie, Y. Wang and G. Chen, *J. Cell. Mol. Med.*, 2017, **21**, 648–657.
- V. Inguscio, E. Panzarini and L. Dini, *Cells*, 2012, **1**, 464–491.
- J. J. Reiners, P. Agostinis, K. Berg, N. L. Oleinick and D. H. Kessel, *Autophagy*, 2010, **6**, 7–18.
- J. Dang, H. He, D. Chen and L. Yin, *Biomater. Sci.*, 2017, **5**, 1500–1511.
- D. C. Yang, X. Z. Yang, C. M. Luo, L. F. Wen, J. Y. Liu and Z. Lin, *Eur. J. Med. Chem.*, 2022, **243**, 114749.
- Y. Li, L. Zhao and X. F. Li, Targeting hypoxia: hypoxia-activated prodrugs in cancer therapy, *Front. Oncol.*, 2021, **11**, 700407.
- N. Baran and M. Konopleva, Molecular pathways: hypoxia-activated prodrugs in cancer therapy, *Clin. Cancer Res.*, 2017, **23**(10), 2382–2390.
- K. Jagathesan and S. Roy, *ChemMedChem*, 2024, **19**, 202400127.
- Z. Chen, Q. Tu, P. Dai, Y. Xu, W. Xu, J. Xue, H. Ao, X. Hu, W. Jiang, S. Liu and Q. Zhao, *J. Organomet. Chem.*, 2025, 123750.
- F. Qu, S. Park, K. Martinez, J. L. Gray, F. S. Thowfeik, J. A. Lundeen, A. E. Kuhn, D. J. Charboneau, D. L. Gerlach, M. M. Lockart and J. A. Law, *Inorg. Chem.*, 2017, **56**, 7519–7532.
- Y. Zeng, J. Ma, Y. Zhan, X. Xu, Q. Zeng, J. Liang and X. Chen, *Int. J. Nanomed.*, 2018, 6551–6574.
- T. J. Kinsella, V. C. Colussi, N. L. Oleinick and C. H. Sibata, *Expert Opin. Pharmacother.*, 2001, **2**, 917–927.

- 51 A. Hajri, S. Wack, C. Meyer, M. K. Smith, C. Leberquier, M. Kedingier and M. Aprahamian, *J. Photochem. Photobiol.*, 2002, **75**, 140–148.
- 52 T. E. Kim and J. E. Chang, *Pharmaceutics*, 2023, **15**, 2257.
- 53 P. Pashootan, F. Saadati, H. Fahimi, M. Rahmati, R. Strippoli, A. Zarrabi, M. Cordani and M. A. Moosavi, *Int. J. Pharm.*, 2024, **649**, 123622.
- 54 J. F. Algorri, M. Ochoa, P. Roldan-Varona, L. Rodriguez-Cobo and J. M. López-Higuera, *Cancers*, 2021, **13**, 3484.
- 55 W. P. Li, C. J. Yen, B. S. Wu and T. W. Wong, *Biomed.*, 2021, **9**, 69.
- 56 L. B. Josefsen and R. W. Boyle, *Met.-Based Drugs*, 2008, **2008**, 276109.
- 57 S. Mariano, E. Carata, L. Calcagnile and E. Panzarini, *Pharmaceutics*, 2024, **16**, 932.
- 58 S. Ma, S. Shi, X. Hu, Y. Zhao, B. Yang, M. Liao, B. Lu and Q. Xu, *Front. Pharmacol.*, 2025, **16**, 1606372.
- 59 A. Gandosio, K. Purkait and G. Gasser, *Chimia*, 2021, **75**, 845–845.
- 60 S. A. McFarland, A. Mandel, R. Dumoulin-White and G. Gasser, *Curr. Opin. Chem. Biol.*, 2020, **56**, 23–27.
- 61 S. T. Diepstraten, M. A. Anderson, P. E. Czabotar, G. Lessene, A. Strasser and G. L. Kelly, *Nat. Rev. Cancer*, 2022, **22**, 45–64.
- 62 S. Qian, Z. Wei, W. Yang, J. Huang, Y. Yang and J. Wang, *Front. Oncol.*, 2022, **12**, 985363.
- 63 K. A. Sarosiek and A. Letai, *FEBS J.*, 2016, **283**, 3523–3533.
- 64 A. Ashkenazi, *Cytokine Growth Factor Rev.*, 2008, **19**, 325–331.
- 65 R. Jan, *Adv. Pharm. Bull.*, 2019, **9**, 205.
- 66 T. J. Sayers, *Cancer Immunol., Immunother.*, 2011, **60**, 1173–1180.
- 67 N. L. Oleinick, R. L. Morris and I. Belichenko, *Photochem. Photobiol. Sci.*, 2002, **1**, 1–21.
- 68 K. Plaetzer, T. Kiesslich, C. B. Oberdanner and B. Krammer, *Curr. Pharm. Des.*, 2005, **11**, 1151–1165.
- 69 P. Agostinis, H. Breyssens, E. Buytaert and N. Hendrickx, *Photochem. Photobiol. Sci.*, 2004, **3**, 721–729.
- 70 J. N. Ribeiro, A. R. D. Silva and R. A. Jorge, *J. Bras. Patol. Med. Lab.*, 2004, **40**, 383–390.
- 71 Z. Zou, H. Chang, H. Li and S. Wang, *Apoptosis*, 2017, **22**, 1321–1335.
- 72 M. Zhong, J. He, B. Zhang, Q. Liu and J. Fang, *Free Radical Biol. Med.*, 2023, **195**, 121–131.
- 73 S.-f. He, W.-c. Han, Y.-y. Shao, H.-b. Zhang, W.-xin Hong, Q.-h. Yang, Y.-q. Zhang, R.-r. He and J. Sun, *Bioorg. Chem.*, 2023, **141**, 106867.
- 74 Q. Zhou, X.-B. Zhang, A.-L. Liu, Z.-G. Niu, G.-N. Li and F.-B. Yu, *Bioorg. Chem.*, 2025, **161**, 108507.
- 75 J. Hao, H. Zhang, L. Tian, L. Yang, Y. Zhou, Y. Zhang, Y. Liu and D. Xing, *J. Inorg. Biochem.*, 2021, **221**, 111465.
- 76 W. Li, C. Shi, X. Wu, Y. Zhang, H. Liu, X. Wang, C. Huang, L. Liang and Y. Liu, *J. Inorg. Biochem.*, 2022, **236**, 111977.
- 77 Z.-Y. Pan, B.-F. Liang, Y.-S. Zhi, D.-H. Yao, C.-Y. Li, H.-Q. Wu and L. He, *Dalton Trans.*, 2023, **52**, 1291–1300.
- 78 R. Tu, J. Liu, W. Chen, F. Fu and M.-J. Li, *Dalton Trans.*, 2023, **52**, 13137–13145.
- 79 Z. Tan, M. Lin, J. Liu, H. Wu and H. Chao, *Dalton Trans.*, 2024, **53**, 12917–12926.
- 80 E. Zafon, I. Echevarría, S. Barrabés, B. R. Manzano, F. A. Jalón, A. M. Rodríguez, A. Massaguer and G. Espino, *Dalton Trans.*, 2022, **51**, 111–128.
- 81 L.-Z. Zeng, X.-L. Li, Y.-A. Deng, R.-Y. Zhao, R. Song, Y.-F. Yan, M.-F. Wang, X.-H. Wang, X. Ren and F. Gao, *Inorg. Chem.*, 2025, **64**, 967–977.
- 82 T. Dixit, M. Negi and V. Venkatesh, *Inorg. Chem.*, 2024, **63**, 24709–24723.
- 83 M. Negi, T. Dixit and V. Venkatesh, *Inorg. Chem.*, 2023, **62**, 20080–20095.
- 84 N. Neelambaran, S. Shamjith, V. P. Murali, K. K. Maiti and J. Joseph, *ACS Appl. Bio Mater.*, 2023, **6**, 5776–5788.
- 85 C. Reghukumar, S. Shamjith, V. P. Murali, P. K. Ramya, K. V. Radhakrishnan and K. K. Maiti, *J. Photochem. Photobiol., B*, 2024, **250**, 112832.
- 86 K. Xiong, Y. Zhou, X. Lin, J. Kou, M. Lin, R. Guan, Y. Chen, L. Ji and H. Chao, *Photochem. Photobiol.*, 2021, **98**, 85–91.
- 87 Y. Li, B. Liu, C.-X. Xu, L. He, Y.-C. Wan, L.-N. Ji and Z.-W. Mao, *J. Biol. Inorg. Chem.*, 2020, **25**, 597–607.
- 88 C. Gonzalo-Navarro, E. Zafon, J. A. Organero, F. A. Jalón, J. C. Lima, G. Espino, A. M. Rodríguez, L. Santos, A. J. Moro, S. Barrabés, J. Castro, J. Camacho-Aguayo, A. Massaguer, B. R. Manzano and G. Durá, *J. Med. Chem.*, 2024, **67**, 1783–1811.
- 89 Y. Wu, J. Liu, M. Shao, P. Zhang, S. Song, G. Yang, X. Liu and Z. Liu, *J. Inorg. Biochem.*, 2022, **233**, 111855.
- 90 D. Chen, T. Shao, H. Zhao, F. Chen, Z. Fang, Y. Tian and X. Tian, *Dyes Pigm.*, 2023, **215**, 111271.
- 91 S. Shamjith, M. M. Joseph, V. P. Murali, G. S. Remya, J. B. Nair, C. H. Suresh and K. K. Maiti, *Biosens. Bioelectron.*, 2022, **204**, 114087.
- 92 Z. Tan, J. Feng, J. Liu, T. Liu, H. Wu and H. Chao, *Dalton Trans.*, 2025, **54**, 3626–3635.
- 93 S. J. Dixon, K. M. Lemberg, M. R. Lamprecht, R. Skouta, E. M. Zaitsev, C. E. Gleason, D. N. Patel, A. J. Bauer, A. M. Cantley, W. S. Yang and B. Morrison, *Cell*, 2012, **149**, 1060–1072.
- 94 S. J. Dixon and J. A. Olzmann, *Nat. Rev. Mol. Cell Biol.*, 2024, **25**, 424–442.
- 95 D. Tang, X. Chen, R. Kang and G. Kroemer, *Cell Res.*, 2021, **31**, 107–125.
- 96 X. Chen, R. Kang, G. Kroemer and D. Tang, *Nat. Rev. Clin. Oncol.*, 2021, **18**, 280–296.
- 97 G. Lei, L. Zhuang and B. Gan, *Nat. Rev. Cancer*, 2022, **22**, 381–396.
- 98 F. Zeng, S. Nijati, L. Tang, J. Ye, Z. Zhou and X. Chen, *Angew. Chem.*, 2023, **135**, e202300379.
- 99 M. Liu, X. Y. Kong, Y. Yao, X. A. Wang, W. Yang, H. Wu, S. Li, J. W. Ding and J. Yang, *Ann. Transl. Med.*, 2022, **10**, 368.
- 100 Z. Gao, S. Zheng, K. I. Kamei and C. Tian, *Acta Mater. Med.*, 2022, **1**, 411–426.

- 101 T. A. Mishchenko, I. V. Balalaeva, M. V. Vedunova and D. V. Krysko, *Trends Cancer*, 2021, **7**, 484–487.
- 102 Y. Zou, J. Chen, X. Luo, Y. Qu, M. Zhou, R. Xia, W. Wang and X. Zheng, *Front. Pharmacol.*, 2024, **15**, 1481168.
- 103 J. Chen, Z.-G. Sheng, H.-Z. Zhang, C.-H. Huang, M. Qin, B. Shao, J.-Y. Mao, R.-Q. Wang, J. Shao and B.-Z. Zhu, *ACS Appl. Mater. Interfaces*, 2025, **17**, 5684–5694.
- 104 Y. Pei, Y. Pan, Z. Zhang, J. Zhu, Y. Sun, Q. Zhang, D. Zhu, G. Li, M. R. Bryce, D. Wang and B. Z. Tang, *Adv. Sci.*, 2025, 2413879.
- 105 X. Zhao, J. Zhang, W. Zhang, Z. Guo, W. Wei, X. Wang and J. Zhao, *Chem. Sci.*, 2023, **14**, 1114–1122.
- 106 X. He, L. Wei, J. Chen, S. Ge, M. Kandawa-Shultz, G. Shao and Y. Wang, *Inorg. Chem. Front.*, 2023, **10**, 4780.
- 107 L. Zhu, X. Wang, T. Tian, Y. Chen, W. Du, W. Wei, J. Zhao, Z. Guo and X. Wang, *Chem. Sci.*, 2024, **15**, 10499–10507.
- 108 Y. Li, B. Liu, Y. Zheng, M. Hu, L.-Y. Liu, C.-R. Li, W. Zhang, Y.-X. Lai and Z.-W. Mao, *J. Med. Chem.*, 2024, **67**, 16235–16247.
- 109 Y. Ling, W. Wang, L. Hao, X. Wu, J. Liang, H. Zhang, Z. Mao and C. Tan, *Small*, 2022, **18**, 2203659.
- 110 Q. Zhang, D. Chen, X. Liu, Z. Deng, J. Li, S. Zhu, B. Ma, R. Liu and H. Zhu, *Small*, 2024, 2403165.
- 111 D. Lee, I. Y. Kim, S. Saha and K. S. Choi, *Pharmacol. Ther.*, 2016, **162**, 120–133.
- 112 E. Kim, D. M. Lee, M. J. Seo, H. J. Lee and K. S. Choi, *Front. Cell Dev. Biol.*, 2021, **8**, 607844.
- 113 D. Kessel, *Apoptosis*, 2020, **25**, 611–615.
- 114 S. Hanson, A. Dharan, J. PV, S. Pal, B. G. Nair, R. Kar and N. Mishra, *Front. Pharmacol.*, 2023, **14**, 1159409.
- 115 D. Kessel, *Photochem. Photobiol.*, 2019, **95**, 119–125.
- 116 D. Kessel and N. L. Oleinick, *Photochem. Photobiol.*, 2018, **94**, 213–218.
- 117 F. Chen, H. Tang, X. Cai, J. Lin, L. Xiang, R. Kang, J. Liu and D. Tang, *Cancer Gene Ther.*, 2024, **31**, 349–363.
- 118 L. He, K. Wang, Y. Zheng, J. Cao, M. Zhang, C. Tan, L. Ji and Z. Mao, *Dalton Trans.*, 2018, **47**, 6942–6953.
- 119 J. Liao, Y. Zhang, M. Huang, Z. Liang, Y. Gong, B. Liu, Y. Li, J. Chen, W. Wu, Z. Huang and J. Sun, *Bioorg. Chem.*, 2023, **140**, 106837.
- 120 S. K. Tripathy, U. De, N. Dehury, P. Laha, M. K. Panda, H. S. Kim and S. Patra, *Dalton Trans.*, 2016, **45**, 15122–15136.
- 121 K. Yokoi, C. Balachandran, M. Umezawa, K. Tsuchiya, A. Mitrić and S. Aoki, *ACS Omega*, 2020, **5**, 6983–7001.
- 122 K. Yokoi, K. Yamaguchi, M. Umezawa, K. Tsuchiya and S. Aoki, *Biochemistry*, 2022, **61**, 639–655.
- 123 C. Balachandran, K. Yokoi, K. Naito, J. Haribabu, Y. Tamura, M. Umezawa, K. Tsuchiya, T. Yoshihara, S. Tobita and S. Aoki, *Molecules*, 2021, **26**, 7028.
- 124 F. Van Hauwermeiren and M. Lamkanfi, *Cell Res.*, 2022, **32**, 227–228.
- 125 S. K. Hsu, C. Y. Li, I. L. Lin, W. J. Syue, Y. F. Chen, K. C. Cheng, Y. N. Teng, Y. H. Lin, C. H. Yen and C. C. Chiu, *Theranostics*, 2021, **11**, 8813.
- 126 B. T. Cookson and M. A. Brennan, *Trends Microbiol.*, 2001, **9**, 113–114.
- 127 S. L. Fink and B. T. Cookson, *Infect. Immun.*, 2005, **73**, 1907–1916.
- 128 F. Pentimalli, S. Grelli, N. Di Daniele, G. Melino and I. Amelio, *Genes Immun.*, 2019, **20**, 539–554.
- 129 B. Sangiuliano, N. M. Pérez, D. F. Moreira and J. E. Belizário, *Mediators Inflammation*, 2014, **2014**, 821043.
- 130 J. Shi, W. Gao and F. Shao, *Trends Biochem. Sci.*, 2017, **42**, 245–254.
- 131 S. Zeng, J. Wang, H. Kang, H. Li, X. Peng and J. Yoon, *Angew. Chem.*, 2025, **137**, e202417899.
- 132 M. Li, J. Kim, H. Rha, S. Son, M. S. Levine, Y. Xu, J. L. Sessler and J. S. Kim, *J. Am. Chem. Soc.*, 2023, **145**, 6007–6023.
- 133 D. Wu, S. Wang, G. Yu and X. Chen, *Angew. Chem.*, 2021, **133**, 8096–8112.
- 134 Y.-S. Zhi, T. Chen, B.-F. Liang, S. Jiang, D.-H. Yao, Z.-D. He, C.-Y. Li, L. He and Z.-Y. Pan, *J. Inorg. Biochem.*, 2024, **260**, 112695.
- 135 B.-F. Liang, S. Jiang, Y.-S. Zhi, Z.-Y. Pan, X.-Q. Su, Q. Gong, Z.-D. He, D.-H. Yao, L. He and C.-Y. Li, *Inorg. Chem. Front.*, 2025, **12**, 2294.
- 136 Y. Ling, X. Xia, L. Hao, W. Wang, H. Zhang, L. Liu, W. Liu, Z. Li, C. Tan and Z. Mao, *Angew. Chem., Int. Ed.*, 2022, **61**, e202210988.
- 137 M. Wu, X. Liu, H. Chen, Y. Duan, J. Liu, Y. Pan and B. Liu, *Angew. Chem., Int. Ed.*, 2021, **60**, 9093–9098.
- 138 X. Su, W. Wang, Q. Cao, H. Zhang, B. Liu, Y. Ling, X. Zhou and Z. Mao, *Angew. Chem., Int. Ed.*, 2022, **61**, e202115800.
- 139 W. Zhou and J. Yuan, *Semin. Cell Dev. Biol.*, 2014, **35**, 14–23.
- 140 B. Shan, H. Pan, A. Najafav and J. Yuan, *Genes Dev.*, 2018, **32**, 327–340.
- 141 X. Tong, R. Tang, M. Xiao, J. Xu, W. Wang, B. Zhang, J. Liu, X. Yu and S. Shi, *J. Hematol. Oncol.*, 2022, **15**, 174.
- 142 P. Meier, A. J. Legrand, D. Adam and J. Silke, *Nat. Rev. Cancer*, 2024, **24**, 299–315.
- 143 M. J. Morgan and Y. S. Kim, *Exp. Mol. Med.*, 2022, **54**, 1695–1704.
- 144 R. Karlowitz and S. J. van Wijk, *FEBS J.*, 2023, **290**, 37–54.
- 145 Y. Zhou, Y. Xiang, S. Liu, C. Li, J. Dong, X. Kong, X. Ji, X. Cheng and L. Zhang, *Cell Death Discovery*, 2024, **10**, 200.
- 146 Á. C. de Souza, A. L. Mencalha, A. D. S. D. Fonseca and F. de Paoli, *Lasers Med. Sci.*, 2024, **39**, 267.
- 147 Q. Zeng, X. Ma, Y. Song, Q. Chen, Q. Jiao and L. Zhou, *Theranostics*, 2022, **12**, 817.
- 148 X. Wang, P. Hua, C. He and M. Chen, *Acta Pharm. Sin. B*, 2022, **12**, 3567–3593.
- 149 O. Krysko, T. L. Aaes, V. E. Kagan, K. D'Herde, C. Bachert, L. Leybaert, P. Vandenabeele and D. V. Krysko, *Immunol. Rev.*, 2017, **280**, 207–219.
- 150 R. Guan, L. Xie, L. Wang, Y. Zhou, Y. Chen, L. Ji and H. Chao, *Inorg. Chem. Front.*, 2021, **8**, 1788–1794.
- 151 W. Li, T. Li, Y. Pan, S. Li, G. Xu, Z. Zhang, H. Liang and F. Yang, *J. Med. Chem.*, 2024, **67**, 3843–3859.
- 152 E. Řezníčková, O. Bárta, D. Milde, V. Kryštof and P. Štarha, *J. Inorg. Biochem.*, 2025, **262**, 112704.

- 153 L. Xie, L. Shi, K. Xiong, R. Guan, Y. Chen, J. Long, L. Ji and H. Chao, *Eur. J. Inorg. Chem.*, 2023, **26**, e202300001.
- 154 K. Xiong, C. Qian, Y. Yuan, L. Wei, X. Liao, L. He, T. W. Rees, Y. Chen, J. Wan, L. Ji and H. Chao, *Angew. Chem., Int. Ed.*, 2020, **59**, 16631–16637.
- 155 V. Kirkin, *J. Mol. Biol.*, 2020, **432**, 3–27.
- 156 Y. Ohsumi, *Cell Res.*, 2014, **24**, 9–23.
- 157 F. Peng, M. Liao, R. Qin, S. Zhu, C. Peng, L. Fu, Y. Chen and B. Han, *Signal Transduction Targeted Ther.*, 2022, **7**, 286.
- 158 K. K. Mahapatra, S. R. Mishra, B. P. Behera, S. Patil, D. A. Gewirtz and S. K. Bhutia, *Cell. Mol. Life Sci.*, 2021, 1–15.
- 159 S. Das, N. Shukla, S. S. Singh, S. Kushwaha and R. Shrivastava, *Apoptosis*, 2021, 1–22.
- 160 W. K. Martins, R. Belotto, M. N. Silva, D. Grasso, M. D. Suriani, T. S. Lator, R. Itri, M. S. Baptista and T. M. Tsubone, *Front. Oncol.*, 2021, **10**, 610472.
- 161 A. D. Garg, H. Maes, E. Romano and P. Agostinis, *Photochem. Photobiol. Sci.*, 2015, **14**, 1410–1424.
- 162 R. Zhang, C. Zhang, C. Chen, M. Tian, J. H. Chau, Z. Li, Y. Yang, X. Li and B. Z. Tang, *Adv. Sci.*, 2023, **10**, 2301295.
- 163 M.-M. Wang, D.-P. Deng, A.-M. Zhou, Y. Su, Z.-H. Yu, H. K. Liu and Z. Su, *Inorg. Chem.*, 2024, **63**, 4758–4769.
- 164 M. Park, J. S. Nam, T. Kim, G. Yoon, S. Kim, C. Lee, C. G. Lee, S. Park, K. S. Bejoymohandas, J. Yang, Y. H. Kwon, Y. J. Lee, J. K. Seo, D. Min, T. Park and T. Kwon, *Adv. Sci.*, 2025, **12**, 2407236.
- 165 N. Xu, G.-D. Zhang, Z.-Y. Xue, M.-M. Wang, Y. Su, H. Fang, Z.-H. Yu, H.-K. Liu, H. Lu and Z. Su, *Chem. Eng. J.*, 2024, **497**, 155022.
- 166 Y. Chen, C. Liang, M. Kou, X. Tang and J. Ru, *Dalton Trans.*, 2024, **53**, 11836–11849.
- 167 A. Gupte and R. J. Mumper, *Cancer Treat. Rev.*, 2009, **35**, 32–46.
- 168 Z. Wang, D. Jin, S. Zhou, N. Dong, Y. Ji, P. An, J. Wang, Y. Luo and J. Luo, *Front. Oncol.*, 2023, **13**, 1123420.
- 169 P. Zheng, C. Zhou, L. Lu, B. Liu and Y. Ding, *J. Exp. Clin. Cancer Res.*, 2022, **41**, 271.
- 170 J. Xie, Y. Yang, Y. Gao and J. He, *Mol. Cancer*, 2023, **22**, 46.
- 171 Y. Yang, M. Li, G. Chen, S. Liu, H. Guo, X. Dong, K. Wang, H. Geng, J. Jiang and X. Li, *Coord. Chem. Rev.*, 2023, **495**, 215395.
- 172 P. Zheng, C. Zhou, Y. Ding and S. Duan, *J. Exp. Clin. Cancer Res.*, 2023, **42**, 103.
- 173 S. Zhou, J. Liu, A. Wan, Y. Zhang and X. Qi, *J. Hematol. Oncol.*, 2024, **17**, 22.
- 174 X. Liu, L. Zhuang and B. Gan, *Trends Cell Biol.*, 2024, **34**, 327–337.
- 175 W. Zhen, T. Zhao, X. Chen and J. Zhang, *Small*, 2025, 2500880.
- 176 T. Li, Y. Song, L. Wei, X. Song and R. Duan, *Cell Commun. Signaling*, 2024, **22**, 491.
- 177 Y. Zhou, L. Liu, S. Tao, Y. Yao, Y. Wang, Q. Wei, A. Shao and Y. Deng, *Pharmacol. Res.*, 2021, **163**, 105299.
- 178 G. Gupta, M. Afzal, E. Moglad, A. Goyal, W. H. Almalki, K. Goyal, M. Rana, H. Ali, A. Rekha, I. Kazmi and S. I. Alzarea, *EXCLI J.*, 2025, **24**, 351.
- 179 P. Huang, G. Chen, W. Jin, K. Mao, H. Wan and Y. He, *Int. J. Mol. Sci.*, 2022, **23**, 7292.
- 180 K. Moloudi, H. Abrahamse and B. P. George, *Front. Oncol.*, 2023, **13**, 1225694.
- 181 L. Zhou, J. Li, J. Chen, X. Yao, X. Zeng, Y. Liu, Y. Wang and X. Wang, *Dalton Trans.*, 2024, **53**, 15176–15189.
- 182 C. Huang, Y. Yuan, G. Li, S. Tian, H. Hu, J. Chen, L. Liang, Y. Wang and Y. Liu, *Eur. J. Med. Chem.*, 2024, **265**, 116112.
- 183 S. Tian, Q. Nie, H. Chen, L. Liang, H. Hu, S. Tang, J. Yang, Y. Liu and H. Yin, *J. Inorg. Biochem.*, 2024, **256**, 112549.
- 184 H. Zhang, X. Liao, X. Wu, C. Shi, Y. Zhang, Y. Yuan, W. Li, J. Wang and Y. Liu, *J. Inorg. Biochem.*, 2022, **228**, 111706.
- 185 P. Wang, H. Fang, M. Wang, G. Zhang, N. Xu, Y. Su, H. Liu and Z. Su, *Chin. Chem. Lett.*, 2024, 110099.
- 186 Y. Lu, S.-S. Wang, M.-Y. Li, R. Liu, M.-F. Zhu, L.-M. Yang, F.-Y. Wang, K.-B. Huang and H. Liang, *Acta Pharm. Sin. B*, 2024, **15**, 424–437.
- 187 Y. Niu, S. Tang, J. Li, C. Huang, Y. Yang, L. Zhou, Y. Liu and X. Zeng, *J. Inorg. Biochem.*, 2025, **264**, 112808.
- 188 J. Zheng, A. Zhang, Q. Du, C. Li, Z. Zhao, L. Li, Z. Zhang, X. Qin, Y. Li, K.-N. Wang and N. Yu, *J. Colloid Interface Sci.*, 2025, **683**, 420–431.
- 189 T. Feng, Z. Tang, J. Karges, J. Shen, C. Jin, Y. Chen, Y. Pan, Y. He, L. Ji and H. Chao, *Biomaterials*, 2023, **301**, 122212.
- 190 M. Shee, D. Zhang, M. Banerjee, S. Roy, B. Pal, A. Anoop, Y. Yuan and N. D. P. Singh, *Chem. Sci.*, 2023, **14**, 9872–9884.
- 191 Y.-L. Zeng, L.-Y. Liu, T.-Z. Ma, Y. Liu, B. Liu, W. Liu, Q.-H. Shen, C. Wu and Z.-W. Mao, *Angew. Chem., Int. Ed.*, 2024, **63**, e202410803.
- 192 L. Ke, F. Wei, L. Xie, J. Karges, Y. Chen, L. Ji and H. Chao, *Angew. Chem., Int. Ed.*, 2022, **61**, e202205429.
- 193 H. Yuan, Z. Han, Y. Chen, F. Qi, H. Fang, Z. Guo, S. Zhang and W. He, *Angew. Chem., Int. Ed.*, 2021, **60**, 8174–8181.
- 194 Y. Lu, W. Sun, J. Du, J. Fan and X. Peng, *JACS Au*, 2023, **3**, 682–699.
- 195 G. Canti and V. Rapozzi, *Photochem. Photobiol. Sci.*, 2024, **23**, 1749–1755.
- 196 D. Nowis, T. Stokłosa, M. Legat, T. Issat, M. Jakóbsiak and J. Gołab, *Photodiagn. Photodyn. Ther.*, 2005, **2**, 283–298.
- 197 H. S. Hwang, H. Shin, J. Han and K. Na, *J. Pharm. Invest.*, 2018, **48**, 143–151.
- 198 Y. Zheng, G. Yin, V. Le, A. Zhang, S. Chen, X. Liang and J. Liu, *Int. J. Biol. Sci.*, 2016, **12**, 120.
- 199 R. Alzeibak, T. A. Mishchenko, N. Y. Shilyagina, I. V. Balalaeva, M. V. Vedunova and D. V. Krysko, *J. ImmunoTher. Cancer*, 2021, **9**, 001926.
- 200 J. Li, E. Pang, J. An, Z. Xiong, E. Kim, M. Lan, Q. Y. Cao and J. S. Kim, *Adv. Funct. Mater.*, 2025, **35**, 2419598.
- 201 X. Liu, H. Zheng, Y. Peng, D. Ji, C. Wang, D. Wang, Z. Jia, Y. Chang, X. Cai, L. Wang and Y. Ling, *Mol. Pharmaceutics*, 2025, **22**, 882–894.
- 202 Q. Lie, H. Jiang, X. Lu, Z. Chen, J. Liang, Y. Zhang and H. Chao, *J. Med. Chem.*, 2025, **68**, 8894–8906.
- 203 G. Vigueras, L. Markova, V. Novohradsky, A. Marco, N. Cutillas, H. Kostrhunova, J. Kasparkova, J. Ruiz and V. Brabec, *Inorg. Chem. Front.*, 2021, **8**, 4696–4711.

- 204 J. Y. Zhou, Q. H. Shen, X. J. Hong, W. Y. Zhang, Q. Su, W. G. Li, B. Cheng, C. P. Tan and T. Wu, *Chem. Eng. J.*, 2023, **474**, 145516.
- 205 J. Zhao, X. Dai, M. Lv, H. Liu, M. Ren, G. Hu, X. Xue and H. K. Liu, *Inorg. Chim. Acta*, 2025, **580**, 122601.
- 206 F. Chen, H. Ma, G. Wen, X. Wu, X. Lin, D. Li, D. Wang, A. Dao, H. Huang and P. Zhang, *J. Med. Chem.*, 2025, **68**, 13019–13029.
- 207 J. An, K. P. Lv, C. V. Chau, J. H. Lim, R. Parida, X. Huang, S. Debnath, Y. Xu, S. Zheng, A. C. Sedgwick and J. Y. Lee, *J. Am. Chem. Soc.*, 2024, **146**, 19434–19448.